universität wien

DIPLOMARBEIT

Titel der Diplomarbeit

TTP-Mediated mRNA-Decay in Acute and Chronic Inflammation

Verfasser

Florian Ebner

angestrebter akademischer Grad

Magister der Naturwissenschaften (Mag. rer. nat.)

Wien, 2011

Studienkennzahl lt. Studienblatt:	A 490
Studienrichtung lt. Studienblatt:	Diplomstudium Molekulare Biologie
Betreuerin / Betreuer:	Ao. Univ.-Prof. Mag. Dr. Pavel Kovarik

ABSTRACT

Regulation of gene expression is indispensible for environmental adaption of cells, and is a prerequisite for all living organisms. Classically, transcription and post-translational modifications are the most extensively studied levels of gene expression control, but in recent years the regulation at the level of mRNA stability gained more and more attention. Governing the stability of the message is an elegant and quick way for cells to change gene expression. Regulation of gene expression by means of changes in mRNA stability is particularly important for the immune system. To combat pathogens the immune system needs to generate a sufficiently strong response which however needs to be precisely limited in terms of time and amplitude to avoid adverse effects.

One mechanism utilized in this type of regulation is achieved by proteins binding so-called adenine/uridine-rich elements (AREs) within the 3' untranslated regions of target mRNAs. Tristetraprolin (TTP) is an ARE-binding protein that recruits decapping and deadenylating proteins upon binding to its target mRNAs thereby causing degradation by 5' to 3' exonucleolytic decay or 3' to 5' degradation via the exosome complex. Mice deficient in TTP are viable but display a general pro-inflammatory phenotype demonstrating that TTP is involved in limiting inflammatory responses by degradation of inflammatory mRNAs.

The strong phenotype of conventional knockout mice is not well suited to study roles of TTP in different pathologies and cell-types, therefore conditional knockout mice were employed in this current study. The aim of the thesis was to investigate roles of TTP-mediated mRNA-decay in acute inflammatory responses and in inflammation-associated colon carcinogenesis. We could show that conditional knockout in the myeloid lineage renders mice less susceptible to invasive infection with a highly virulent strain of *Streptococcus pyogenes.* These animals displayed decreased dissemination of *S. pyogenes* and exhibited improved survival. This was most likely caused by a stronger immune response of mice lacking myeloid TTP since experiments employing low- and high-virulent strains of *S. pyogenes* suggested the requirement of efficient immune response for clearance of the pathogen. Experiments addressing colitis-associated cancer revealed that, surprisingly, TTP has a cell type-specific function in this model of inflammation-associated cancer. Mice lacking TTP in myeloid cells displayed enhanced susceptibility to the disease whereas animals with T cell-specific TTP ablation were more resistant.

ZUSAMMENFASSUNG

Regulation der Genexpression ist für zelluläre Adaptation an die Umwelt unersetzlich und Voraussetzung für alle Lebewesen. Kontrollmechanismen der Transkription und der post-translationalen Modifikationen sind zwar am besten studiert, aber in den letzten Jahren wurde die Wichtigkeit der Regulation der mRNA Stabilität immer mehr erkannt. Steuerung dieser Stabilität ist für Zellen eine elegante und schnelle Möglichkeit Genexpression zu ändern und diese Flexibilität ist für das Immunsystem besonders wichtig. Pathogene müssen einer effizienten Immunantwort ausgesetzt sein, diese muss aber auf der anderen Seite präzise in der Zeit und Stärke limitiert werden, um schädigende Folgen zu vermeiden.

Ein Mechanismus dieser Regulation wird durch Bindung von Proteinen an sogenannte Adenin/Uridin-reiche Elemente (AREs) im 3‘ untranslatierten Bereich von mRNAs vermittelt. Tristetraprolin (TTP) ist ein solches ARE-bindendes Protein und rekrutiert Enzyme, die das Cap und den Poly-A Schwanz von mRNAs degradieren, gefolgt von exonukleolytischem Abbau der gebundenen mRNA durch Degradation in 5‘ zu 3‘ oder 3‘ zu 5‘ Richtung. Mäuse denen TTP fehlt sind zwar lebensfähig, haben aber einen starken pro-inflammatorischen Phänotyp. Das zeigt, dass TTP durch Vermittlung von mRNA-Degradation bei der Limitierung der inflammatorischen Antwort eine wichtige Rolle spielt.

Dieser starke Phänotyp macht es schwierig, Rollen von TTP in verschiedenen Krankheiten und Zelltypen zu studieren, deswegen wurden in dieser Studie konditionale knockout Mäuse verwendet. Das Ziel dieser Arbeit war es, Effekte von TTP-vermittelter mRNA-Degradation in akuten inflammatorischen Antworten und Entzündungs-assoziierter Dickdarmkarzinogenese zu studieren. Wir zeigen, dass Mäuse mit Deletion von TTP in myeloiden Zellen bei einer Infektion mit einem virulenten Stamm von *Streptococcus pyogenes* Vorteile haben. Die Bakterien sind weniger invasiv und die Tiere zeigen höhere Überlebensraten, höchstwahrscheinlich weil sie eine stärkere Antwort des Immunsystems auslösen. Versuche mit hoch- und niedrig-virulenten Stämmen haben nämlich gezeigt, dass eine effizientere Antwort zur Beseitigung des Pathogens vielleicht der Grund für die geringere Virulenz ist. Überraschenderweise ergaben Experimente mit Colitis-assoziierten Karzinomen, dass TTP Zelltyp-spezifische Funktionen in einem Modell von Entzündungs-assoziiertem Krebs hat. Fehlte TTP in myeloiden Zellen, waren die Mäuse anfälliger für induzierte Karzinogenese, fehlte es jedoch in T Zellen waren sie resistenter.

TABLE OF CONTENTS

1 ACKNOWLEDGEMENTS

First of all I want to thank Pavel Kovarik for giving me the opportunity to do the work for my diploma thesis in his research group. Thanks for the numerous discussions, for general guidance, all the scientific advice, advancing me and last but not least for enabling a high degree of independence.

I'm deeply grateful to Franz and Nina. Franz for being a great and patient mentor – I can't imagine a better way of guiding and helping me. Nina for teaching me how to work with Streptococcus, without you I would have been like "da Butta in da Sun". Naturally I'm thankful to all my lab members for making the laboratory not only a working place but as well a place of social interaction and fun. Special thanks to former lab-member and diploma-buddy Marton – I never expected finding a colleague sharing so many commonalities with.

As a matter of course this thesis is dedicated to my beloved family. Thanks for supporting me in any case and in any situation of life and thanks for the great acceptance and encouragement in everything I did, I'm currently doing and I will be doing.

Naturally, there are other mentionable people who didn't contribute directly to this work, but indirectly by enriching my daily life. Manuel Leeb always takes my moaning (even in the middle of the night), is a great accomplice for everything and triggers creativity buried deep in me. Thanks to many of my colleagues and friends I found during the studies for support. Chris thanks for productive (and sometimes not so productive) discussions on the terrace. Dagmar thanks for being so entertaining and supportive all the time. Muriel thanks for self-purled caps and teaching me some art. Nici, your archetypical straightforwardness is admirable. Susi thanks for dancing nights away together. Albin, you're cool.

Additionally I want to thank Michaela for being very cooperative and helpful with the endoscopy and teaching me a lot about colitis-associated cancer. Thanks to Bella for being very patient and helpful when I'm asking about colitis and Stefanie for performing the phagocytosis assays.

And last and as well least in this case I wanted to thank some people I've never met (so far?) but still they are enriching my life with their creativity. In particular Shigeru Miyamoto for creating awesome entertainment for more than 20 years now, Allan Ball for high-quality television series, Charlaine Harris and Stephen King for balancing "light" literature besides all the read publications and text books and Stefani Germanotta for reaching an incredibly huge audience with the messages to embrace individuality and to love who you are.

2 INTRODUCTION

2.1 Regulation of Gene Expression: mRNA Stability

One prerequisite for higher organisms and environmental adaption in general is the possibility to regulate gene expression differently in different cells. This regulation takes place on many different layers from a gene on its way to a functional protein. Chromatin can be silenced or activated by multiple mechanisms[1], transcription factors can enhance or repress transcription[2,3], different splicing patterns often generate multiple different proteins out of one original gene[4], translation can be influenced in different ways[5] and proteins themselves are heavily affected by post-translational modifications and spatiotemporal distribution[6,7] and many more.

In recent decades mRNA gained more and more attention: The view of mRNA as passive bystander product of gene expression changed dramatically and the mRNA level is nowadays considered to be extensively regulated. Stability of mRNA is of special interest, as decay of template messenger RNA is a very efficient way for cells to diminish synthesis of a protein quickly. This type of regulation is important in situations where prolonged expression of a protein could be potentially harmful and a very strict and potent mechanism is needed. Limiting the production of cytokines is of special importance in innate mediated inflammatory responses, as spill-over potentially entails septic shock. Misbalanced production of pro-inflammatory proteins in immune homeostasis can be harmful as well, as illustrated by e.g. inflammatory bowel disease (IBD). Furthermore, mRNA decay is a way of quality control to protect cells against potentially harmful mutant proteins.

Eukaryotic mRNA is known to be processed and bound by many proteins from the very beginning of transcription to translation, therefore mRNA is never appearing as a single molecule and is always forming a circular structure which contributes to stability[8]. The general machinery for mRNA turnover usually starts with deadenylation by e.g. Ccr4p mRNA deadenylase followed by removal of the 5'-cap structure by a decapping enzyme complex, consisting of Dcp1p and Dcp2p. Decapping leads to 5' to 3' digestion and, alternatively, deadenylation alone is thought to expose mRNA to the exosome complex,

degrading in 3' to 5' direction. Other suggested pathways involve recognition of mRNA without any stop codon or endonucleolytic pathways[9]. **Fig. 1** illustrates these undirected, unspecific general mRNA turnover pathways employed by eukaryotic cells. Besides formerly mentioned undirected mRNA turnover, cells employ mechanisms to degrade mRNA specifically.

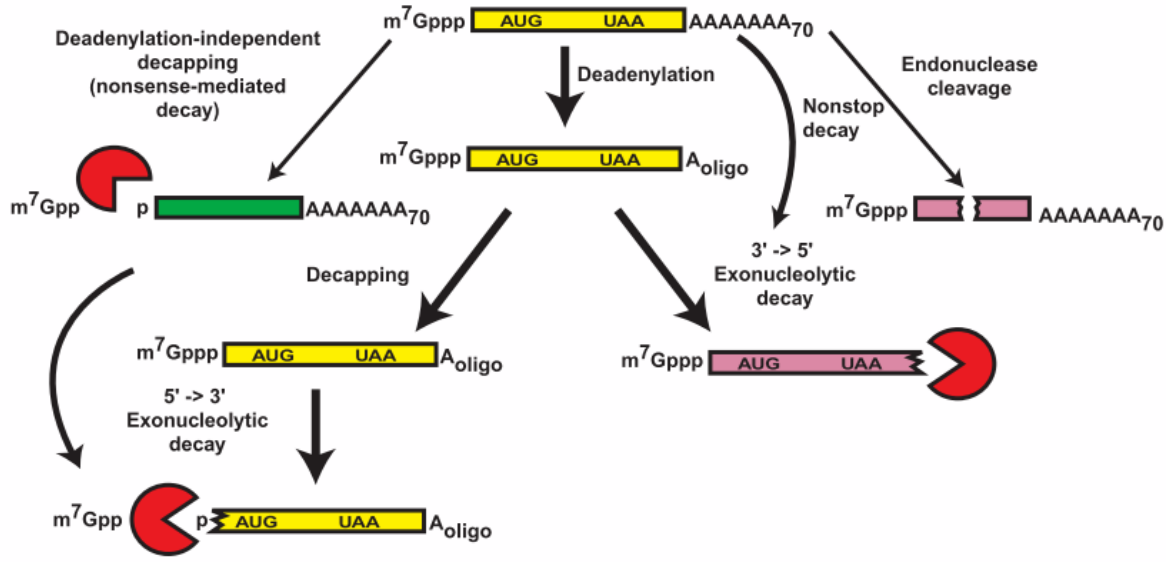

Figure 1 | Suggested pathways of eukaryotic mRNA turnover. From: R. Parker & H. Song, 2004[9]

2.1.1 RNA interference (RNAi)

The discovery that small RNAs can induce the degradation of mRNA in a sequence-specific way unraveled a new layer of regulating gene expression. Small RNA is generated by introducing foreign long double-stranded RNA (dsRNA) into the cytoplasm, which is then cut down as defense mechanism against viral infections. This pathway is nowadays widely used in molecular biology to knock down specific genes with target RNAs. The other category of small RNAs is generated from genome encoded hairpin RNAs which form characteristic stem loop structures, get cut and are then referred as microRNAs (miRNAs). In brief, RNA interference is carried out through three steps. It starts with RNAse III-like enzymes Dicer and Drosha recognizing exogenous dsRNA or endogenous hairpin RNA and processing it to small duplexes. After unwinding, one single strand is introduced into the RNA-induced silencing complex (RISC). RISC screens for homologous endogenous sequences, binds them and the single-stranded RNA guides one paralogue of the Argonaute (AGO) family proteins to cleave targeted mRNAs[8,10].

2.1.2 Nonsense Mediated Decay (NMD)

Spontaneous point mutations or deletions of bases in coding regions of genes potentially lead to the generation of a premature termination codon (PTCs). When translated, mRNAs containing PTCs can lead to possibly harmful proteins. In brief, ribosomes stall at stop codons (UAG, UGA and UAA) and if this happens at a PTC, it either fails to receive termination signals from the protein complex bound to the Poly-A tail of an mRNA[11] or the PTC is upstream of an Exon-Intron Junction Complex (EJC), both events triggering NMD[12]. A decay inducing complex (DECID) assembles, mainly mediated by UPF1 phosphorylation of different SMG proteins. Following this assembly, mRNA is degraded either by exonucleases or through endonucleolytic cleavage, depending on different SMG proteins in the DECID. Apparently NMD is not only a quality-control mechanism but also involved in active regulation of gene expression, because reports describe that mature, non-mutated mRNAs are targeted for degradation utilizing NMD[13].

2.1.3 Staufen1 Mediated Decay (SMD)

Staufen (STAU)1 was originally defined as being important for posterior-anterior definition by transporting mRNAs in *Drosophila*. But it gained entrance into the world of mRNA decay when demonstrated that STAU1 initiates decay of ADP-ribosylation factor 1 (ARF1) in human cells[14]. STAU1 mediates mRNA decay by recruiting the aforementioned NMD factor UPF1 to double stranded mRNA secondary structures in the 3' UTRs of its targets[15]. The involvement of UPF1 makes it's regulation even more complex, as it was shown that NMD and SMD are possibly opposing pathways involved in cellular differentiation[16]. Remarkably, long non-coding RNAs are proposed co-factors to create STAU1-binding sites in unstructured 3' UTRs via base pairing of *Alu* elements. The importance for this type of initiating SMD is questionable for rodents, as *Alu* elements are equivocal to be one of the key drivers of primate evolution[17].

2.1.4 A-U-rich Element Mediated Decay (AMD)

A-U-rich element mediated decay (AMD) is mediated as well by certain elements in the 3'UTRs of messages, namely adenine/uridine-rich elements (AREs). AMD seems to be one central mRNA destabilizing pathway throughout eukaryotes, as it was reported for yeast[18], *Drosophila melanogaster*[19], *Xenopus leavis*[20], *Mus musculus*[21], etc. First evidence for mRNA destabilization mediated via AREs was found in 1986 in the regulation of the

gm-csf mRNA[22]. Further investigations led to the discovery of the first ARE binding protein (BP) AUF1, which was reported to destabilize *c-myc* mRNA[23,24]. Since these start-ups, many more targets and more ARE BP were identified and showed that AMD is a very (if not the most) important pathway of targeted mRNA destabilization. AREs are nowadays considered to be 50 to 150 nt long sequences in the 3' UTR of mRNAs and contain the AUUUA pentamer accompanied with a certain U enrichment within the sequence[25]. The so far best bet for a consensus sequence is the UUAUUUA(U/A)(U/A) nonamer, as it was reported that just one AUUUA pentamer is not sufficient to induce AMD[26]. As the exact sequence for AREs is not conserved among all reported targets for AMD, AREs have been classified into three types. Class I AREs contain more core pentamers distributed over a U-rich region, class II AREs have at least two overlapping nonamers and class III AREs just have an U-rich region, but don't contain any AUUUA pentamer[27]. Even if this classification was not connected to any biological function, it's worth mentioning that cytokines cluster in the class II subgroup and transcription factors and mRNAs coding for proteins involved in cell cycle regulation contain mostly class I and class III AREs[25]. Most ARE BPs do not execute degradation of mRNAs themselves, but rather elucidate deadenylation and decapping followed by ribonucleolytic degradation of the targeted molecule[28]. Implicated mechanisms will be discussed in greater detail below for the prominent ARE BP tristetraprolin (TTP).

2.2 Tristetraprolin (TTP)

2.2.1 Biochemical Properties

TTP (other aliases TISII, Gos24, Tis11, Nup475, TIS11-D, ZFP-36) is encoded by the *Zfp36* gene, and is a 319 amino acids long protein containing three eponymous Pro-Pro-Pro-Pro repeats[29]. It belongs to the TIS11-family all of which are ARE BPs, with BRF1 (TIS11b) and BRF2 (TIS11d) sharing 70% sequence identity with TTP. In mice, Zfp36l3 is a fourth member of this family, but it's expression is restricted to the placenta in mice[30]. All TIS11-family ARE BPs share a common tandem zinc finger (TZF) domain including two C_3H zinc fingers. The spacing within these zinc fingers is steady among all TIS11 proteins ($CX_8CX_5CX_3H$) with an 18 residues long linker between the two fingers (**Fig. 2a**). NMR structure of the TZF of TIS11d bound to the UUAUUUAUU nonamer showed, that the two

fingers bind the mRNA in a single stranded, stretched conformation with U2 and U6 as central bases with defined pucker conformations (**Fig. 2b**)[31].

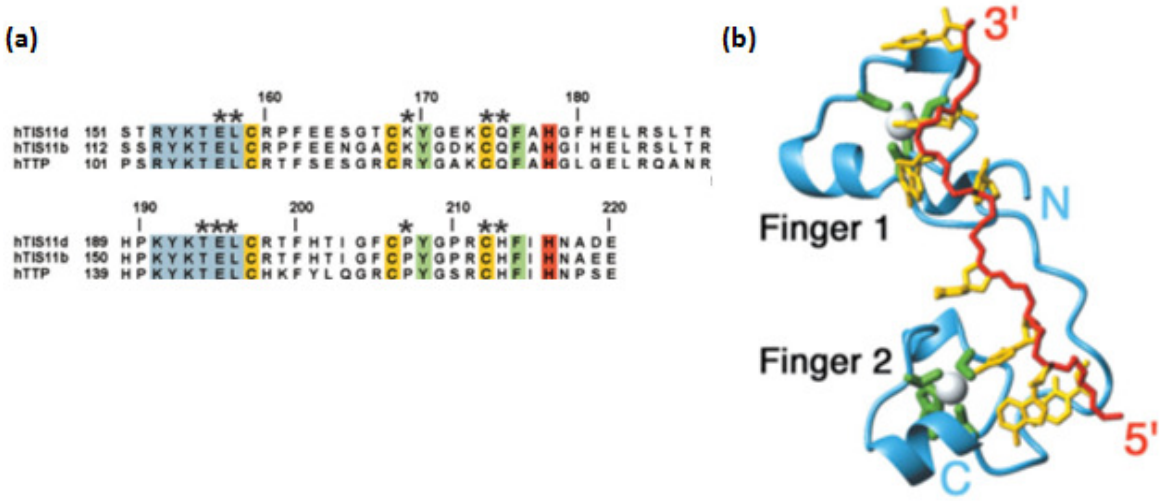

Figure 2 | Sequence alignment and RNA-binding of TIS11 proteins. (a) Sequence alignment of the three best known vertebrate members of the TIS11-family. Conserved and structurally important residues are highlighted. **(b)** Structure of TIS11d TZF domain bound to UUAUUUAUU. Taken and modified from: Hudson et al, 2004[31]

By binding to AREs, the current model suggests that TTP recruits components administrating the prerequisite for mRNA degradation. Reports showed that it induces deadenylation and decapping by interacting with the Ccr4-Not1 complex, the PARN (poly A-specific ribonuclease) complex and decapping proteins (Dcps)[32-34].

This actions lead to mRNA deprived of its circular structure and this is suspected to initiate the actual mRNA degradation. Either directly in the cytoplasm via the 3'-5' exonuclease complex termed as exosome or by nucleating P(processing)-body formation leading to 5'-3' decay via Xrn1 (**Fig. 3**). A third pathway was proposed in 2005 by a study of Jing *et al.*, demonstrating data that TTP complexes together with a microRNA (miR16) and the RNA interference protein AGO2 to induce endonucleolytic cleavage of bound mRNA[35]. Remarkably, the exact timing of these events or which nucleolytic pathway is initiated preferentially by TTP remain elusive[32,36,37].

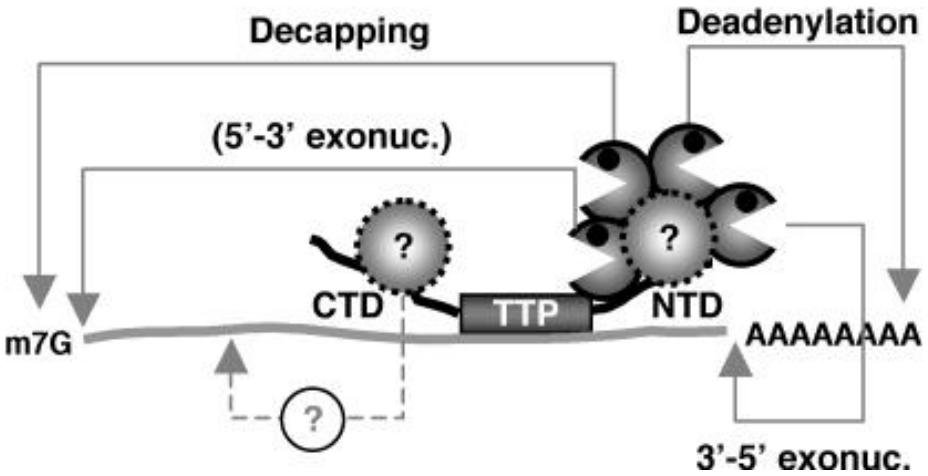

Figure 3 | Illustration of TTP binding to mRNA and recruitment of effectors. The conserved TZF domain binds to AREs within the 3'UTRs of mRNAs and proteins initiating and executing decay are thought to be recruited through interactions with the N- and C-terminal domains of TTP. From: J. Lykke-Anderson et al, 2005[32]

2.2.2 Regulation on the Transcriptional and Post-Transcriptional Level

Transcription of the *Zfp36* gene is induced by a variety of stimuli, including TPA (12-O-tetradecannoylphorbol-13-acetate), anisomycin, glucocorticoids, cinnamon polyphenol extracts, green tea, insulin, interferons and stimulation of p38 mitogen-activated kinase (MAPK) in various cell types. Lipopolysaccharide (LPS) induces TTP within 30' in BMDMs via Toll-like receptor (TLR) 4 signaling resulting in p38 phosphorylation[36,38,39].

p38 MAPK is activated upon stress signals, like stimulation of B cells via CD40/BAFF, activation of T cells via TCR, IL-12R signaling or LPS-recognition by TLR4. These receptors initiate a classical MAPK pathway comprising two upstream kinases (which differ for different receptors) leading to phosphorylation and therefore activation of p38 MAPK[40]. Downstream effectors of p38 are other kinases, e.g. MAPK-activated protein kinases (MKs) 1 and 2 and mitogen- and stress-activated kinases (MSKs) 1 and 2. Activated transcription factors by the p38-pathway initiate wide transcriptional changes in cells, leading to the expression of pro- and anti-inflammatory cytokines, chemokines and other proteins, including TTP[36,40,41].

Even if the p38 MAPK pathway activates transcription of TTP, further effects were reported on the protein level. It was shown that MK2 is capable of phosphorylating TTP at different serine residues. This phosphorylation inhibits proteasomal decay, creates binding sites for the 14-3-3 protein stimulating export of TTP from the nucleus to the

cytoplasm. One hallmark of the stress response of a cell is formation of so-called stress granules (SG). Herein mRNAs are temporarily stored for reinitiation of translation at later time points and therefore SGs can be seen as an energy saving strategy for cells[42]. Within these granules are other ARE BPs (like TIA-1 and HuR) partially opposing or competing TTPs effects[43]. Data indicating dynamic interactions between SGs and P-bodies and TTPs ability to nucleate P-body formation led to the hypothesis, that TTP shuttles stalled mRNA from SGs to P-bodies to determine its fate to be degraded and not reused by the translational machinery[44,45]. Association of 14-3-3 complexes with TTP leads to exclusion of TTP and its bound mRNA from SGs, therefore inhibiting AMD mediated by TTP (**Fig. 4**). The net effect is that upon pro-inflammatory stimuli anti-inflammatory TTP enriches in an inactive, but stable form in the cytoplasm, awaiting its activation[46].

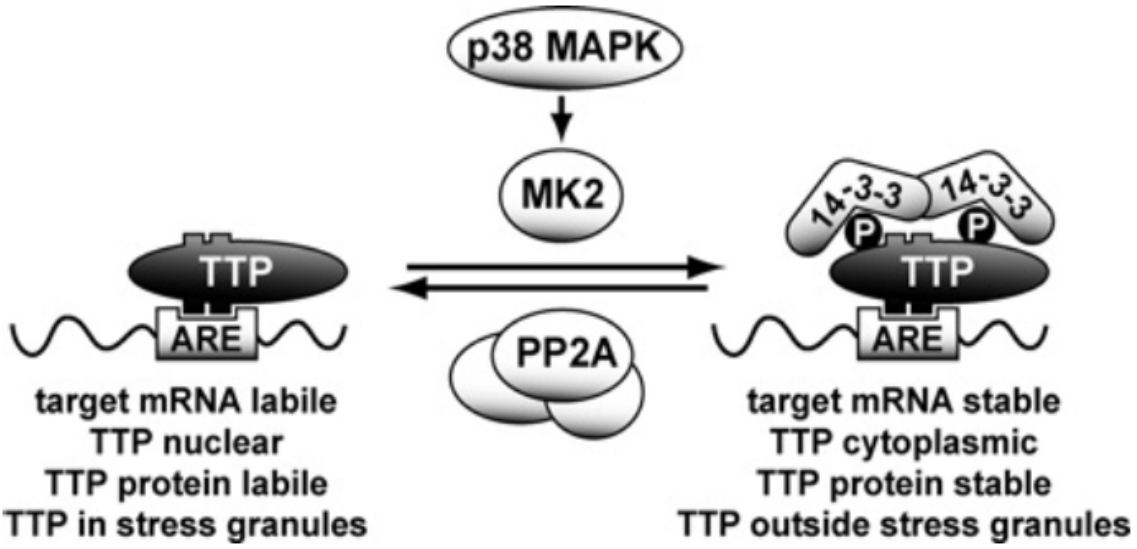

Figure 4 | Effects of posttranslational phosphorylation on TTP. Shown is a scheme for competing kinase MK2 and phosphatase PP2A. Phosphorylation leads to docking of 14-3-3 proteins. Outcomes of these posttranslational modifications of TTP are depicted. From: Sandler et al, 2008[46]

Activation is realized by dephosphorylation of TTP. To date, the dual specificity protein phosphate 1 (DUSP1) and protein phosphatase 2A (PP2A) are known to be important key players in this negative feedback loop. Though, IL-10 is one of the major anti-inflammatory cytokines, it's induced by macrophages upon LPS stimulation. One downstream effect of IL-10 signaling on macrophages is the induction of DUSP1 and recent data indicates that DUSP1 dephosphorylates and therefore inactivates p38 MAPK. This inactivation translates into less active MK2 and shifts the equilibrium to the dephosphorylated form of TTP via competing PP2A. This negative-feedback loop quickly

generates a pool of cytoplasmic active TTP realizing an elegant mechanism for cells to shut of transient expression of potentially harmful pro-inflammatory cytokines quickly to resolve the inflammatory reaction on the cellular level[41,46,47].

2.2.3 Targets of TTP

TTPs most prominent and most extensively physiological target is tumor necrosis factor α (TNF-α). Conventional knockout mice show a general pro-inflammatory phenotype displaying among others signs of arthritis, conjunctivitis, dermatitis, cachexia and myeloid hyperplasia. Moreover this phenotype is reversible by treating the mice with neutralizing antibodies against TNF-α[48]. The fact that *Il10* and *Zfp36l* mRNA themselves are targeted by TTP indicates, that the regulatory network built up by the former mentioned mechanisms is even more complex and self-regulating[49,50]. With time, more and more targets were identified and the number is still growing (a few examples are listed in **Table 1**). Although, most targets are implicated in immune responses, some are implicated in carcinogenesis, including mRNAs encoding proteins important in cell cycle control and angiogenesis.

Table 1 | Examples of reported mRNAs targeted by TTP[36,37].

Inflammation associated mRNAs	*Tnfa*
	Il6
	Il2
	Il3
	Tis11
	Ccl2
	Ccl3
	Gmcsf
	Il10
Carcinogenesis (cell cycle/angiogenesis)	*Cyclin D1*
	p21
	c-myc
	c-fos
	E6-AP
	Vegf

To date, the exact timing and different affinities for different targets of TTP during its inflammation resolving activity is not well understood. The general model can be simplified as upon stimulus of p38 MAPK, TTP is highly expressed and is enriching in the cytoplasm, but inhibited in mediating its destabilizing functions. After deactivation of p38 MAPK, TTP gets active and initiates rapid mRNA decay of targets in a timely resolved gradual manner, i.e. targeting some targets earlier and more efficiently than others (Kratochvill et al, Mol Syst Biol, *in press*).

2.3 Other mRNA Binding Proteins

2.3.1 TTPs Siblings: The TIS11-Family

The TIS11 family in vertebrates contains so far five identified members and TIS11 (TTP) is the best characterized among them. The human family contains furthermore the closely related TIS11b (ZFP36L1 gene, also called BRF1, Berg36, cMG-1, ERF1, RMF162B, PubMed Gene ID: 677) and TIS11d (ZFP36L2 gene, also called BRF2, ERF2, RNF162C, PubMed Gene ID: 678) and share a 67 amino acid highly conserved core region spanning the TZF domain[51]. All three of them display the two conserved zinc fingers and the characteristic RYKTEL sequence preceding each finger (**Fig. 2a**). The murine TIS11 family contains additionally Zfp36l3 which was shown to be strictly expressed in the placenta of mice. Zfp36l1.2 (XC3H-4) was defined to belong to the Tis11 family as well, but is strictly expressed in reproductive tissues in *Xenopus leavis* and fish[30,52].

The TIS11 family seems to be conserved among eukaryotes, hence the two C_3H zinc finger proteins CTH1 and CTH2 in *Saccharomyces cerevisiae* and DTIS11 of *Drosophila melanogaster* share the characteristic $CX_8CX_5CX_3H$ motifs and are implicated in mRNA degradation[36,53].

TIS11b and TIS11d share more than 70 % amino acid identity with TTP and they have overlapping targets, as all of them are reported to target *Tnfa* or *Gm-csf* mRNA for degradation[36,51]. Knockout of TIS11b results in embryonic lethality and TIS11d is involved in reproduction and a critical regulator of hematopoiesis[54-56]. Double knockout of TIS11b and TIS11d in early stages of thymic development caused mice to develop T cell acute lymphoblastic leukemia (T-ALL)[21]. These studies indicate that these two TIS11 proteins are

more important in development and reproduction than TTP. Although TIS11b was shown to be very similarly regulated on the posttranscriptional level by MK2 and inhibitory serine phosphorylations, TIS11b and TIS11d differ in their expression pattern[57]. Both proteins are strongly down-, whereas TTP is upregulated upon LPS stimulation of BMDMs, substantiating the prominent role of TTP in inflammatory reactions (Kratochvill et al, Mol Syst Biol, *in press*).

2.3.2 Stabilizing HuR

The Hu family consists of four encoded proteins in the mammalian genome (HuR or HuA, HuB or ELAVL2, HuC and HuD), with HuR being the best studied[58]. Similarly to TTP, HuR has a nuclear localization signal (NLS) and the ability to shuttle between the nucleus and the cytoplasm. HuR is proposed to bind up to 15 % of all human mRNAs via three RNA-recognition motifs (RRMs) by targeting all three classes of AREs[59]. Slightly opposing results from a very recent study mapped the binding site to overrepresented uridine heptamers and not to adenine/uridine enriched sequences, but this remains to be approved by more detailed investigation[60].

HuR is generally considered to have stabilizing effects when binding to mRNA, especially to class I and II AREs and can be recruited to SGs. As many of TTPs targets have been reported to be targeted and stabilized by HuR, competitive functions of these proteins are suggested[36,43,61]. Opposing function was shown for Tis11b and HuR, as the double knockdown of both proteins compensated for the destabilizing effects of siRNA against HuR alone[62]. More evidence for antagonistic functions was found in the differentially disregulated expression of HuR and TTP in colorectal cancer, where upregulation of HuR is generally accompanied by downregulation of TTP[63].

As microRNA came into play with TTP, it did so for HuR in 2006 when a report showed that cationic aminoacid transporter 1 (CAT-1) mRNA could be released and translationally reactivated from P-bodies by HuR with assistance of miR122 mediated by imperfectly base-pairing with 3'UTR of CAT-1[64].

2.3.3 AUF-1

AUF-1 (also A/U-rich element RNA-binding protein 1, heterogeneous nuclear ribonucleoprotein D, hnRNPD, P37) is another regulatory protein capable of binding AREs

in 3' UTRs, and was the first one identified to do so[24]. Like the formerly mentioned ARE BPs, AUF-1 is shuttling from the nucleus to the cytoplasm[65]. In 1999 a study identified targets on a larger scale by *in vitro* analysis. Besides verifying the known targets like *Gm-csf*, *Tnfa* and *Il2*, they reported that AUF-1 binds to mRNAs encoding for IL-8, Cathepsin L8, EF2, Poly-A binding protein, etc[66]. The initial data always suggested a rather destabilizing role for AUF-1, mediated by a huge complex consisting of heat shock proteins, translation initiation factor eIF4G, PABP and more recruited ribonucleases[67]. In recent years reports were published showing opposing results and suggested a stabilizing function of AUF-1 for some of its targets, e.g. *Tnfa*, *c-myc*, *c-fos*. These inconsistencies could be partially, but not satisfyingly, explained by cell-type specific effects of AUF-1[25]. Remarkably, Hsp27 is associating in the complex with AUF-1, and this heat shock protein is known to be phosphorylated via p38 MAPK and MK2 activation on three serine residues. This phosphorylation leads most probably to polyubiquitinylation of AUF-1 followed by proteasomal degradation[68].

Although AUF-1 shares some pro-inflammatory targets with TTP (e.g. *Tnfa*, *Il1b*), conventional knockout of AUF-1 does not resemble the complex phenotype of TTP knockout mice. They develop normally, but are more susceptible to LPS-induced endotoxin shock. In contrast to TTP, AUF-1 achieves destabilization of *Tnfa* only upon stimulation, whereas the TIS11 proteins do so in homeostatic conditions[69].

2.3.4 TIA-1 and TIAR

T cell intracellular antigen 1 (TIA-1) and TIA-1 related (TIAR) are closely related proteins within the RNA recognition motif (RRM) family of RNA BP. $TIA1^{-/-}$ mice develop mild arthritis, although this is strongly strain dependent[70]. Macrophages derived from these mice produce similar amounts of *Tnfa* transcripts but secrete significantly more mature TNF-α. This showed that TIA-1 is not destabilizing mRNAs per se, but inhibits their translation[71]. Under stress conditions TIA-1 and TIAR shuttle from the nucleus to the cytoplasm to induce the assembly of an alternative so-called noncanonical translation-initiation complex, which is then recruited to SGs. After removal of the stress stimulus stress granules first enlarge through fusion and disappear with time[42]. TIA-1 and TIAR were identified being distinct markers for SG, since cells lacking the proteins failed to induce SGs after stimulus[72].

2.4 Inflammation: From Initiation to Resolution

Detecting pathogens for the first time and initiating a full-fledged innate immune response is mainly mediated by cells belonging to the mononuclear phagocyte system (**Fig. 5**). These cells are derived from committed hematopoietic stem cells in the bone marrow and leave it as monocytes. In homeostatic conditions monocytes circle the blood stream, enter tissues and differentiate to dendritic cells (DCs) or tissue-resident macrophages. Neutrophils, DCs, macrophages and monocytes are professional phagocytic cells, comprising the first line of defense against invading pathogens or danger signals[73].

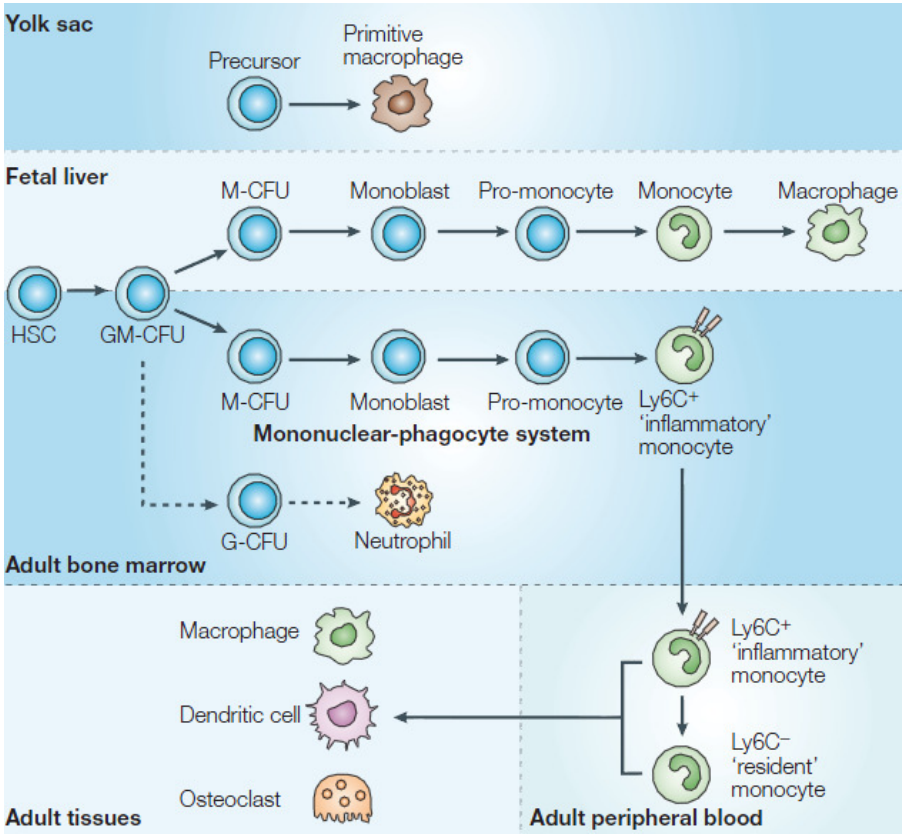

Figure 5 | Mononuclear phagocyte system. Illustrated is differentiation from committed stem cells to different innate immune cells. Ly6C$^+$ monocytes enter the blood stream and differentiate within tissues to different cell types depending tissue-specific signals. From: Gordon and Tayler, 2005[74]

In the classical view DCs are immune sentinels primarily instructing adaptive immunity via antigen-presentation in lymph nodes and have a minor role in innate immune reaction. But advances in cell culture techniques and techniques distinguishing different cell types led to the conclusion that DCs, macrophages and monocytes are highly dynamic and heterogeneous cells[75]. When pathogens manage to overcome the physical barriers like

epithelial cells, they face a plethora of antimicrobial defense mechanisms to protect the body. One of the most important reactions is the cellular based innate immune response to the potentially dangerous invader, executed mainly by APCs (as macrophages or DCs), neutrophils and monocytes[76].

2.4.1 Tissue-resident Macrophages as Immune Sentinels

Tissue-resident macrophages are distributed throughout the body, fulfilling their guarding functions and are highly adapted to different tissues[74]. These cells act as immune sentinels, but are rather anti-inflammatory in many organs, when not stimulated with various ligands derived from pathogens and/or tissue destruction. Especially, at "semi-opened" sites to the exterior like the gut or the spleen, tissue-resident macrophages need to display an anti-inflammatory state, as shown by many studies[77,78].

They express a lot of different germline encoded receptors implicated in recognizing different stimuli, such as signals like microbe-associated molecular patterns (MAMPs), dead cells, tissue injury and cytokines[79,80]. Invading pathogens cause a combination and prolonged exposure to such signals and activate macrophages to a state referred to as pro-inflammatory M1 macrophage[73]. These cells start a full-fledged response by producing antimicrobial agents, such as nitric oxide or Fe-binding molecules, by upregulating phagocytosis-efficiency and production of various cytokines and chemokines[76,81]. The produced and secreted cytokines and chemokines alert the environment and potentiate the response. The molecules enter the blood stream creating a chemotactic gradient for recruitment of other immune cells and they are shaping the inflammatory site by affecting endothelial cells, mainly mediated by TNF-α, pro-inflammatory IL-6, CXCLs and CCLs[79,82]. Additionally, secreted metalloproteinases by macrophages are capable of enhancing the signaling by cleaving chemokines[83].

2.4.2 Outdated Stereotype: Neutrophils and their Bad Reputation

Neutrophils are the most abundant immune cells in the body and differentiate in the bone marrow. Only a small part enters the blood stream (less than 2 % of all neutrophils) and they patrol to sense chemotactic signals. CXCL2 for example leads to massive mobilization of neutrophils from the bone marrow[84]. Following chemotactic signals neutrophils then encounter inflammation-upregulated adhesion proteins on endothelial cells next to the inflammatory site. The penetration through endothelium is mediated by

different integrins, but CD11b/Mac-1 interacting with ICAM-1 is of special interest as this interaction initiates maturation to inflammatory neutrophils[85]. These activated neutrophils execute a number of defense mechanisms, which are potentially harmful to the host (**Fig. 6**). Different vesicles containing granule proteins are released upon different stimuli of the cell, some of them very unspecifically just upon or during transmigration through endothelia[86]. Reactive oxygen species (ROS) act very broadly on host cells and microbes. Neutrophil extracellular traps (NETs) are formed by a mechanism referred to as NETosis, when the inflammatory neutrophil is directly stimulated with a MAMP, ROS or by binding to activated platelets. This stimulation induces an apoptosis-like program in neutrophils and the net effect is spilling out of DNA associated with histones and antimicrobial proteins. NETs are not only reported to kill microbes but are also implicated in just binding pathogens to prevent dissemination[87,88].

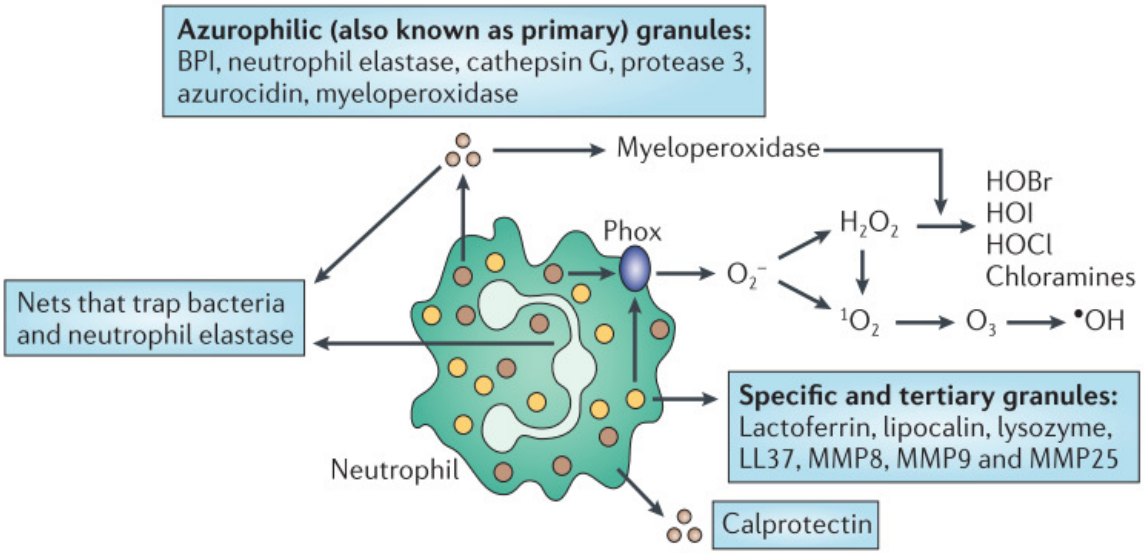

Figure 6 | The antimicrobial armour utilized unspecifically by neutrophils. From: C. Nathan, 2006[89]

The granule components shown in **Fig. 6** are partially highly reactive proteases, metalloperoxidases and antimicrobial peptides. These proteins are mediating massive tissue destruction, which leads to the well known phenomenon of pus formation. These abscesses gave the neutrophils its bad reputation of being undirected destroyers as ultima ratio against pathogens. Over the last decade, this view changed completely as this tissue breakdown implies several defense mechanisms. Breakdown of blood vessels cuts off potential routes for pathogens to get systemic, degrading extracellular matrix (ECM) proteins facilitates infiltration of cells of the adaptive immune system and creates further

danger signals to amplify the response, and last but not least, some truncated proteins resulting from proteolytic cleavage provide anti-inflammatory and resolving signals[76,79,86,90]. A study showed very recently that certain serine proteases within secreted vesicles and NETs of neutrophils are able to induce and regulate the coagulation-cascade *in vivo*. Coagulation is an ancient mechanism to avoid dissemination and is mainly carried out via platelet activation[91,92].

2.4.3 The Third Man: Monocyte Recruitment

Together with secreted CXCL8, CCL2, CCL3, CCL4, CCL6, etc. and granule proteins (e.g. LL-37), inflammatory neutrophils and M1 macrophages create an environment chemoattracting additional monocytes[79,93]. The chemokine CCL2 was shown to recruit inflammatory $CCR2^{+}Li6C^{+}$ monocytes (also termed “classical” monocytes) from the bone marrow to enter the bloodstream[94]. Even if recruiting-cascades of neutrophils and monocytes are very similar, the difference is buried in the endothelium. Monocytes use different adhesion molecules to penetrate into tissues and expression of e.g. vascular cell adhesion molecule 1 (VCAM1 or CD106) is induced by IL-6 *trans*-signaling. Signaling via IL6 needs a membrane heterodimer composed of IL-6Rα and gp130. Expression of IL-6Rα is mainly restricted to cells of the immune system, whereas gp130 is widely expressed. Activated neutrophils secrete not only IL-6 but a soluble form of the receptor as well. These two molecules associate in the extracellular space to IL6-sIL-6Rα complexes. Shedding off the receptor enables IL-6 therefore to potentiate its target cell types, and is able to affect endothelial cells to induce adhesion molecules in this particular case[82,95].

When entering tissues, the general view is that inflammatory monocytes rapidly differentiate into M1 macrophages and/or TNF and iNOS-producing DCs (TipDCs). This step of the cascade is thought to substantiate the macrophage pool for further defense and/or initiating anti-inflammatory mechanisms. The role of TipDCs is not well understood, but studies with *Leishmania major* infections suggest that they enter the lymph-nodes via the blood vessels and are suggested to act as APCs to activate adaptive immunity[73,96,97].

2.4.4 Viva la Resolución: Macrophages Resolve the Reaction

When pathogens are cleared, the immune-stimulatory signaling via PRRs is diminishing and this enables the system to set some breaks. Professional phagocytes at the site of inflammation cooperate via many different mechanisms to generate a rather anti-inflammatory milieu to initiate the resolution of inflammation[76]. A process termed as lipid-mediator class switching gradually generates different anti-inflammatory mediators like lipoxins and resolvins. Lipoxin A4 arrests and inhibits further recruitment of neutrophils, only allowing infiltration of newly recruited monocytes[98,99].

Annexin A1 is another molecule widely exhibiting anti-inflammatory pro-resolving effects. After release by apoptotic (or NETotic) neutrophils and various other stimuli, it downregulates neutrophil recruitment, is an pro-apoptotic signal for neutrophils and enhances their uptake by macrophages[100,101]. Macrophages internalize dead neutrophils, NET-trapped and opsonized pathogens and dead cells. Phagocytosis of apoptotic cells triggers macrophages to produce the widely anti-inflammatory cytokines IL-10 and TGF-β and others, like vascular endothelial growth factor (VEGF), which are considered to resolve the response, restore homeostasis and initiate tissue repair[102,103]. More anti-inflammatory and pro-resolving effects are illustrated in **Fig. 7**.

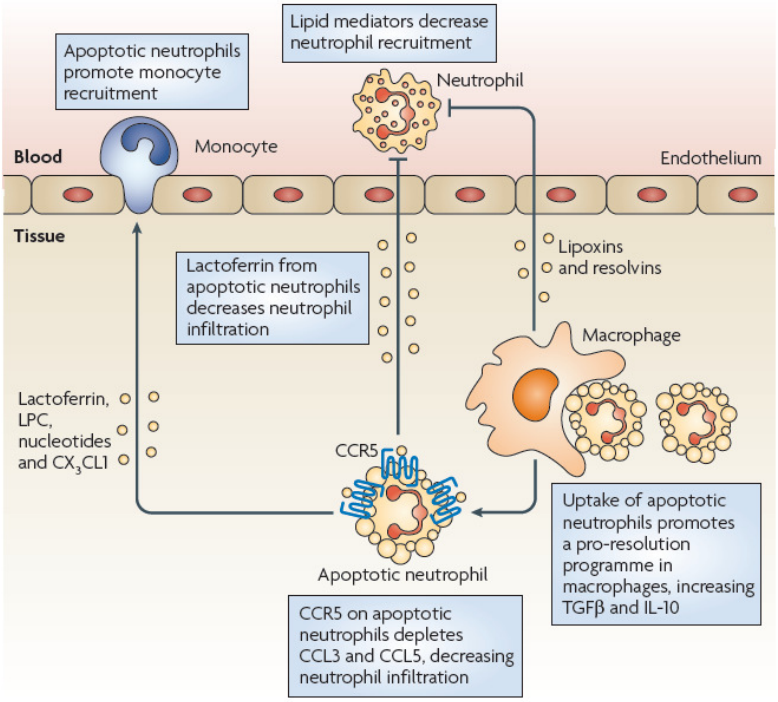

Figure 7 | Concerted action of phagocytes leads to resolution of inflammation. Depicted are the mechanisms inhibiting further neutrophil recruitment and setting up an anti-inflammatory milieu (TGF-β and IL-10), to stop the inflammatory cascade. From: Soehnlein et al, 2010[79]

All the above described mechanisms (and more) were wonderfully reviewed by O. Soehnlein and L. Lindbom in 2010 (Nature Reviews Immunology). They divided this cascade into four distinct phases, which are illustrated in **Fig. 8** at a glance[79].

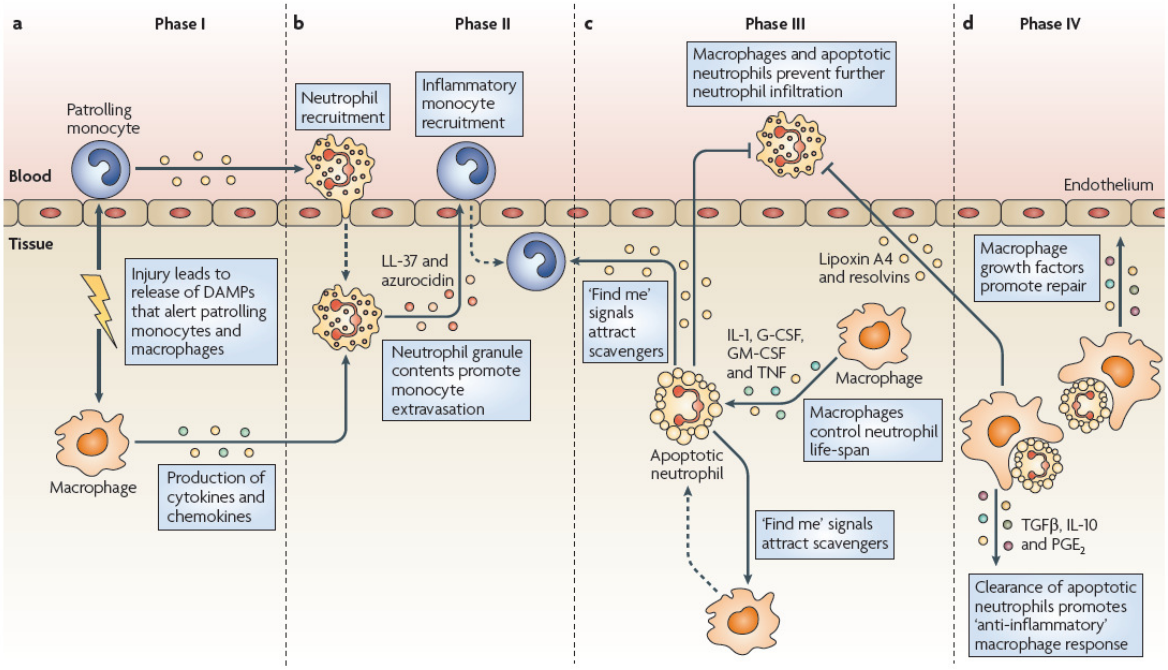

Figure 8 | Phases from initiation to resolution of inflammation. After recognition of pathogens and sensing of danger signals, macrophages recruit neutrophils followed by monocytes. Phase III already turns the system towards resolving mechanisms but it is still in an alerted state. Inflammation is finally resolved mainly by macrophages in phase IV. From: Soehnlein & Lindborn, 2010[79]

2.4.5 Model: Infections with *Streptococcus pyogenes*

Streptococcus pyogenes are gram-positive, non-motile cocci and often part of the human flora by colonizing the skin and/or throat. Although remaining sensitive to penicillin, there is a resurgence of invasive, virulent strains since 1980s. Historically, streptococcal strains are categorized based on the *emm*-gene (coding for the M protein) and to date more than 150 different serotypes were defined, whereas their evolutionary origins can be traced back to 4 different subtypes of the *emm*-gene, arranged in five patterns (A to E)[104]. Infections can cause a variety of different diseases, like pharyngitis, impetigo, scarlet fever, to severe, life-threatening pathologies as Streptococcal Toxic Shock Syndrome (STSS), necrotizing fasciitis or Septicemia with relatively high mortality rates. Furthermore autoimmune pathologies can occur post-infection, like myocarditis or rheumatic fever. Strains M1 and M3 are often but not exclusively associated with severe infections, but

were also isolated from mild-infections indicating that outcome depends on host factors[105]. One hypervirulent strain spread globally during the last 30 years, termed M1T1 and it is not well understood what exactly renders this strain to be so invasive[106].

Streptococci possess an arsenal of mechanisms to evade the immune system and to initiate inflammation, only a few should be mentioned. The very famous M protein has many different functions. Adhesion and colonization are partially mediated via the M proteins, as it was shown to bind to glycosaminoglycans enhancing attachment to epithelial cells[107]. Recognition by the scavenger receptor A (SR-A) of macrophages is inhibited by M proteins and the capsule, and this impairs internalization and bacterial clearance[108]. Interactions with fibrinogen are suspected to inhibit opsonization by complement factors and furthermore M protein and fibrinogen build up three-dimensional supramolecular networks activating neutrophils[109]. Structural analysis of the M protein uncovered similarities to myosin and tropomyosin, and this mimicry suggests that antibodies generated against the M protein are probably causing the autoimmune diseases myocarditis and rheumatic fever post-infectional[110].

Other important virulence factors are the NETs-degrading DNase Sda1, the hyaluronic acid capsule which is implicated in preventing opsonization, different secreted proteases cleaving and inactivating human chemokines and cytokines. Streptolysin O is mediating escape out of phago-lyososomes and is suspected to be one key factor leading to internal survival of *S. pyogenes* in host cells[88,104,111]. A general illustration of the different virulence factors and their effects can be found in **Fig. 9**.

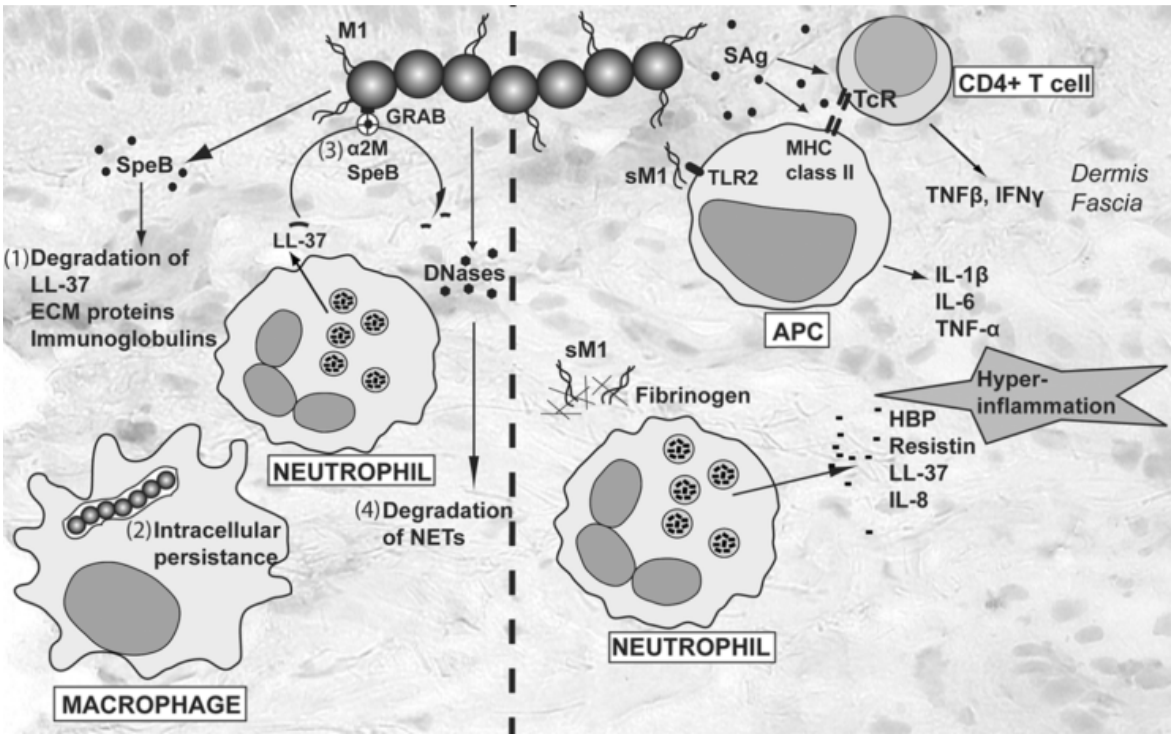

Figure 9 | Mechanisms employed by streptococci and affected cell types. The protease SpeB cleaves not only host immune factors but streptococcal virulence factors. This is partially avoided when caught in a membranous structure termed as GRAB. Within this complex its activity is sterically restricted to small peptides, like the anti-microbial LL-37. Streptococcal Superantigen A, a soluble form of M protein and host Fibrinogen lead to the hyperinflammation. From: Johansson et al, 2010[104]

A study published 2002 linked invasiveness and poor prognosis of streptococcal infections to elevated cytokine levels in the host due to genetic factors[112]. Another study suggested that the inflammatory reaction initiated in concerted action by APCs to recruit neutrophils, puts selective pressure on the bacteria enhancing virulence and invasiveness[113].

2.5 The Gastrointestinal Tract

The gastrointestinal tract provides a mucosal surface of approximately 300 m² in humans and can be considered to be a semi-opening of the organism to the exterior. Following the stomach, the gut consists of the small and the large intestine, interrupted by the ceacum. Most digestive mechanisms take place in the small intestine, which is further subdivided into the duodenum, jejunum and ileum. Considering the fact that the mucosal epithelium is constantly exposed to a plethora of antigens, comprising food and commensal derived ones, it is not surprising that the gut is a system of astonishing complexity[114,115].

2.5.1 Homeostasis: Different Layers of Protection

The intestine contains the highest amount of immune cells all over the body, tightly regulated and coordinated avoiding chronic inflammatory reactions to all the foreign antigens on one hand but initiating effective responses to invading pathogens on the other one.

Many different mechanisms and cell types correspond to this complex system, to ensure two conditions important in homeostasis: Firstly, commensals are physically divided from host cells, and secondly, the intestinal immune system is generally tolerogenic.

The epithelium from the stomach to the rectum is constantly secreting mucus, thereby building up a protective layer over the whole surface. The mucus in the intestine is generally produced by Goblet cells of the epithelia and is composed of MUC2, but its organization differs from small intestine to colon. In the small intestine the mucus is rather variable in height and density, whereas the mucosal structure in the colon is well defined. The colonic mucosa consists of two layers: The inner layer is relatively firm and almost sterile and is converted to the relatively loose outer layer. Both layers consist mainly of the MUC2 protein with the same brush bristle like appearance through massive post-translational modification by attaching O-glycans. The mechanisms transforming the firm to the loose layers at a very well defined sharp border are not well understood. Extending protein structure and loosening the net-forming force of MUC2 by proteolytic cleavages and reduction of disulfide-bonds most probably play a role. Commensals cannot penetrate the inner layer in general and live in the loose outer layer, where MUC2 is providing food for commensals and by digesting it, they limit the thickness of the outer layer[116].

The epithelium itself and its structure are implicated in both conditions (**Fig. 10**). Firstly, zinc, lysozyme and anti-micorbial peptide secreting Paneth cells deep in the crypts of Lieberkühn create an antiseptic gradient to protect neighboring stem cells. This production can be adapted according to sensing bacterial density via PRRs. By expressing a certain set of PRRs, intestinal epithelial cells (iECs) can act as immune sentinels. Importantly, the expressed TLR-subset is restricted in healthy individuals and it seems

that iECs generally express rather cytosolic sensors in order to be sensitive to intracellular but rather tolerogenic to extracellular bacteria[117,118]. One group of cytosolic sensors turned out to have a key function in intestinal homeostasis, namely the NLR-proteins. NOD1 and NOD2 by activating NF-κB, and other NLRs by initiating the assembly of supramolecular inflammasomes, leading to IL-1β and IL-18 secretion[119-121]. Besides these two, iECs produce a wide variety of immunomodulatory molecules and participate in shaping immune responses in the intestine[122].

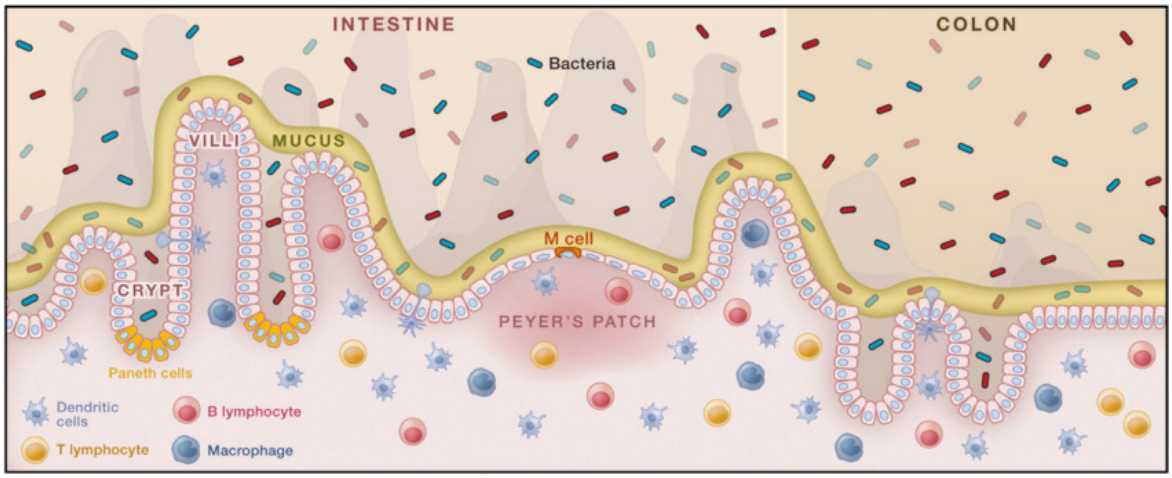

Figure 10 | Simple illustration of the anatomy of the gut. Along the whole gut are structures to enlarge the epithelial absorptive surface. Villi stretching into the lumen can only be found in the small intestine and crypts are found throughout the gut. Peyer's patches are organized tissues for antigen-sampling (by specialized epithelial cells, the M cells) and a major site of immunological mechanisms in the small intestine. Other organized immunological relevant tissues are lymphoid follicles and colonic patches. From: W. S. Garrett et al, 2010[123]

The microbiome itself is participating in shaping homeostatic conditions. Commensals of the human outnumber host cells by a factor of approximately 100, reaching an immense density of 10^{10} to 10^{12} organisms per gram luminal content in the descending colon[124]. This community is in general dominated by Firmicutes and Bacteroidetes, and recent sequencing studies revealed that the whole metagenome consists of compelling ~3.3 million different genes, outnumbering human genes by a factor of approximately 150[125]. The microbiome is passively defending against invading pathogens by occupying every niche in the intestine, not leaving "space" for pathogens. Furthermore commensals actively shape the immunogenic state of the intestine via soluble mediators or direct contact with iECs in some special cases[126,127]. These modulatory mechanisms by symbiotic microorganisms and their importance just started to be elucidated as emphasized by two recently published studies showing that regulatory $Foxp3^+$ T cells are induced in the colon,

and that TLR4 expression of iECs is reduced via histone modifications – both effects depending on the colonic microbiome[128,129].

Other components of this complex system are all the different known immune cells contributing to homeostasis and inflammation in the gut. Even if once considered to be potentially colitogenic, innate immune signaling of commensal organisms in the gut and a certain level of physiological inflammation is of great importance to homeostasis[130]. Macrophages have key roles in downregulating and suppressing immune responses by secretion of mainly IL-10 induced by stromal signals[131]. Different subsets of phagocytic monocytes (like DCs) can shape T cell responses and instruct them to be tolerogenic or inflammatory, mainly via activation of TGF-β[132,133]. Examples how homeostasis is maintained via innate immune signaling are given in **Fig. 11**.

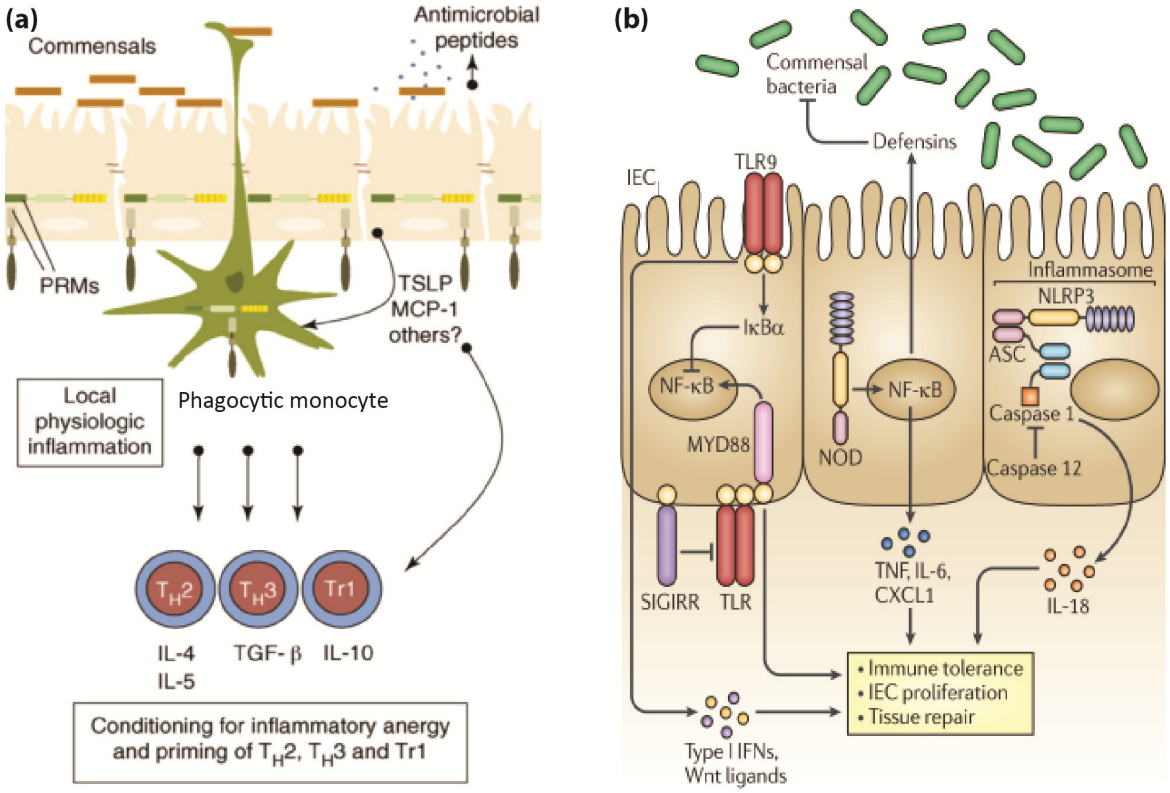

Figure 11 | Innate immune signaling of commensal bacteria. (a) Illustrates that phagocytic monocytes (like macrophages or dendritic cells) in concerted action with epithelial cells provide signals to instruct adaptive immunity to be anergic. Adapted from: JH Fritz et al, 2008[122] **(b)** Sensing of commensals by iECs via innate mechanisms and consequences. From: M. Saleh & G. Trinchieri, 2011[130]

2.5.2 Ulcerative Colitis

Ulcerative colitis is one of the two major forms of inflammatory bowel diseases (IBD), differing from the other form, Morbus Crohn or Crohn's disease, in respect to site and nature of the pathology. IBD is one of the rising diseases, with increasing patient numbers in developed countries. Both forms of IBD appear to result from misbalanced immune responses to the microbiome. Ulcerative colitis usually affects the colon, with a pathology starting at the rectum and progressing into the proximal parts of the colon[134].

Although more than 100 different gene loci are associated with IBD, one usually cannot predict the disease or its pathology. One bioinformatical study in 2011 showed impressively, how these so-called "risk-genes" physically interact and created a huge network of different genes with important knots. Exactly this net-like structure enforces the hypothesis, that different genetic risk-variants may be compensated by the system using another way in this network[135].

To date the whole pathology of IBD and all the different variants cannot be explained by host factors alone and therefore the host-microbiome-dialog is heavily investigated. A huge meta-genomic study of 2010 not only identified the 3.3 million commensal genes, but could show that IBD patients differ in their microbiome-composition. Furthermore these compositions clustered for Crohn's disease and ulcerative colitis[125]. Remarkably, this study is not solving the question whether dysbiosis is cause or consequence of IBD.

Literally every aspect of homeostatic conditions in the intestine is somehow implicated in colitis. Mice lacking TGF-β activation by DCs develop colitis, because they fail to induce a tolerogenic T cell response to commensals[136]. The T_H subset composition is very important and labile, as some imbalancing can lead to immunopathology[122]. Innate immune mechanisms like inflammasome activation or NOD2-signaling are very important and when disturbed or disrupted, this leads in general to colitogenic mice heavily impaired in tissue repair[137]. Remarkably, such imbalance is very often caused by impaired sensing of microbes with innate immune mechanisms[138].

2.5.3 Colitis-Associated Cancer (CAC)

Neoplastic lesions are almost always accompanied by infiltrating immune cells. Exactly this wide variety of tumor-associated immune cells is nowadays known to have opposing effects. Although the immune system exhibits anti-cancer strategies like cytotoxic T cells (CTLs) or natural killer (NK) cells, other pro-inflammatory mechanisms support carcinogenesis in many ways. The immunological microenvironment of incipient neoplasias is considered to support tumor formation mainly, but not only, through innate immune cells. Though activating anti-tumor mechanisms, inflammation mediated by M1 macrophages or neutrophils promotes acquirement of certain hallmarks of cancer. Just to name a few, pro-inflammatory signals boost proliferation and growth in surrounding tissues, reactive oxygen species induce additional mutations, metalloperoxidases (e.g. MMP9) from neutrophils change the surrounding tissue alleviating metastasis, and secreted VEGF enhances angiogenesis[73,139,140].

In patients suffering from ulcerative colitis the risk factor to develop colorectal-cancer rises to 18 % after 30 years[141] and this form of cancer is generally termed as colitis-associated cancer (CAC). Interestingly, mutations or failure in innate immune mechanisms to sense the microbiome are paradoxically often reported to have a colitogenic, pro-inflammatory phenotype accompanied by enhanced CAC development, most probably due to impaired wound healing mechanisms[137,142].

A murine model for CAC is achieved by administering the cancerogen azoxymethane (AOM), which shows strong organotropism for the colon. Mode of action is mostly linked to O^6-methyl-guanine modifications leading to G-to-A transitions during replication. Mutations in several important signaling pathways, like Wnt-β-catenin, TGF-β or p53 are initiating tumor formation. Tumorigenesis is advanced by chronic colitis, as induced by repeated treatment of the animals with dextran sulfate sodium (DSS)[143].

3 PROJECT AIMS

3.1 How does Modulation of Immunity by TTP-Dependent mRNA-Decay Affect Infectious Disease Caused by *Streptococcus pyogenes*?

Streptococcal strains EC700 and ISS3348 are both M1-serotype strains, but differ in their pathogenicity in a subcutaneous infection model of wildtype C57BL/6N mice. Mice are more prone to die upon infection with ISS3348 whereas animals survive infections with EC700 with comparable MOI. Remarkably, EC700 induces more cytokine expression in BMDMs infected *in vitro* (data not shown). Mice conditionally ablating TTP ($TTP^{fl/fl}$ LysMcre, from now on ΔM mice) in the myeloid lineage (macrophages, neutrophils and potentially dendritic cells)[144] are more susceptible to LPS-induced endotoxin shock, because of elevated serum levels of pro-inflammatory cytokines (Kratochvill et al, 2011; Manuskript submitted). As described in the introduction, many cytokines of the innate inflammatory reaction to pathogens are targeted by TTP on the mRNA level and therefore we hypothesized that ΔM mice elicit a stronger immune reaction upon ISS3348 infection and that this enhancement implies advantages resembling the phenotype of EC700 infections of wildtype mice. This would be contradictory to the mentioned study, which linked streptococcal virulence with higher serum cytokine levels resulting from differences in HLA loci[112]. Notably, the study didn't provide any molecular link and therefore the question remains if these elevated levels are just caused by dissemination.

3.2 Can TTP-Controlled Intestinal Homeostasis Influence the Development of Inflammation and/or Tumors in the Colon?

Franz Kratochvill could show that mice ablating TTP in T-cells ($TTP^{fl/fl}$ LckCre mice, from now called ΔT mice) or ΔM mice are coping better with DSS-induced colitis compared to WT littermates. For the latter he gained evidence that DSS-treated ΔM mice display lower histological scores of Swiss rolls and expressed more IL-18 in the colon, which is implicated in wound healing and proliferation of intestinal epithelia (data not shown)[120,121]. As ulcerative colitis patients are prone to developed so-called colitis-associated cancer (CAC)[141] and abnormalities in TTP expression are correlated with various forms of cancer[145], the second project addressed the question whether these initial phenotypes of ΔT and ΔM mice translate into differences in AOM-DSS-induced CAC.

4 RESULTS

4.1 TTP in Acute Inflammation: *Streptococcus pyogenes*

Bone-marrow derived macrophages (BMDMs) of ΔM mice and $TTP^{fl/fl}$ (referred from now on as WT mice) were infected with both streptococcal strains and TTP expression was monitored with Western blotting. Both strains induced comparable TTP expression, even if the MOI differed approximately 10-fold. This experiment confirmed furthermore the ablation of TTP in ΔM BMDMs (**Fig. 12a**). As higher pathogenicity of *S. pyogenes* strains is linked to impaired immune recognition by macrophages[108], Colony Forming Unit (CFU) assays were performed to monitor internalization of bacteria. Results show that EC700 forms approximately 100-fold more units 1 hour post-infection of WT BMDMs substantiating the hypothesis that EC700 induces stronger innate immune reactions than ISS3348 (**Fig. 12b**).

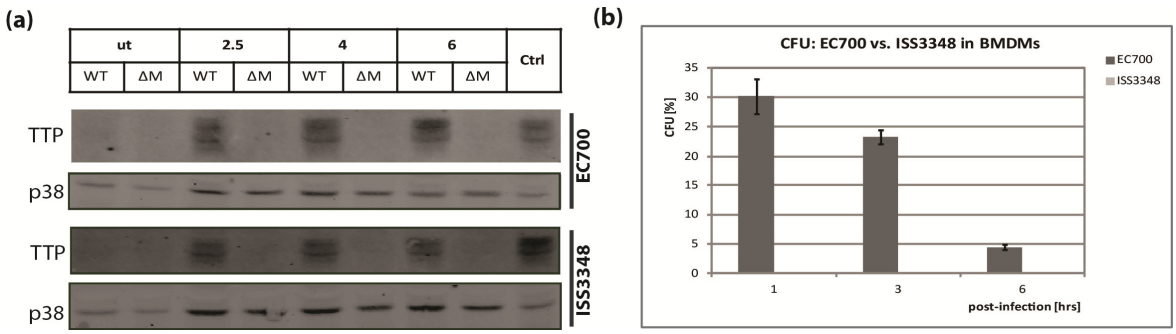

Figure 12 | Comparison of streptococcal M1-strains. (a) BMDMs differentiated from WT and ΔM mice were infected with EC700 and ISS3348 (MOI 10 and 100, respectively) for 30' before changing medium to DMEM supplemented with 60 ng/ml Penicillin or stimulated with *E. coli* LPS (1 ng/ml) for 3 hrs as control. Whole cell extracts were prepared at indicated time points post-infection and were analyzed by Western blotting with a serum antibody against TTP. After stripping of the membrane, reprobing with an antibody against p38 MAPK served as loading control. **(b)** BMDMs were infected with EC700 and ISS3348 for 45' and CFU assays were performed at indicated time points. As inocula between strains differed approximately 10-fold, CFUs are normalized to inoculum per strain (= 100%). Error bars show SD (n = 3).

As WT BMDMs produce more pro-inflammatory cytokines (e.g. TNF-α, IL-6) after infection with EC700 (data not shown) and survive subcutaneous infections, we employed the ΔM mice as an *in vivo* model to test whether these mice cope better with an ISS3348 infection. Bacterial suspension was injected subcutaneously into lower legs of anesthetized mice and their health-status was monitored for the next five days. Mice were euthanized when they reached one of the defined humane endpoints (see Material

and Methods) or on the fifth day post-infection. ΔM mice showed significantly higher survival rates (**Fig. 13a**). Random tissue samples of the lesion were taken and prepared for immunohistochemistry. Comparison of early dying with surviving mice showed a trend that more infiltrating immune cells were present at the site of infection of surviving mice (**Fig. 2b and 2c**). Detailed statistical analysis and histological scoring for differences of surviving vs. dying and WT vs. ΔM mice has to be performed in the future, for now the differences in infiltrating cells, acanthosis and tissue destruction were just observations.

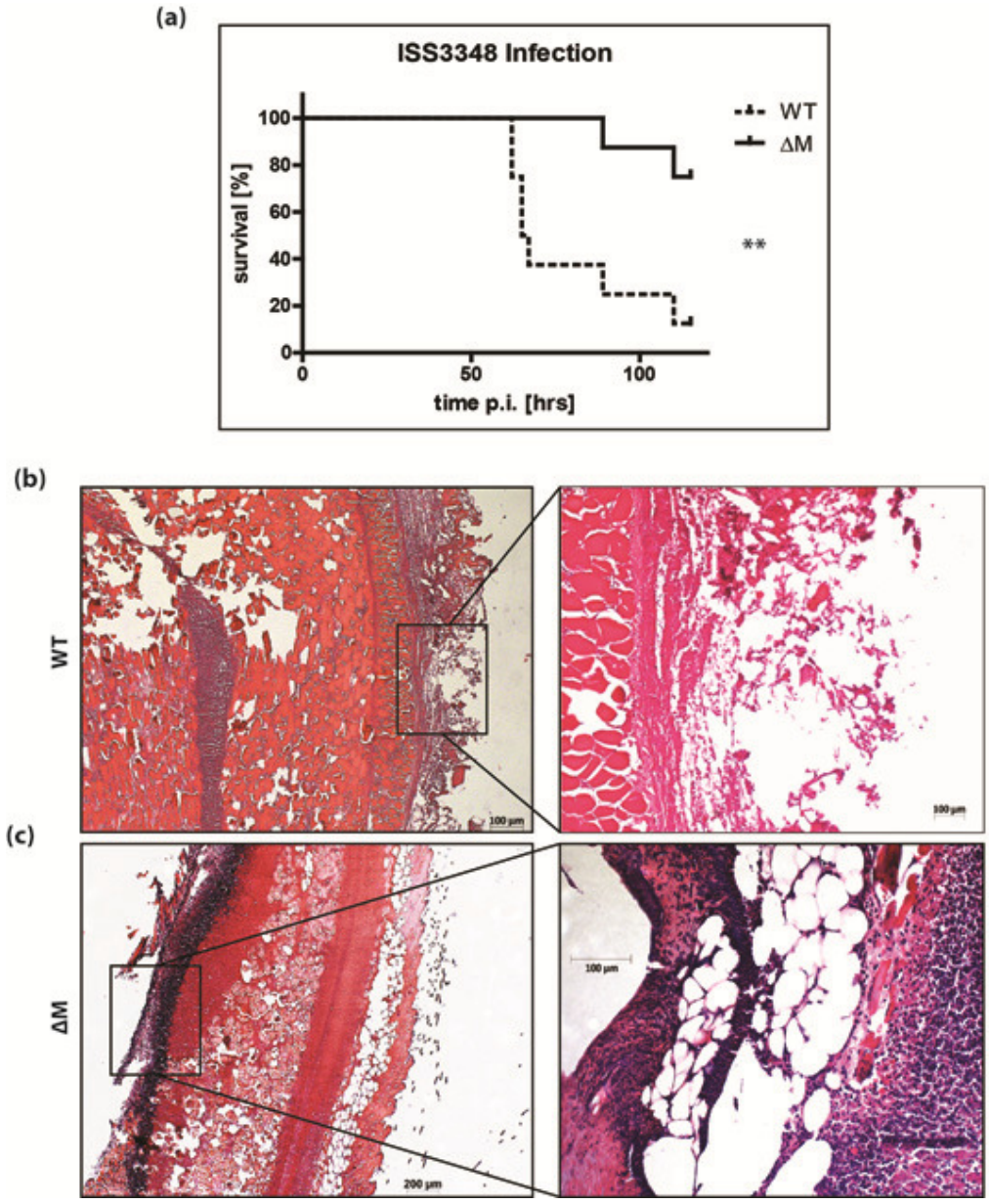

Figure 13 | ΔM mice show enhanced survival upon subcutaneous ISS3348 infection. (a) Mice were infected with MOI $1x10^8$ per mouse and depicted is a Kaplan-Meier blot showing survival (%) over 5 days of monitoring. Shown is one blot out of three independent experiments. Statistical significance was calculated using Log-rank (Mantel-Cox) test: ** = P < 0.001, n = 8 per genotype; **(b)** H&E staining of a lower leg sample derived from a WT mouse dying 65 hrs post-infection

and **(c)** a surviving ΔM mouse. Infected tissue was cut longitudinally through the lesion and paraffin slices (3 nm) were prepared. Magnification is 25-fold for the left and 100-fold for the right panel. Note the striking amount of immune infiltrates in **(c)** compared to **(b)**.

As it's known that macrophages and dendritic cells are important cell types for immunity against streptococcal species, *in vitro* infection of these cells with ISS3348 was further investigated[104]. CFU assays (**Fig. 12b**) are not the method of choice to assess phagocytosis of BMDMs, because bacteria which are just adherent to cells but not internalized are potentially not killed and could bias the result. To get rid of this potential "noise" Stefanie Sigel infected BMDMs differentiated from WT and ΔM mice with fluorescent labeled bacteria and performed phagocytosis assays. Consistently, internalization of EC700 was approximately 100-fold higher compared to ISS3348 (**Fig. 14a**). Interestingly, ΔM BMDMs showed higher phagocytosis indexes not only for EC700 and ISS3348, but as well for *Streptococcus pneumoniae*, the gram-negative *Escherichia coli* but not for synthetic latex beads (**Fig. 14b and data not shown**).

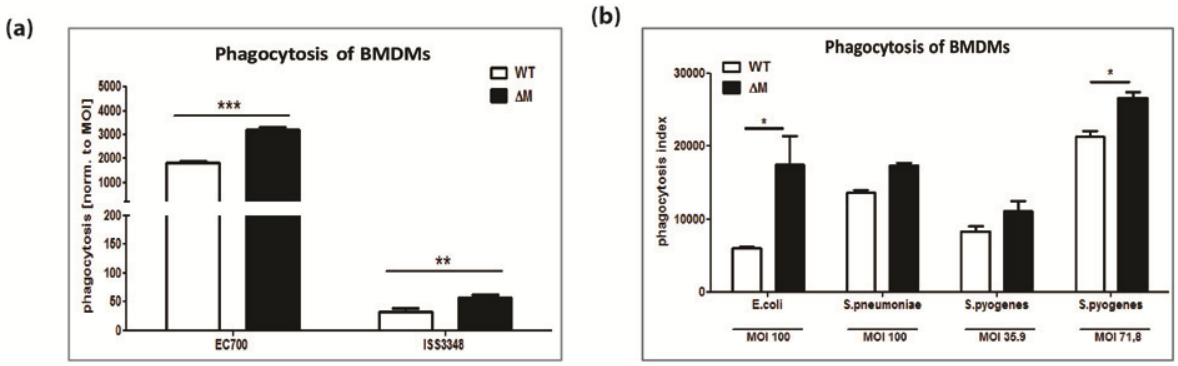

Figure 14 | BMDMs derived from ΔM animals show enhanced phagocytic efficiency. (a) WT and ΔM BMDMs were infected with BacLight-green (molecular probes) labelled EC700 or ISS3348. Internalization of bacteria is expressed as phagocytosis index determined by flow cytometry as mean fluorescence within the gate for living cells multiplied with the cell number and further normalized to inocula. Values represent mean (n = 8) and indicated error bars are SD. Significance between the two genotypes was calculated using Mann Whitney test. Significance: ***, $P < 0.001$ (EC700) and **, $P < 0.01$ (ISS3348). **(b)** Differences in efficiency of phagocytosis of WT and ΔM BMDMs for internalization of *Escherichia coli*, *Streptococcus pneumonia* and *Streptococcus pyogenes* (ISS3348). In essence, the experimental setup was the same as in **(a)** but phagocytosis index was not normalized to the inocula (MOIs are indicated below the graph and n=4). Significance: * = $P < 0.05$.

As enhanced phagocytosis upon stimulation with bacteria could be the result of higher activated cells, BMDMs and conventional dendritic cells (cDCs) were infected with ISS3348 and TTP expression and p38 mitogen-activated protein kinase (MAPK) activation

were monitored by Western blotting. Phosphorylation (i.e. activation) of p38 MAPK clearly increased with time post-infection in WT and ΔM BMDMs and cDCs and correlated with expression of TTP (**Fig. 15a and 15b**). Ablation of TTP in *in vitro* differentiated cDCs derived from ΔM mice could be shown on the protein level, which is in line with published data, that the LysMcre system affects about 16% of dendritic cells *in vivo*[144]. The decrease in expression of total p38 MAPK in cDCs originates from dying of mature dendritic cells upon overstimulation with activating ligands[146]. Notably, TTP expression in cDCs could be visualized only upon long exposure time with the ODYSSEY Imaging System, which points to generally lower protein levels compared to BMDMs (**Fig. 15b**). Although WT and ΔM BMDMs and cDCs showed differences in p38 phosphorylation, these results were inconsistent between experiments (**Fig. 15a and 15b**). As phagocytosis assays showed internalized bacteria already 1 hr post-infection (**Fig. 14a**), activation of p38 should be analyzed at earlier time points in the future.

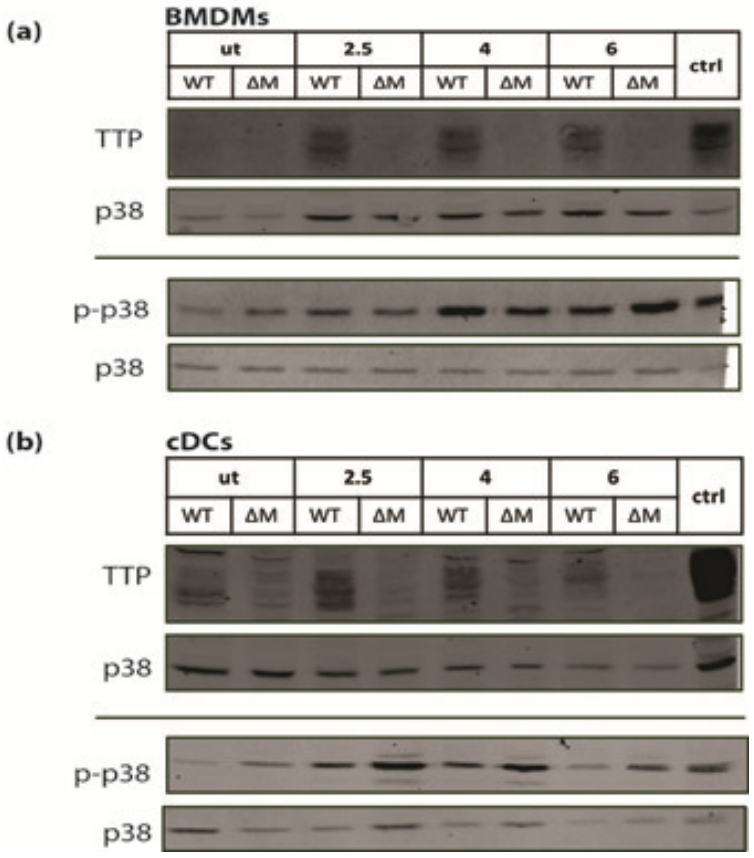

Figure 15 | Difference of p38 MAPK activation upon ISS3348 infection of ΔM compared to WT cells. (a) BMDMs were stimulated with ISS3348 (MOI 100) for 30', medium was replaced by DMEM (+ 60 ng/ml Penicillin) and whole cell extracts were prepared. **(b)** cDCs were stimulated the same way as described for **(a)**, but after 30' 60 ng/ml Penicillin was added to the medium and whole cell extracts were prepared after indicated times post-infection. For **(a)** and **(b)** cells were stimulated for 3 hrs with *E. coli* LPS (1 ng/ml) as positive control. p38 MAPK activation was analyzed by

Western blotting using an antibody against phosphorylated p38 (p-p38). TTP expression was determined using a serum antibody against TTP. Membranes were reproped with an antibody against unphosphorylated p38 MAPK (p38) as loading control.

Downstream effects of p38 MAPK activation is the expression of different target genes (e.g. TNF-α, IL-6, IL-1α, different chemokines and TTP itself) and as many of these mRNAs are known TTP targets (Kratochvill et al, Mol Syst Biol, *in press*), BMDMs and cDCs were infected with ISS3348 and total mRNA or supernatant were collected. Expression levels were assessed with qRT-PCR on the mRNA level and with enzyme-linked immunosorbent assay (ELISA) on the protein level. ΔM BMDMs and cDCs showed reproducibly higher mRNA levels for TNF-α already 2.5 hours post-infection (**Fig. 16a**). These differences translated to the protein level, as ELISA measurements of TNF-α were consistently higher in supernatants of stimulated ΔM cells (**Fig. 16b**). Additionally higher levels in supernatants of ΔM BMDMs of TNF-α, IL-6 and MCP-1 were measured using Flowcytomix™ Multiplex Technology (eBioscience) (**data not shown**).

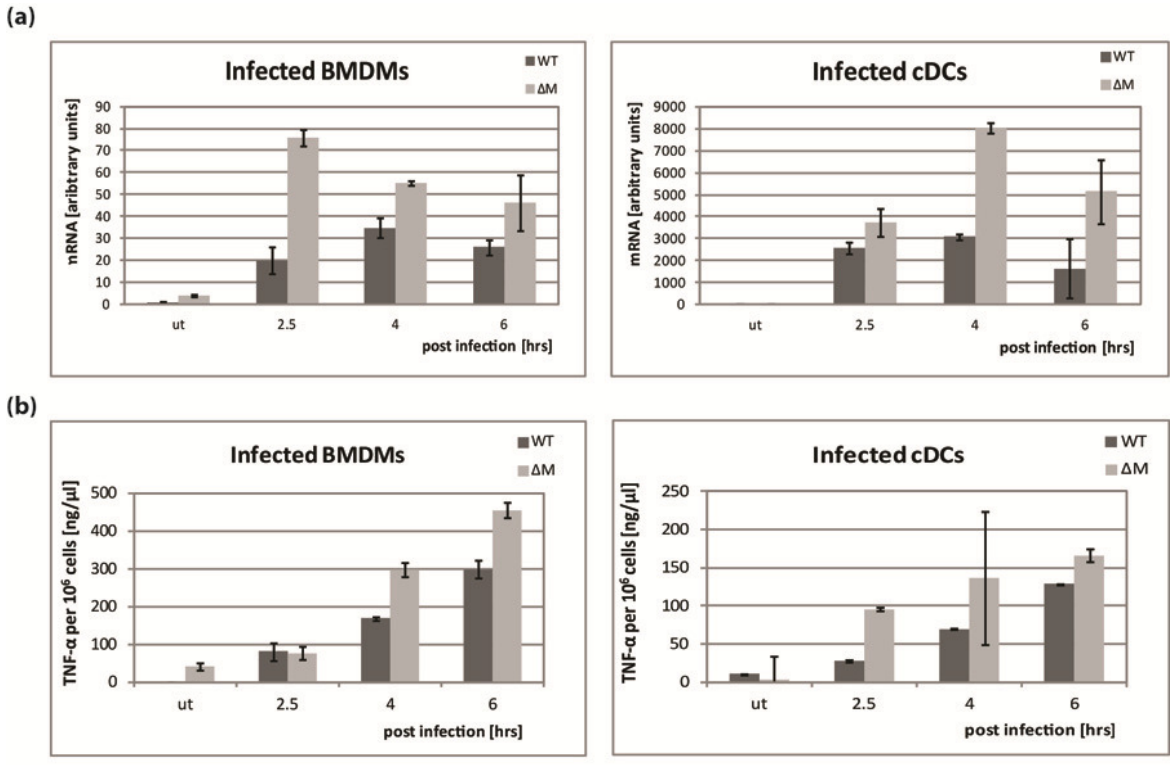

Figure 16 | BMDMs and cDCs lacking TTP secrete more TNF-α upon ISS3348 infection. Cells differentiated from bone marrow of WT or ΔM mice were infected with ISS3348 (MOI 100). After 30' medium was exchanged with DMEM + 60 ng/ml Penicillin or 60 ng/ml Penicillin was added (in case of cDCs). mRNA and supernatant were prepared at indicated time points post infection. **(a)** mRNA expression levels were determined by qRT-PCR using primers for *Tnfa*. Shown are relative expression levels normalized to a housekeeping gene (*Hprt*). **(b)** Secretion of TNF-α was quantified

by ELISA. Protein levels were normalized to $1x10^6$ cells for comparability between experiments. Shown is one representative out of three independent experiments for mRNA and protein level analysis.

As the first WT mice died approximately 55 hours post-infection (**Fig. 13a**), mice were infected subcutaneously with ISS3348 and euthanized earlier for the following experiments. Area of inflammation was measured 48 hrs post-infection and ΔM mice displayed bigger lesions in general (**Fig. 17a and 17b**). This result is consistent with enhanced survival of ΔM mice (**Fig. 13a**) and the observation of more infiltrating immune cells in surviving mice (**Fig. 13b**) upon ISS3348 infection.

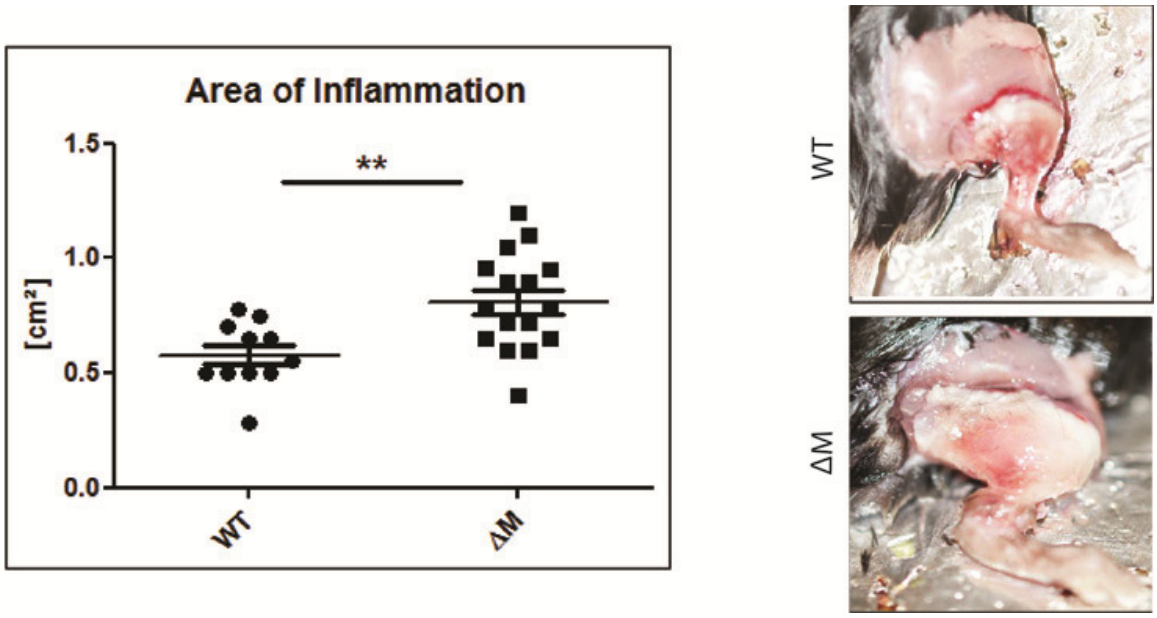

Figure 17 | ΔM mice display signs of enhanced innate responses upon subcutaneous ISS3348 infection. ΔM and WT littermates were infected subcutaneously into lower legs with $1x10^8$ bacteria per mouse. They were euthanized 48 hrs post-infection and skin was removed to measure visible area of inflammation. The dot blot (left panel) shows areas of inflammation pooled from three different experiments and significance was determined using t test: **, $P < 0.01$. The photographs (right panel) show representative infected lower legs.

As differences in lesion size could be the result of earlier events, mice were infected and euthanized 24 and 48 hrs post-infection and infected tissue was prepared for immunohistochemistry. H&E stained samples were scored for amount of infiltrating immune cells and their localization, grade of tissue destruction, acanthosis, formation of thrombi, neutrophil-mediated abscess formation and blood vessel destruction (results in spreading of erythrocytes into tissue). Histological scoring resulted in higher scores for ΔM samples at both time points with significance at 48 hrs post-infection (**Fig. 18a**). As expected, Gr-1 staining showed that most infiltrating cells were neutrophils or monocytes

and we observed that they co-localized with streptococci. Another impression we got was that bacteria seemed to disseminate within WT whereas dissemination was impaired in ΔM samples, probably due to higher neutrophil and monocyte load (**Fig. 18b**). Importantly, histological scoring and analysis of co-localization of bacteria and immune infiltrates has to be reproduced by a pathologist in the future.

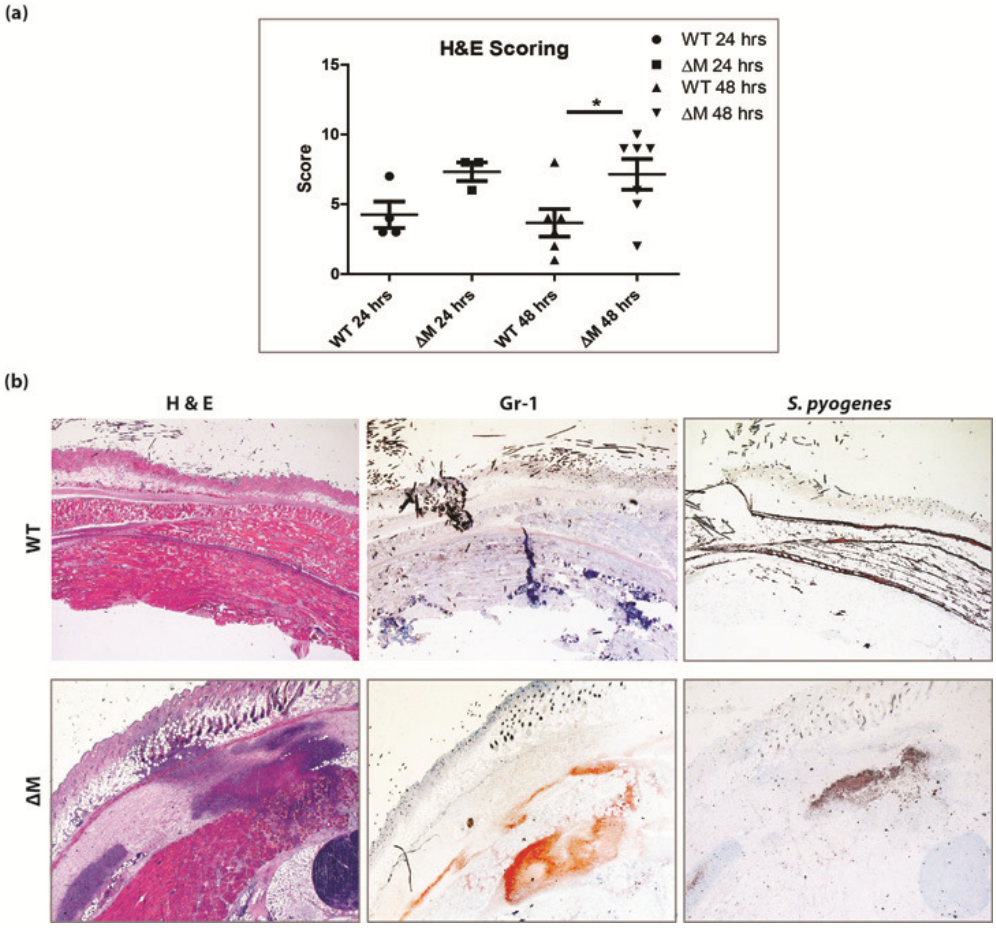

Figure 18 | Recruitment of inflammatory infiltrates to the site of infection. Lower legs of animals were infected subcutaneously (MOI 1x10^8 ISS3348 per mouse). After 24 and 48 hours animals were euthanized and infected tissue was prepared for immunohistochemistry. **(a)** Histological grading (criteria: Infiltrated area, depth of infiltration, acanthosis, swelling, vasodilation, tissue destruction, abscess formation) of WT and ΔM samples 24 and 48 hrs post-infection. Significance was determined with t test: *, $P < 0.05$ (48 hrs). **(b)** Immunohistochemical staining of two representative samples derived from mice euthanized 48 hrs post-infection. Shown are 3 nm sections of H&E staining, staining using an antibody against Gr-1 (Ly6C/Ly6G) and an antibody against *S. pyogenes* (from left to right). Magnification: 25x.

Tissue-resident macrophages serve as immune sentinels and are responsible for initiating an inflammatory innate immune response upon infection. One of the first hallmarks of such a reaction is the recruitment of circulating neutrophils via cytokines and chemokines, like e. g. TNF-α or IL-6[76]. As we could show that ΔM BMDMs and cDCs

produce more of these two cytokines most probably due to lacking TTP-mediated mRNA-destabilization *in vitro*, we infected mice subcutaneously and prepared protein extracts from the lesion 24 and 48 hrs post-infection. Cytokine and chemokine levels of these extracts were measured using Flowcytomix™ Multiplex Technology. Expression was measurable at both time points, but was increased 48 hrs post-infection. Notably, these measurements unraveled that levels of IL-1α, MCP-1/Ccl2, IL-6, MIP-1α/Ccl3, IL-1β and TNF-α were comparable between WT and ΔM samples at both time points. A trend to rather lower levels in ΔM samples was visible at 48 hrs post-infection but was not significant (**Fig. 19**).

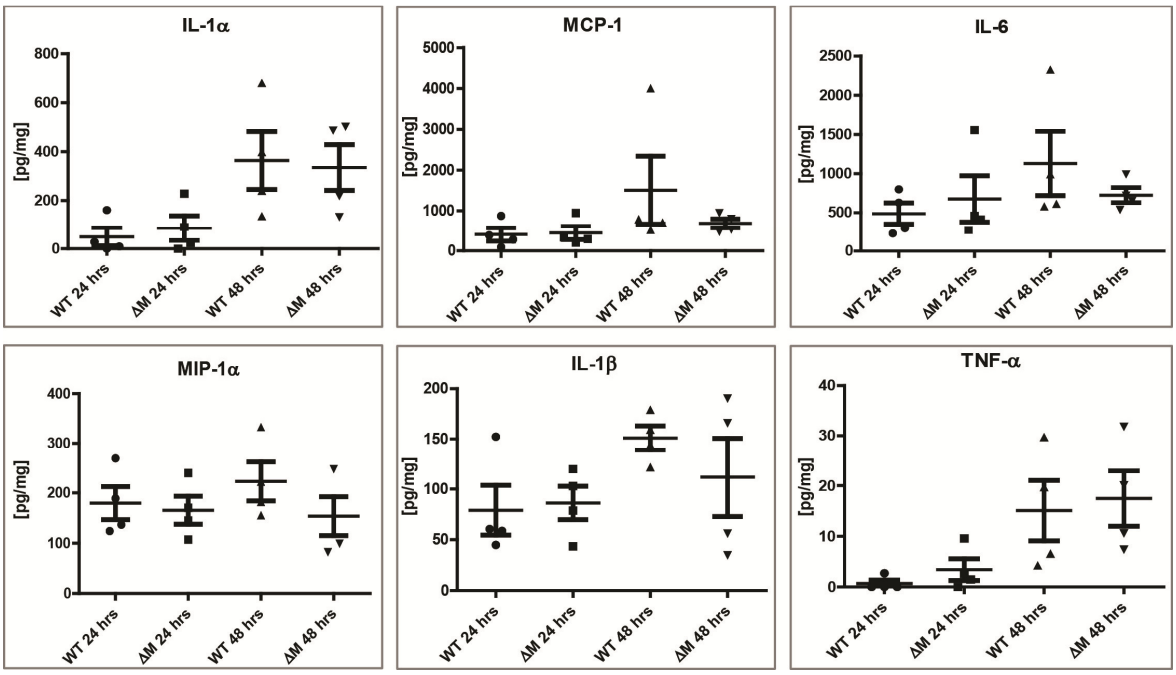

Figure 19 | Cytokine production at the lesion 24 and 48 hrs post-infection. Animals were infected subcutaneously with *S. pyogenes* strain ISS3348 (MOI 1x10^8 bacteria per mouse). Mice were euthanized 24 and 48 hrs post-infection, respectively, and infected tissue was homogenized. Protein levels were determined using Flowcytomix™ Multiplex Technology (eBioscience) and normalized to total protein content of the lysate. Shown are six representative dot blots out of twelve screened cytokines. Significance between WT and ΔM samples for both time points was determined using t test: ns in all cases. Error bars: Mean (SEM).

Besides measuring cytokine expression within the lesion, blood serum was prepared from the same mice and protein levels were determined. Only two out of ten screened cytokines were detectable at both time points. Levels for MCP-1/Ccl2 and IL-6 dropped drastically 48 hrs post-infection in blood sera of ΔM mice (**Fig. 20**). One could speculate of two reasons for this observation, either, bacteria are cleared in ΔM mice at this time

point and the innate immune reaction is resolving, or disseminated bacteria in WT mice are triggering the release of these cytokines.

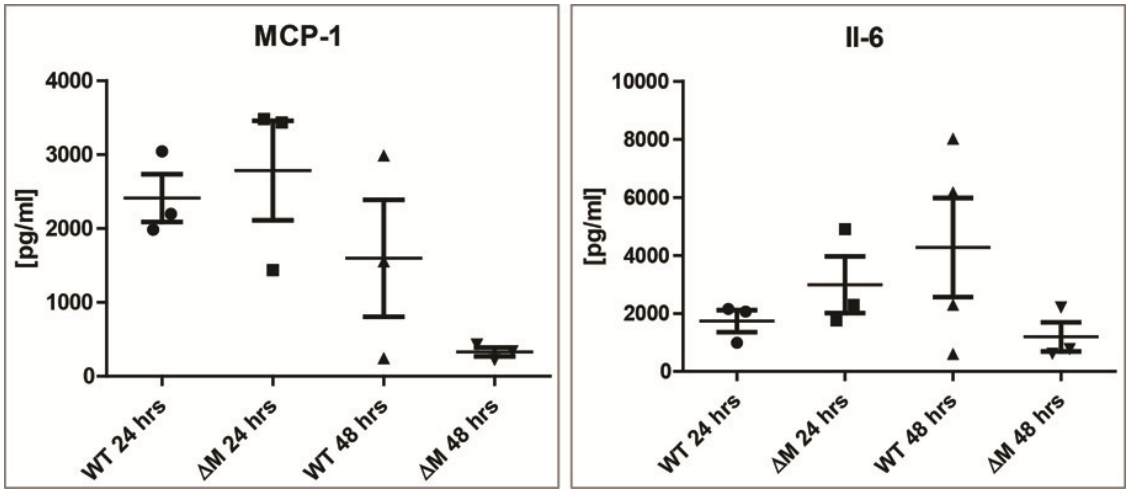

Figure 20 | Serum cytokines 24 and 48 hrs post-infection. Serum samples were obtained from the same animals as described for Fig. 8 before euthanization. Protein levels were determined using Flowcytomix™ Multiplex Technology (eBioscience). Significance between WT and ΔM samples for both time points was determined using t test: ns. Error bars: Mean (SEM).

Dissemination of virulent strains and following multi-organ failure (MOF) are correlated with lethal outcomes of streptococcal infections[105]. Though we already head the impression of impaired dissemination of ISS3348 in ΔM mice (**Fig. 18b**), *in vivo* CFU assays were employed to measure bacterial loads in different organs. ISS3348 was disseminating in these experiments almost exclusively in WT mice. Dissemination could be demonstrated for almost all WT blood samples, but for liver and spleen as well (**Fig. 21**). Remarkably, high CFU values within the blood correlated with high values in the liver and the spleen. This correlation suggests a sequential dissemination of ISS3348 from the lesion, via the blood stream into organs resulting in MOF most probably.

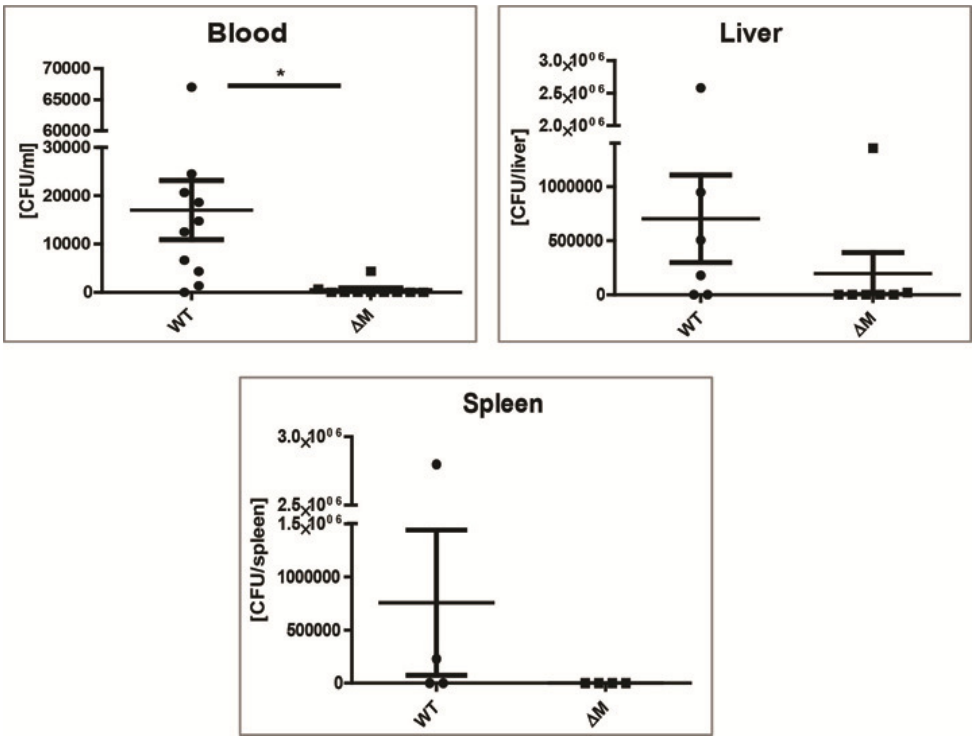

Figure 21 | Dissemination of ISS3348 in WT and ΔM mice. Mice were infected subcutaneously with $3x10^8$ bacteria per mouse and euthanized 48 hrs post-infection. Blood was extracted via heart-puncture, organs were taken and homogenized. To determine CFUs, dilution series of either the blood or the organ lysates were prepared, plated on blood agar plates and colonies were counted the following day. Colony-forming units are depicted per ml blood or normalized per organ. Results for blood and liver CFUs show a pool of two independent experiments. Significance was tested using t test: *, $P < 0.05$ (blood). Error bars: Mean (SEM).

So far, all *in vivo* experiments were performed with high MOIs (1 to 5 x 10^8 bacteria per lower leg). One could speculate that such bacterial loads and late time points are potentially hiding measurable cytokine differences of myeloid TTP-knockout mice in this subcutaneous infection model. To address this question and to screen more time points, MOI was reduced 10- and 100-fold and mice were euthanized 6 and 12 hrs post-infection. Lesions and blood sera were prepared for protein measurement as described. Neutrophil-attracting MIP-2/Cxcl2, KC/Cxcl1, TNF-α and IL-6 are all known to be secreted by tissue-resident macrophages[79]. Additionally, their mRNAs are known to be degraded in an TTP dependent way during inflammatory responses of BMDMs (Kratochvill et al, Mol Syst Biol, *in press*). Protein levels in the blood sera rose between 6 and 12 hours indicating that neutrophils are recruited between these time points to the site of infection (**Fig. 22**).

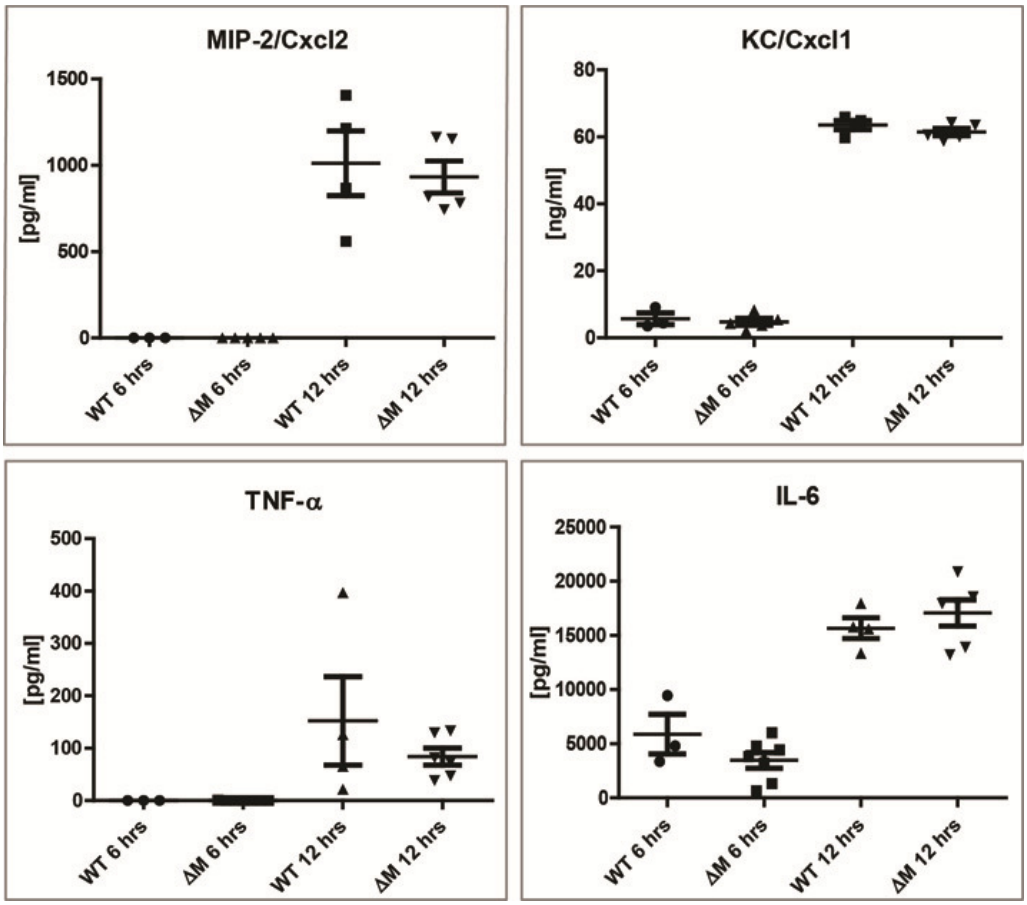

Figure 22 | Neutrophil attracting serum cytokines at 6 and 12 hrs post-infection. WT and ΔM mice were infected subcutaneously with ISS3348 (MOI $1x10^6$ and $1x10^7$ bacteria in left and right lower leg, respectively). Blood serum was extracted before euthanizing the animals at indicated time points and cytokine levels were determined using Flowcytomix™ Multiplex Technology (eBioscience). Depicted are cytokines important for neutrophil recruitment to the site of infection. Significance between WT and ΔM samples for both time points was determined using t test: ns. Error bars: Mean (SEM).

CCLs are known to recruit inflammatory monocytes to site of infections and are produced by neutrophils and other tissue-resident cell-types[79,94]. Measurement of TTP-targeted CCLs unraveled no differences between ΔM and WT mice and showed again, that levels of these proteins rose between 6 and 12 hrs post-infection (**Fig. 23**).

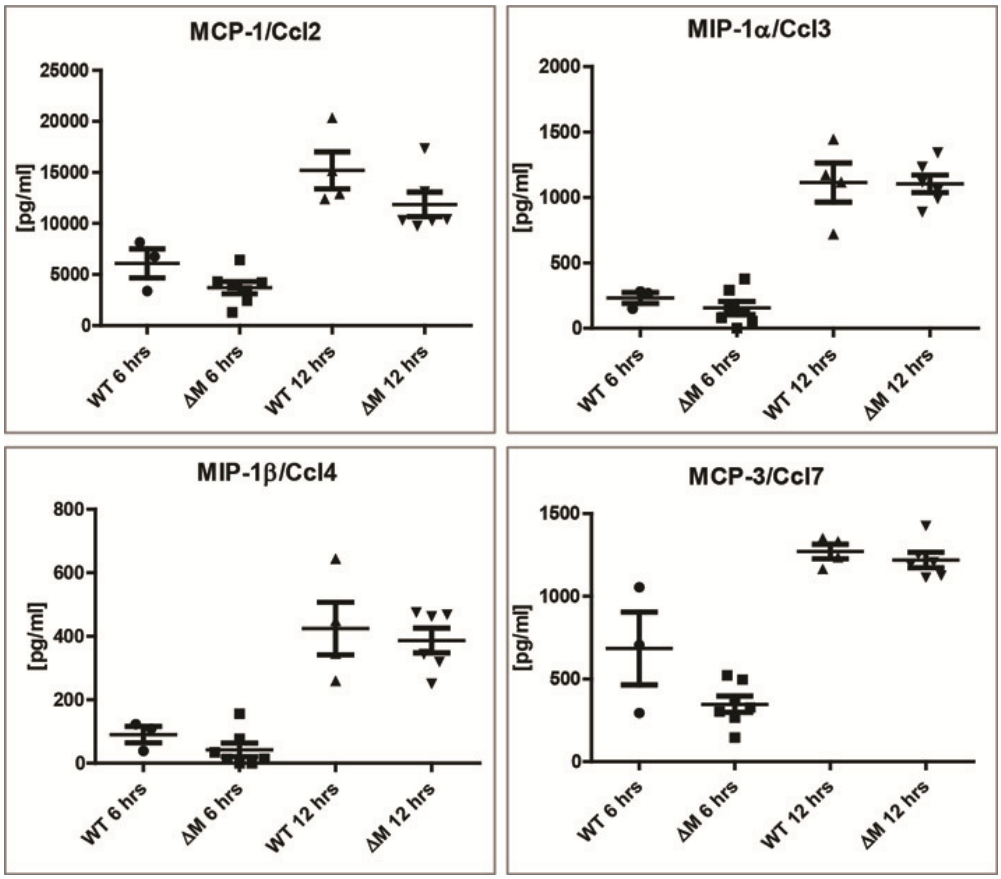

Figure 23 | Monocyte recruiting serum cytokines at 6 and 12 hrs post-infection. Same experiment as described for Fig. 11, but depicted are chemokines attracting monocytes to the site of infection. Significance between WT and ΔM samples for both time points was determined using t test: ns. Error bars: Mean (SEM).

4.2 TTP in Chronic Inflammation: Colitis-Associated Cancer

For the first experiment with ΔT mice, 10 kg/mg AOM were injected intraperitoneally followed by cycles of DSS-treatment to induce colonic inflammation and drive cancer progression. After the third cycle, the animals were analyzed by minimal invasive *in vivo* endoscopy. Endoscopic scoring implicated number of polyps, size of polyps, thickening of colonic epithelium and overall appearance of the colon. Expectedly, ΔT mice were partially protected against CAC induction with AOM-DSS compared to WT (**Fig. 24**).

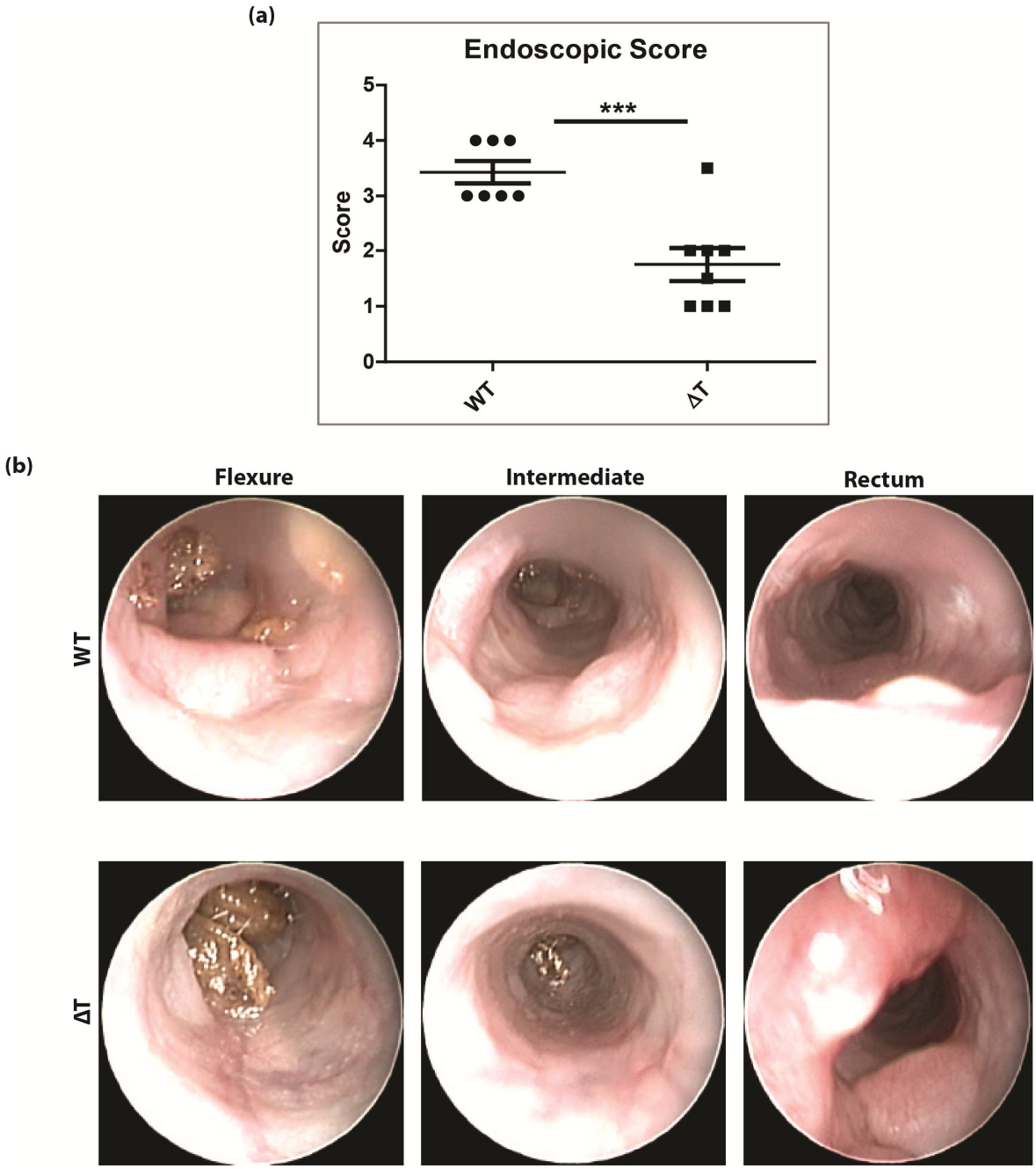

Figure 24 | ΔT mice develop less polyps upon AOM-DSS mediated CAC induction. After CAC induction (see text) non-invasive *in vivo* endoscopic analysis was carried out. **(a)** Dot blot showing endoscopic grading by three individuals, taking into account number of polyps, size of polyps, proximal progression into the colon, epithelial thickening and overall appearance. t test revealed significance: ***, $P < 0.001$. Error bars: Mean (SEM). **(b)** Shown are cut-outs of representative movies recorded during endoscopy from the proximal flexure of the colon to the distal rectum.

Because the induced polyp-number was already very high after the third cycle, mice didn't receive a fourth cycle of DSS-treatment and were euthanized after two more weeks. After opening and determination of polyp-count, the colons were prepared for immunohistochemistry and protein level measurement by ELISA. Macroscopic counting of polyps revealed again, that ΔT mice developed fewer polyps in this model of CAC (**Fig. 25a**

and 25b). Counting the polyp number and histological grading of H&E stained samples showed this effect again, though less strikingly compared to macroscopic grading before (**Fig. 25c and 25d**). Notably, histological analysis requires expertise and will be performed by an experienced pathologist in the future. TNF-α and IL-6 protein levels were comparable between WT and ΔT mice (**data not shown**).

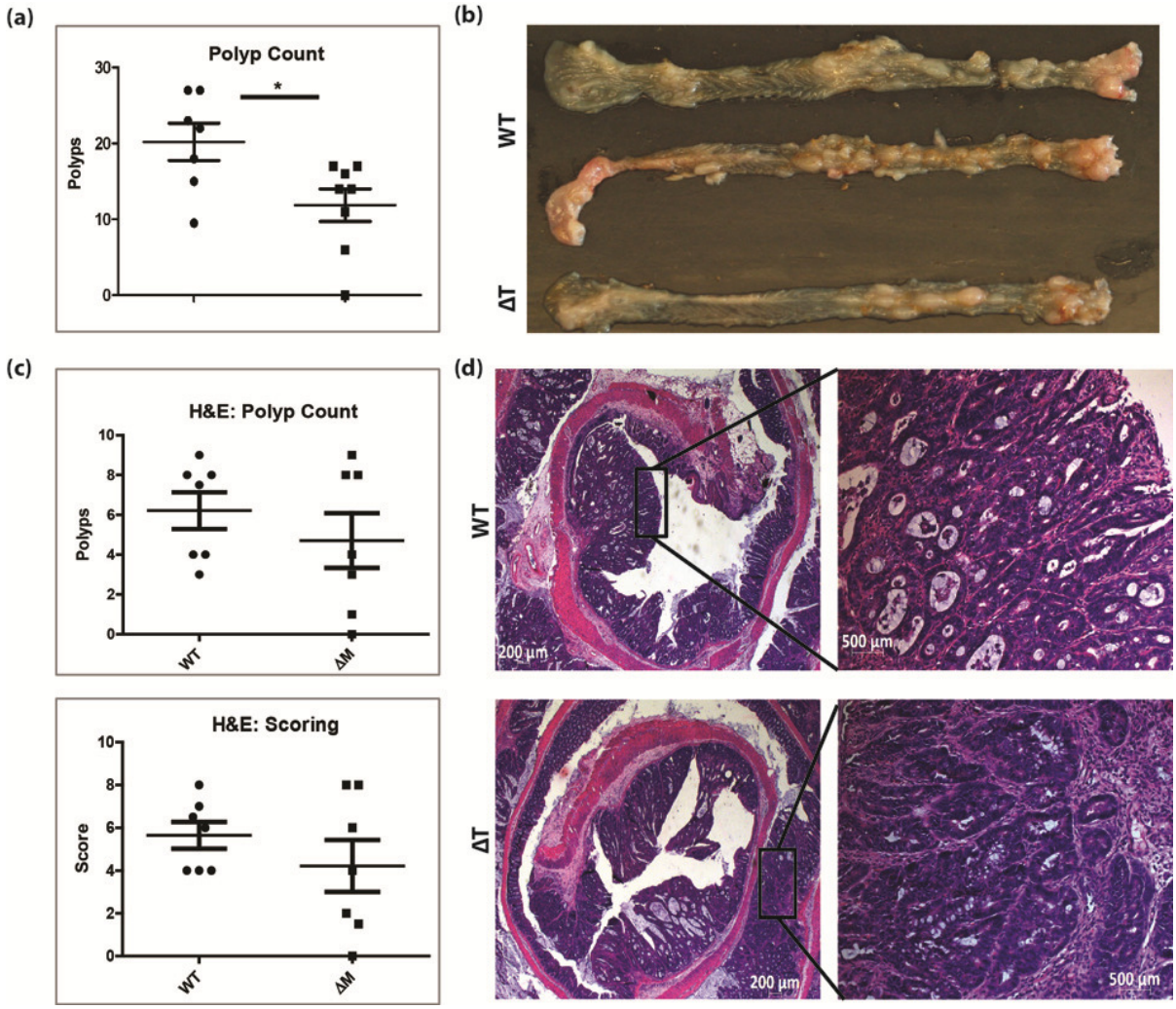

Figure 25 | Macroscopic and histological analysis of ΔT and WT mice. Two weeks after endoscopic analysis (see Fig. 13) mice were opened, colon was removed, flushed and cut longitudinally. **(a)** Developed polyps in the colon were counted and the result is represented as dot blot. Polyp counts from WT and ΔT were tested for significance with t test: *, $P < 0.05$. Error bars: Mean (SEM). **(b)** Representative photographs of WT (upper two) and ΔT (lower) colons. **(c)** Colons were cut again longitudinally and one half was prepared for immunohistochemistry (Swiss rolls). Shown are the polyp count and the histological grading of H&E stained samples. Grading took into account: Overall number and size of visible polyps, grade of neoplasia (if present), general hallmarks of cancer of the polyps (detaching and enlargement of nuclei, multinucleic cells, loosening of crypt structure, invasiveness, connective tissue formation) and unaffected areas. Shown results were tested for significance with t test: ns. Error bars: Mean (SEM). **(d)** Representative H&E stained sections. Note that unaffected epithelium is only present in the ΔT sample compared to WT (left panel, magnification: x25). Right panel shows indicated cut-outs of two polyps in higher magnification (x100). Note the higher grade of tumor progression of the lower polyp. Important: The right panel is not representative. These were chosen to illustrate the grading procedure.

Preliminary experiments showed that TTP ablation within the T-cell compartment leads to a certain degree of protection against AOM-DSS induced CAC. We were wondering if ΔM mice display comparable protective effects in this model. 10 mg/kg AOM were injected intraperitoneally one week prior to cycles of DSS-treatment. As feces was problematic in the above mentioned experiment, mice were deprived of food the day before and were given additional electrolytes in the drinking water. After the fourth DSS cycle, endoscopic analysis indicated that ΔM mice are not protected against polyp development like ΔT mice. Counting polyps and overall grading revealed that ΔM mice are if anything more susceptible (**Fig. 26a and 26b**).

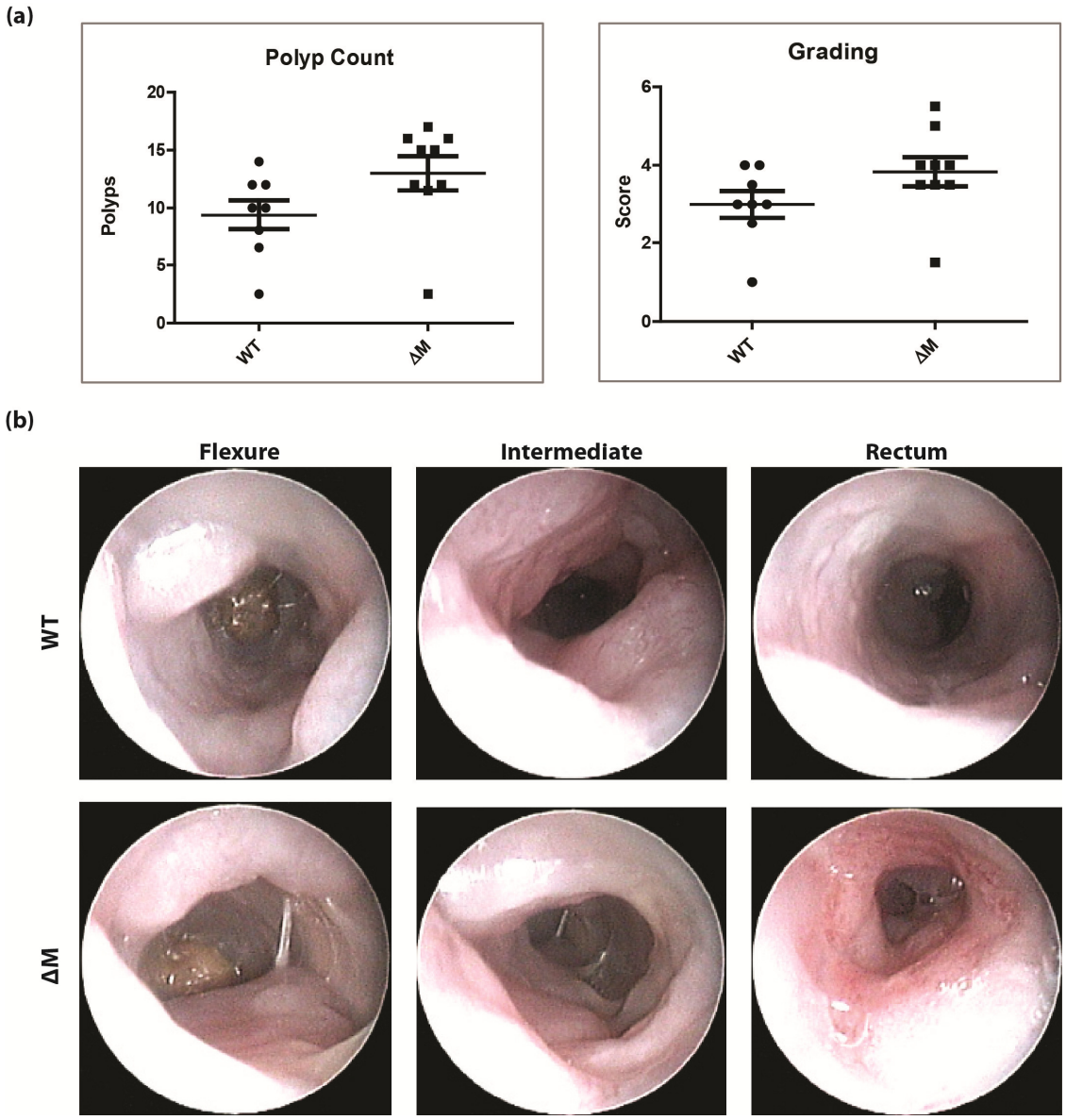

Figure 26 | ΔM mice develop more polyps upon AOM-DSS induced CAC. After CAC induction (see text) non-invasive *in vivo* endoscopic analysis was carried out. **(a)** Dot blots showing polyp count and grading by two individuals, taking into account number of polyps, size of polyps, proximal progression into the colon, epithelial thickening and overall

appearance. t test revealed no significance (ns). Error bars: Mean (SEM). **(b)** Shown are cut-outs of representative movies recorded during endoscopy from the proximal flexure of the colon to the distal rectum. Note the visible blood vessels through colonic epithelium in the WT colon (upper right).

These mice were already severely affected by the treatment and therefore they were euthanized the next day and analyzed macroscopically. Overall grading and counting of the polyps showed again the same trend towards more susceptibility of ΔM mice. Worth mentioning, polyp size, polyp count and thickening of the epithelium (**Fig. 27a and 27b**) were generally more pronounced compared to the former experiment. This originated in the additional fourth cycle of DSS, most probably. Colons were prepared for immunohistochemical and mRNA-level analysis, which will be performed in the future.

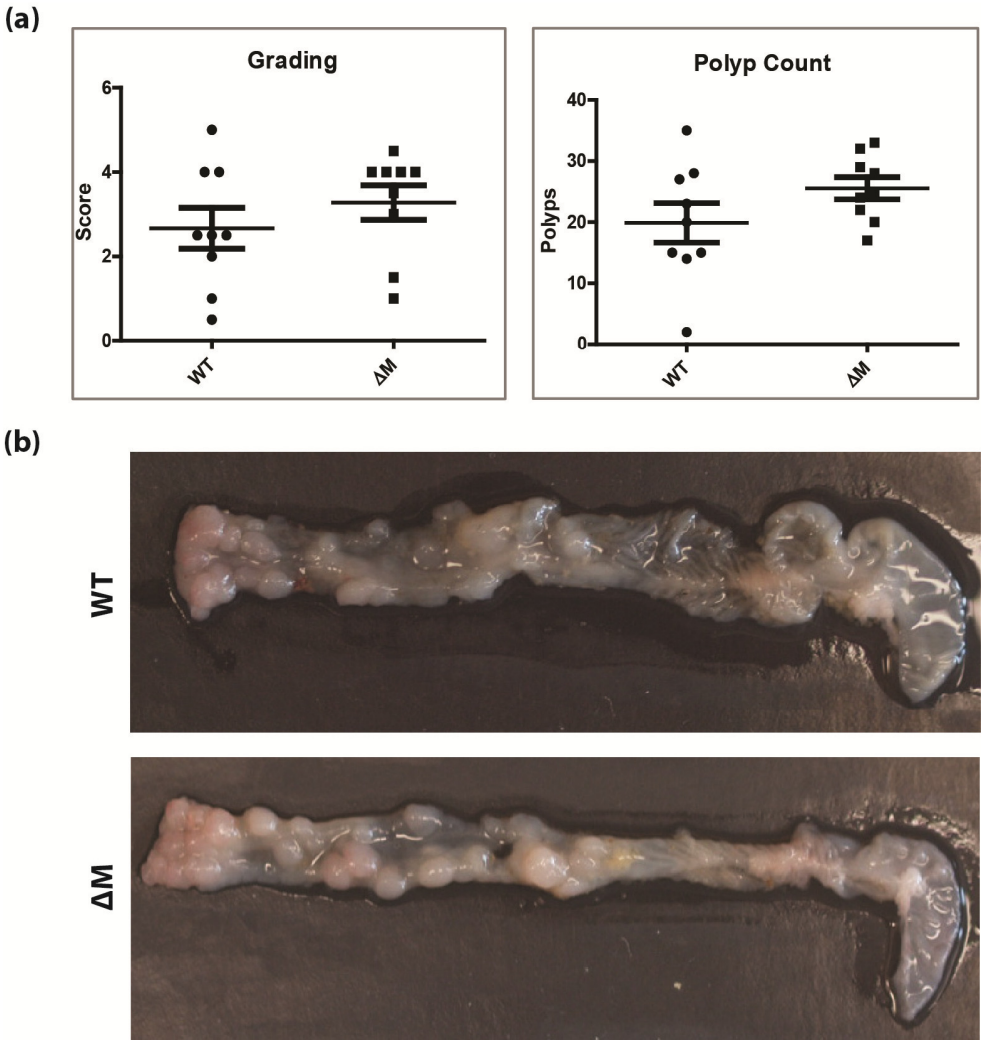

Figure 27 | Macroscopic analysis of polyp development in ΔM and WT mice. The day after endoscopic analysis mice were opened, colon was removed, flushed and cut longitudinally. **(a)** Developed polyps in the colon were counted and overall appearance of the colon was graded. The results are represented as dot blots. Determined significance with t test: ns. Error bars: Mean (SEM). **(b)** Representative photographs of WT (upper) and ΔM (lower) opened colons.

Because of the contrasting effects of TTP deletion in different immune cell compartments, we performed an experiment with conventional knockout mice (from now on referred as KO mice). As these mice show a pro-inflammatory phenotype and are more susceptible in general, less AOM (8 mg/kg mouse) and softer DSS-treatment (2% w/v) were used to induce CAC. This resulted in hardly any colonic polyps after the fourth DSS-cycle analyzed by endoscopy (data not shown). Therefore the animals were subjected to a fifth DSS-cycle before euthanizing. KO mice developed less and smaller polyps and hardly any in the colon (**Fig. 28a and Fig. 28b**). Additionally, colons were prepared for immunohistochemical and mRNA-level analysis in the near future.

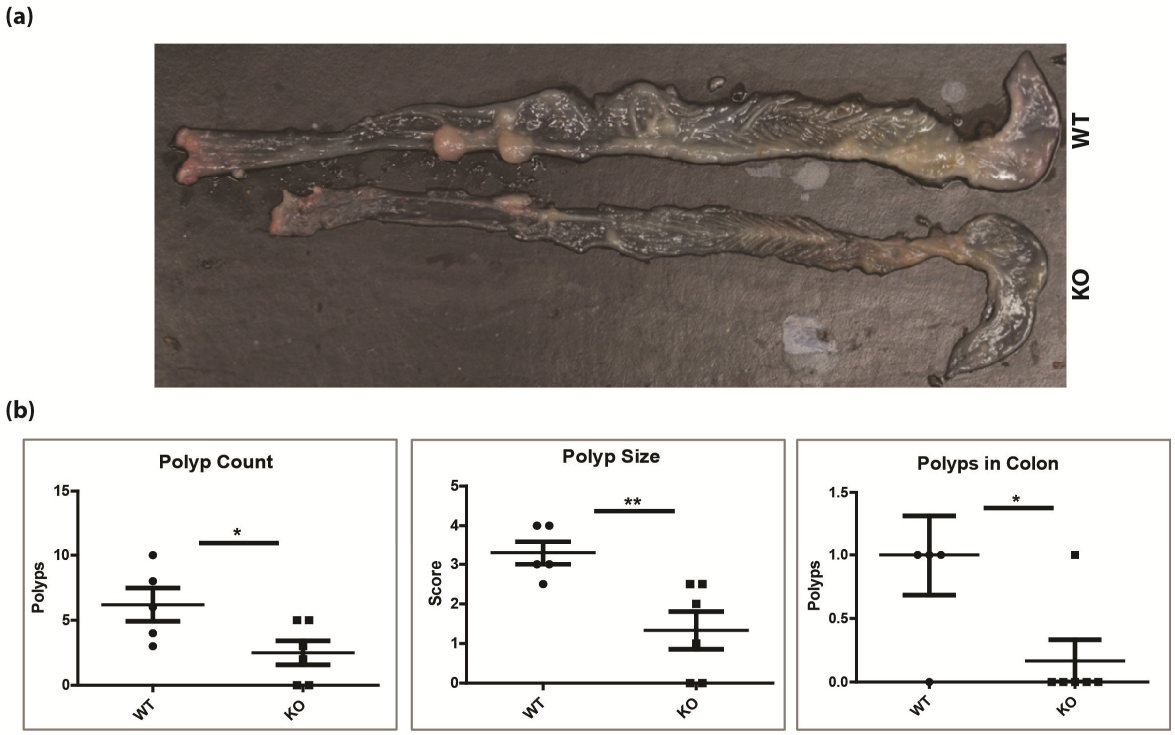

Figure 28 | Macroscopic analysis of CAC induction in KO and WT mice. Mice were euthanized and opened after five cycles of 2% DSS in drinking water **(a)** Representative photographs of WT (upper) and KO (lower) colons. Note: Two polyps are visible only in the colon of a WT mouse. **(b)** Developed polyps were counted, graded according to their size and polyps in the colon were counted independently. Significance was tested with t test: *, $P < 0.05$ (polyp count and polyps in colon); **, $P < 0.01$ (polyp size). Error bars: Mean (SEM).

5 DISCUSSION

5.1 TTP in Acute Inflammation: *Streptococcus pyogenes*

A study by M. Kotb *et al.* correlated human leukocyte antigen (HLA) class II variations of humans with different outcomes of streptococcal infections. The study showed that the invasiveness of the infection and the severity of the outcome (STSS or necrotizing fasciitis) are correlated with higher cytokine release[112]. As the study focuses on the activation of the adaptive immune system (HLA class II) and many reports showed that cells of the innate immune system are of crucial importance for host defense against *S. pyogenes*[108,88,147], the shown correlation must not be generalized and has to be further investigated. Whereas GAS infections are usually mild and non-invasive, about 0.1 % out of 700 million infections worldwide per year lead to invasive manifestations at normally sterile sites with potentially very serious consequences (25 % mortality)[111]. Rising of invasive manifestations of streptococcal infections is reported since late 80s, with the threatening prevalence of one very virulent strain (M1T1)[106]. Among all isolates from patients (with mild or severe infections) strains belonging to the emm1 (M1) serotypes are predominant[111]. But as M1T1 shows, not all strains within one serotype display the same virulence and this is most likely linked to different characteristics of the strain, like the nature of the hyaluronic acid capsule[148] or other proteins like Sda1 DNase[88] or SpyCEP[149] expressed differently.

Here we could show that although the two compared strains EC700 and ISS3348 are both classified belonging to the M1 serotype, *in vitro* behavior and virulence in subcutaneously infected mice differ. C57BL/6N mice cope with EC700 infection, whereas mice die approximately 55 hrs post-infection with ISS3348. Analysis of *in vitro* infected BMDMs revealed that EC700 leads to elevated cytokine levels (TNF-α, IL-6) which is in contrast to the afore mentioned study, that grade of invasiveness is linked to higher cytokine levels[112]. This first result challenges this correlation, as higher cytokine levels could be a secondary effect of already manifested invasive infection and not the cause. Furthermore, macrophages internalize EC700 a 100-fold more efficiently compared to ISS3348, shown by CFU and phagocytosis assays. Taken these *in vitro* results together, one could speculate that EC700 displays more accessible MAMPs alleviating immune recognition by

innate immune cells or ISS3348 is actively downregulating and evading the immune response by an unknown mechanism. *S. pyogenes* is inducing programmed cell death in macrophages and one of the first measurable parameters in this process is loss of mitochondrial membrane potential[150]. As this potential is involved in the phagocytic capacity of macrophages[151] one possible molecular mechanism for the differences in internalization of the two strains could be their efficiency of inducing cell death. This and other possible mechanisms leading to the different virulence of the two strains will be explored in the future.

Innate immune defense mechanisms against invading *S. pyogenes* are still lacking a lot of investigation and are currently only partially understood. Whereas it's known that the bacteria are triggering IFN-β production in BMDMs and cDCs, the molecular nature of ligand(s) and receptor(s) are still elusive[152]. Importantly, interferons exert their anti-inflammatory functions via triggering TTP expression[153]. Myeloid knockout of TTP in mice (ΔM) renders them very susceptible to lipopolysaccharide endotoxin-shock. Lack of TTPs anti-inflammatory effects[47,154] leads to misbalanced serum cytokine secretion followed by septic shock of these mice (Kratochvill et al, Mol Syst Biol, *in press*). As the LysMcre system knocks out TTP in the myeloid lineage (granulocytes, monocytes/macrophages and related dendritic cells)[144], these mice served as a tool to test the hypothesis, that elevated innate immune reactions are beneficial in streptococcal infections *in vivo*. Indeed, mice ablated in myeloid TTP (ΔM) show significantly enhanced survival upon infection with the virulent ISS3348 strain. Histological specimen of dead mice showed hardly any recruitment of immune cells whereas large amounts of infiltrates were present at the site of infection of surviving mice. Sites of infection in ΔM mice were more swollen and the area of inflammation was bigger compared to WT mice, emphasizing the enhanced reaction triggered in ΔM mice.

Thus one could speculate that enhanced immune recognition by tissue resident immune sentinels (as macrophages or dendritic cells) leads to enhanced recruitment of neutrophils and monocytes and facilitates fighting the streptococcal infection at an early stage. All of these innate immune cell types are reported to be important in defense against *S. pyogenes* and are prone to be affected by LysMcre[88,147,155,156]. Upon an arsenal

of antimicrobial mechanisms, like ROS production or anti-microbial proteins, phagocytosis of invading bacteria remains one of the key characteristics and specialties of macrophages[76]. Therefore we tested whether BMDMs lacking TTP show enhanced phagocytic properties. All tested pathogens (gram-positive and –negative) were internalized more efficiently compared to BMDMs derived from WT cells. No difference could be found with synthetic latex beads, leading to the conclusion that not enhanced phagocytic capacity but rather stronger activation upon pattern recognition receptor (PRR) engagement of ΔM BMDMs is responsible for this effect.

p38 MAPK activation is a cardinal feature of cells reacting to stress or immune stimuli and is crucial for TTP expression[46]. *In vitro* differentiated ΔM and WT BMDMs and cDCs showed inconsistent and inconclusive differences in phosphorylated (i.e. activated) p38 MAPK on the protein level at investigated time points. In the future, earlier time points should be investigated to check whether ΔM cells show higher p38 MAPK activation upon ISS3348 infection affecting subsequent events like higher phagocytic rates and survival of the animals. These events are partially controlled by mRNA stability and as TTP targets many pro-inflammatory mRNAs (*Tnfa*, *Il6*, *Ccl2*, *Ccl3*, etc.) the former result was not surprising to us[48,145,153]. Consistently, ΔM BMDMs and cDCs showed elevated mRNA levels of tested cytokine mRNAs (namely *Tnfa* and *Il6* in BMDMs and *Tnfa* in cDCs) confirming the effects of a TTP knockout. These differences on the mRNA-level translated (literally) to differences in secreted cytokine levels, as measurements of supernatants of infected ΔM cells showed consistently higher concentrations.

Time-resolved *in vivo* infection experiments confirmed the stronger innate immune reaction by two striking results: *(i)* area of inflammation of ΔM mice was significantly bigger compared to WT mice and *(ii)* histological grading of sites of infection was higher for ΔM mice. These histological analysis for H&E and Gr-1 (neutrophil/monocyte marker[157]) suggested that ΔM mice recruit more infiltrates to sites of infection, which is in line with the former observation that H&E staining of lesions of surviving animals (WT or ΔM) show the similar phenomenon. A cardinal feature of tissue resident macrophages is recruitment of neutrophils and monocytes via cytokine secretion[79]. As many of chemoattracting and activating cytokines/chemokines for these cells are targets for TTP,

like MCP-1/Ccl2, IL-6, MIP-1α/Ccl3 and TNF-α, we tried to determine cytokine/chemokine concentrations within the tissue 24 and 48 hrs post-infection. These experiments revealed no striking differences among WT and ΔM samples.

Severe, life-threatening diseases caused by GAS are always linked to invasiveness and dissemination of bacteria[105]. Almost no IL-6 and MCP-1/Ccl2 was measurable in blood sera derived from ΔM mice 48 hrs post-infection. It was tempting to speculate that dissemination of *S. pyogenes* is impaired in these mice. Indeed, CFU assays showed that ISS3348 is almost not disseminating with the used MOI per mouse 48 hrs post-infection. Consistent with the concept of invasive GAS spreading via the blood stream to organs causing MOF, most bacteria were measured in livers and spleens of mice[158]. Remarkably, first mice died roughly 55 hrs post-infection, suggesting that lethal outcome at later stages of the invasive disease is determined at earlier time points. The immune system employs different mechanisms to avoid dissemination of bacteria, with neutrophils playing a key role therein[79].

Neutrophils employ different clearance mechanisms against invading bacteria, namely secretion of antimicrobial peptides (e.g. cathelicidin LL37), phagocytosis and trapping by neutrophil-extracellular trap (NET) formation[76,87,88]. Furthermore, they inhibit dissemination by degrading extracellular-matrix proteins unspecifically. Breakdown of vessels and liquefaction of surrounding tissue is cutting off ways for bacteria to escape into the organism and is freeing the way for infiltrating cells of the adaptive immune system at later stages[89]. Recruitment of neutrophils to inflamed sites results from a combination of expressed cytokines and chemokines[159,160]. Exact roles of these chemoattractants and activators *in vivo,* and whether they are redundant or not, are currently under investigation. TNF-α and IL-6 are important players in orchestration of local and systemic inflammatory responses, CXCL1 and CXCL2 are important in chemoattraction of neutrophils (and to a minor extend monocytes) in particular[80,82,161]. ISS3348 infected ΔM and WT mice displayed comparable levels of the mentioned activating and chemoattracting cyto- and chemokines for neutrophils in the blood stream and sites of infection, although all of them are targets for TTP in BMDMs. Monocytes are the next important players in the activation cascade of innate immune reactions against

bacteria. Tissue-resident macrophages and neutrophils are involved in their recruitment and activation, mainly but not only by expression of chemoattractants of the CCL-family[79,94,96]. Tested CCLs (CCL2, CCL3, CCL4 and CCL7) revealed the same as for tested factors for neutrophils, namely comparable levels at the tested time points. Lower MOI and earlier timepoints showed the same results, worth mentioning for future experiments is that measurable amounts of tested cytokines and chemoattractants appeared between 6 and 12 hours post-infection within the bloodstream.

All in all we could show that knockout of mRNA-destabilizing TTP in the myeloid lineage is not detrimental in a subcutaneous model of infection with *Streptococcus pyogenes*. ΔM mice displayed increased areas of inflammation and number of polymorphonuclear cells recruited to the site of infection. The molecular basis for the observed phenotype remains unknown. The question, whether enhanced phagocytosis of tissue resident macrophages ablated in TTP is the only mechanism leading to this protective phenotype will be addressed in the future. One could think that one so far unknown target of TTP or a downstream effect of elevated levels of a known target causes this difference.

Furthermore detailed investigation of other cytokines (e.g. IL-1α, IL-1β, etc.) and different time points for already tested cytokines is necessary. Another *in vivo* attempt will be to measure mRNA-levels within the sites of infection, because measuring protein levels could have been biased for several reasons: *(i)* bigger lesion sizes of ΔM mice could have led to a “normalization-bias” (i.e. higher protein levels were hidden by normalization to the weight or total protein levels), *(ii)* higher amounts of tissue-degrading neutrophils could have degraded the proteins of interest to a certain extent.

Histological grading of lesions 48 hrs post-infection will be performed again by a pathologist, to rule out any artifacts resulting from non-professional grading due to lacking experience. As LysMcre is affecting neutrophils to 100% and TTP targets within these cells are elusive, it’s tempting to analyze these cells in detail *in vitro*. This analysis should address new targets for TTP, if they express more effectors (e.g. metalloperoxidases, LL-37) or show enhanced recruitment in co-culture experiments with activated ΔM BMDMs or stimulated with ISS3348 and if differences in phagocytosis of

bacteria seen in macrophages are present in neutrophils as well. Blood-clotting is another mechanism avoiding dissemination of GAS and neutrophils are implicated in this mechanism[109,162]. Another hallmark of inflammatory reactions is vasodilation induced by nitric oxide (NO) signaling, TNF-α and IL-6. Neutrophils, monocytes and macrophages produce nitric oxide via inducible Nitric Oxide Synthase (iNOS) and therefore it would be interesting to do experiments addressing vasodilation upon ISS3348 infection *in vivo*[79,163].

5.2 TTP in Chronic Inflammation: Colitis-Associated Cancer

The intestine of humans is colonized by a plethora of microorganisms. Sensing of all the present MAMPs is obviously not inducing pathogenic conditions in healthy individuals but is rather required for homeostasis and health[127]. Signaling through PRRs is of special interest, since knockouts of TLR4, TLR2 or MyD88 make mice more susceptible to DSS-treatment through impairment of wound healing[164]. As conventional knockout of TTP in mice is leading to a general pro-inflammatory phenotype, it was surprising that these mice did not develop spontaneous colitis[48]. On the other hand, ablating the A-U-rich element from the 3'-end of the *tnf* gene makes mice prone to develop intestinal inflammation[165]. This controversy could be partially explained by Franz Kratochvill, who obtained data with ΔM knockout mice and could show that these mice are coping better with DSS-induced colitis (data obtained in the laboratory and not published yet). The phenotype seems to be the result of elevated intestinal cytokine-signaling elucidating higher levels of IL-18. IL-18 recently gained prominence in the field of ulcerative colitis, because of its wound-healing and proliferative effects on intestinal epithelial cells[120,137].

In human T cells TTP is up-regulated by transforming growth factor β (TGF-β)[166] and one target in T cells is *Il2* mRNA[167]. TGF-β plays a special role in intestinal homeostasis by participating in shaping the T cell response towards subtypes inducing inflammatory anergy[122,136]. For these reasons, mice ablating TTP specifically in T cells were treated with DSS by Franz Kratochvill as well and these mice displayed comparable results as the myeloid TTP knockout mice, namely amelioration of DSS-induced colitis compared to WT mice.

Another prerequisite to the currently described work is the fact, that TTP and inflammation in general are implicated in several forms of cancer[145,168,169]. As $CD4^+$ TH_1

cells and $CD8^+$ cytotoxic T cells are very prominent to exert anti-cancer effects[170], we were curious if the protective effect in DSS-induced colitis shown by Franz Kratochvill is translating into protection against polyp formation in AOM-DSS induced CAC.

As expected, AOM-DSS induced CAC was less pronounced in mice ablating TTP specific in T cells (ΔT) determined by endoscopic grading according to recommendations[171] and by macroscopic grading upon opening of the colons. Histological analysis revealed no differences, most probably due to two problems. Firstly, we are not sophisticated in grading carcinogenesis due to lack of experience and secondly, for proper analysis in the future, several layers of the specimen should be stained to cover the whole colon vertically.

A possible scenario could be, that the onset is delayed because ΔT are not as susceptible to DSS-induced colonic inflammation as WT mice and progression could be delayed due to better $CD8^+$ T cell mediated killing of cancerogenic cells. The latter will be tested by cytotoxic T cell killing assays. Immunohistochemical stainings of proteins associated with tumorigenesis will help to grade the polyps for different stages, like stainings for phosphorylated STAT3, Wnt-5a, IL-6 or the proliferation marker Ki67[142,172]. Since different T cell subsets are heavily implicated in shaping immune responses in the gut, other upcoming experiments will illuminate T cell subset composition with flowcytometry in untreated and DSS-treated colons, to decipher whether colonic immune homeostasis in ΔT mice is biased to the mentioned anergic state[127,173,174].

Not only cells belonging to the adaptive branch are important in shaping the immunologic state in the gut, but innate immune cells are heavily implicated as well. Antigen-presenting cells (APCs) as macrophages and dendritic cells have a special role in the gut and are very heterogenous[73,130,138,175]. Franz Kratochvill obtained data showing that DSS-induced colitis was ameliorated in mice lacking myeloid TTP. This might be caused by elevated levels of IL-18 in these mice, because this cytokine is known to exhibit proliferative and wound healing effects on intestinal epithelial cells[119,120]. Inducing colorectal cancer in ΔM mice revealed very similar polyp-development to WT mice. This was rather surprising, as we expected less polyp formation due to less pronounced

inflammatory response to DSS in ΔM mice. Reasons for this result could be the following. Firstly, DSS is a polymer synthesized by bacteria and every lot exerts different inflammatory effects, secondly the number of polyps was so high, that one could speculate about a saturated system. Another aspect is, that IL-18 exerts maybe counter-acting effects on cancer induction and cancer progression, as it was reported to be the case for STAT3[172]. Proliferative effects could have led to less inflammation driven tumor induction but, at later stages, it's conceivable that exactly these effects lead to faster polyp growth compensating the initial effect.

The question whether IL-18 is the only cytokine causing the protective phenotype will be addressed by using neutralizing antibodies before DSS-induction. IL-18 is expressed by monocytes, macrophages and epithelial cells, but as macrophages in the intestine are known to produce almost solely IL-10, the measured differences are likely to originate from intestinal epithelial cells (iECs)[78,125,176]. To test this hypothesis and to shed more light on the molecular mechanism, we plan to do *in vitro* experiments with primary iECs[177]. Co-culture with macrophages will decipher, whether iECs produce more IL-18 in response to generally elevated cytokine levels in the gut or if IL-18 originates from intestinal macrophages in this model. This question is very important to answer, as resident intestinal macrophages differ fundamentally from other macrophage subsets due to lamina propria derived stromal regulation, instructing them to be rather anti-inflammatory[78,131].

The experiment with conventional TTP knockout mice revealed a certain level of protection against AOM-DSS-induced CAC, though the grade of protection was less pronounced compared to amelioration of CAC in ΔT mice. This is in line with the results of the former two experiments as these indicate a compensating effect of T cell and myeloid knockout, whereas influence of other cell types must not be ruled out as a matter of fact.

Another interesting aspect of using LysMcre-mediated and conventional TTP knockout mice is to analyze different dendritic cell types in the gut, especially the $CD11b^{+}CD11c^{+}CD103^{+}$ and $CD11b^{+}CD11c^{+}CD103^{-}$ subsets. They are potentially ablating

TTP in ΔM mice and these cells are implicated in orchestrating the tolerogenic state via TGF-β activation and T cell subtype shaping[133,136,178].

As future plan for all experiments addressing DSS-induced colitis and colitis-associated cancer, time-resolved *in vivo* endoscopy during the treatment(s) will help to decipher onset and progression of inflammation and polyp growth in the different used mouse models. Furthermore consulting a pathologist for detailed analysis of histological specimens will ensure proper grading on the microscopic level.

6 MATERIAL AND METHODS

6.1 Animal Models

Mice carrying floxed alleles of TTP ($TTP^{fl/fl}$) (Kratochvill et al, Mol Syst Biol, *in press*) were bred to LysMcre[144] or LckCre[179] mice to obtain offspring conditionally deleting TTP in myeloid (ΔM) or T cells (ΔT), respectively. Breeding pairs of conventional knockout mice of TTP[48] (KO) were kindly provided by Perry Blackshear to set up a colony. All mice were housed under specific pathogen-free conditions. All mice were on C57BL/6 background and sex- and age-matched littermates were used for all experiments. All animal experiments were in accordance with the Austrian and European law and with the recommendations by GV-SOLAS.

6.1.1 Anesthesia and Euthanasia

Mice were anesthetized injecting Ketamine/Xylazine solution intraperitoneally (200 – 300 µl) or shortly anesthetized by inhaling Halothane. Mice were euthanized by cervical dislocation. Eyes of anesthetized mice were covered with a drop of eye ointment for light- and dryness-protection.

6.1.2 AOM-DSS Induced Colitis-Associated Cancer (CAC)

Animals were transferred to in-house individually ventilated microisolator-cages (IVCs) and left untreated at least for five days to acclimatize to the new environment. Azoxymethane (Sigma-Aldrich®) diluted in 0.9 % NaCl was injected intraperitoneally (10 or 8 mg/kg mouse) and mice were left untreated for 7 days. Then cycles of DSS treatment started, each followed by 12 days of recovery. For each DSS-induced colitis cycle DSS was provided ad libitum in drinking water (2.0 to 3.5 % w/v depending on DSS lot and constitution of mice) for 5 days.

6.1.3 *In Vivo* Endoscopy and Opening of Mice

Approximately two weeks after the last DSS cycle, mice were analyzed with non-invasive *in vivo* micro endoscopy. Food was removed the day before and mice were given rehydrating solution supplying with carbohydrates and electrolytes. The setup consisted of the following parts: Endoscope (1.9 mm diameter), an air pump, a light source, an LCD

screen for live-visualization and a computer to record the videos. After anesthetizing mice, air flow was set, the endoscope was inserted carefully into the rectum and the scope was slowly put in as far as possible (max. to the first flexure of the colon, up to ~4 cm). Videos were recorded while moving backwards and grading took into account the following suggested biological characteristics: Thickening of the epithelium (reduced transparency), vascular pattern (focusing on bleeding), fibrin deposits, granularity of the mucosal surface, feces consistency, polyp count, polyp size and distribution of the polyps. This grading follows largely the recommended scheme for colitis-endoscopy-scoring (MEICS: murine endoscopic index of colitis severity) with adaption for CAC grading[180].

Based on the endoscopic results, mice were opened the following day or DSS-treatment was repeated to promote cancer growth. When opened, colon was removed, flushed with cold 1xPBS, cut longitudinally and cleaned from remaining feces. Macroscopic grading was based on rectal bleeding, polyp count, polyp size and distribution over colonic tissue. Photographs were taken, followed by another cut longitudinally. One half was prepared as Swiss roll, put on a Whatman paper for stabilization and put over night into 4 % Paraformaldehyde-solution (at 4 °C) followed by the protocol for immunohistochemistry. The other half of the colon was shock-frozen in liquid nitrogen and put on -80 °C for either mRNA or protein preparation.

6.1.4 *In Vivo* Infections with *Streptococcus pyogenes*

4 ml of overnight culture were pelleted (6500 rpm, 6‘, RT) and resuspended in 1 ml sterile 0.9 % NaCl (Sigma®) (equals $28x10^8$ cells per ml). 700 µl bacterial suspension were diluted to 1 ml with 0.9 % NaCl to reach $1x10^8$ in 50 µl (for different inocula suspension was diluted further). This suspension was injected subcutaneously into lower legs of anesthetized mice (1 to 5 x 10^8 for survival assays, 1 to $3x10^8$ for CFU assays or lower number of bacteria depending on the experiment). Directly after infections, inocula were determined.

For cytokine measurements, mice were euthanized at indicated time points. Blood was extracted by puncture of the retrobulbar venous plexus and left shortly at RT for clotting. After centrifugation (1’, 13200 rpm), blood serum was taken and stored at -80 °C. Infected

tissue was removed without any bones and homogenized in 750 µl PBS (supplemented with 10 µl 10 mM Vanadate and 50 µl Complete Protease Inhibitor (Roche)). After two cycles of freezing and thawing on ice, tissue debris were removed by centrifugation for 1' with 13200 rpm and lysate was stored at -80 °C. Cytokine concentration was determined using ELISA (R&D Systems) or Flowcytomix^{TM} Multiplex Technology (eBioscience). For normalization, total protein concentration of tissue-lysates was measured using Nanodrop Spectrophotometer (Thermo Scientific).

For histology, infected tissue was removed without bones at indicated time points. After cutting longitudinally through the lesion, tissue was put on Whatman paper and into 4 % Paraformaldehyde solution at 4 °C over night and processed as described (see Histology).

6.1.5 Survival Assay

After subcutaneous infection (MOI: 1 to 5x10^8) mice were examined for either death during the night or reaching humane endpoints (HEPs) defined for survival experiments as the following: Inactivity, hunched position, piloerection, poor body condition and disturbed locomotor activity. Humane endpoints were chosen as recommended by the working group Humane Endpoints (HEP) of the Netherlands Association for Laboratory Animal Science (NVP). When showing signs of HEPs mice were euthanized and time of death was recorded. At day five post-infection mice were euthanized and were considered to survive the infection.

6.1.6 Determination of Bacterial Inoculum

Dilution series of *Streptococcus pyogenes* cell suspension used for infection (of mice or cells) were prepared in duplicates: 30 µl suspension in 270 µl sterile 1xPBS (to 10^{-8} dilution). Dilutions were plated on Trypticase Soy agar + 5 % sheep blood plates (Biomerieux) (4 dilutions/plate, 5 drops of 10 µl) and incubated o/n at 37 °C with 5 % CO_2. Next day colonies were counted and original concentration of bacteria/ml was calculated using following equation (**Equation 1**):

Equation 1: Calculating CFUs per 50 µl

$$\frac{\left[\sum_{d_f=-x}^{-y} \frac{\sum_{i=1}^{n} x_i}{n} \times 10^{d_f}\right]}{n_{df}}$$

where …

- n … number of duplicates per dilution
- i … index for duplicates (increment = 1)
- x_i … counted number of colonies
- d_f … dilution factor (increment = 1)
- x … exponent of lowest dilution counted (i.e. -8 for 10^{-8} dilution, therefore first d_f corresponds to 10^8)
- y … exponent of highest dilution counted
- n_{df} … number of counted dilutions

6.1.7 *In Vivo* Colony Forming Unit (CFU) Assay

CFU assays of infected mice were performed to monitor bacterial.

Mice were deeply anesthetized 48 hrs after subcutaneous infection (MOI: 3 x 10^8 in 50 µl) and blood samples were taken by heart-puncture after opening the thorax to avoid contamination by skin resident bacteria. Blood was immediately diluted 1:1 with ddH_2O to lyse host cells. Spleen and liver were removed, put into 750 µl sterile PBS and homogenized using a Potter-Homogenizer. 1:10 dilution series of blood and tissue lysates were prepared in PBS, 4 or 5 drops of 10 or 15 µl, respectively, of dilutions were plated on Trypticase Soy agar + 5% sheep blood plates (Biomerieux) and incubated overnight at 37 °C with 5 % CO_2. Colonies per dilution were counted the next day and CFUs were calculated with **Equation 2**. For normalization CFU/ml was divided by tissue-weight of spleen or liver.

Equation 2: Calculating *in vivo* CFUs

$$V_E/_V \times \frac{\left[\sum_{d_f=-x}^{-y} X_i \times 10^{d_f}\right]}{n_{df}}$$

where …

- x_i … counted number of colonies per dilution
- d_f … dilution factor (increment = 1)
- x … exponent of lowest dilution counted (i.e. -8 for 10^{-8} dilution, therefore first d_f corresponds to 8)
- y … exponent of highest dilution counted
- n_{df} … number of counted dilutions
- V … total volume plated per dilution (i.e. 4 x 15 = 60 µl or 5 x 10 = 50 µl)
- V_E … Endvolume (usually 1000 µl)

6.2 Histology

Tissue (lesions or colons) were put into 4 % PFA solution overnight at 4 °C for fixation, followed by another night on 4 °C in 70 % EtOH. Shandon Excelsior (Thermo Electron Corporation) was used to dehydrate the samples with the following routine:

- 70 % EtOH 5’
- 75 % EtOH 60’
- 80 % EtOH 60’
- 85 % EtOH 60’
- 90 % EtOH 60’
- 95 % EtOH 60’
- 100 % EtOH 60’
- Xylene 3x 60’
- Paraffin 3x 80’

After dehydration tissue was embedded in paraffin with Shandon Histocentre 3 (Thermo Electron Corporation), 3 nm slices were prepared using Microtome LEICA RM 2155 (Leica) and dried.

6.2.1 H&E Staining

For Hematoxilin and Eosin stain an automated staining routine was used after pre-warming slides for 5’ to 50 °C to aid deparaffinization:

- 2x Xylene Substitute (J.T. Baker) for 10’
- 2x 100 % EtOH for 5’
- 90 % EtOH for 2’
- 70 % EtOH for 2’
- washing with tap water for 1’
- Hematoxilin (Sigma-Aldrich) for 6’
- washing with tap water for 1’
- 1 % HCl EtOH 5’’
- washing with tap water for 10’
- 70 % EtOH for 30’’

- 80 % EtOH for 30''
- Eosin (Sigma-Aldrich) for 2''
- 2x 90 % EtOH for 1'
- 2x 100 % EtOH for 1'
- 2x Xylene Substitute for 5'

Before embedding with Entellan (MERCK), slides were incubated for 10' in Xylene. After drying over night slides could be stored.

6.2.2 Immunohistochemistry

Stainings with antibodies against *S. pyogenes* and Gr-1 (BD Pharmingen) were performed as the following.

Solutions:

Wash Buffer: 1x TBST

Antigen Unmasking Solution (S. pyog.): 0.1 M Tris (pH 7.5); 0.5 % SDS, to 35-40 °C and add Pronase stock solution (10 – 20 mg/ml) to give a solution with 0.5 – 2.0 mg/ml Pronase.

Antigen Unmasking Solution (Gr-1): 9 ml 0.1 M Citric Acid, 41 ml 0.1 M NaCitrate with ddH_2O to 500 ml.

Blocking Solution: 3 % Goat Serum (vector) in 1xTBST

Primary antibodies: rabbit anti-*S. pyogenes* diluted 1:1000 in Blocking Solution; rat anti-mouse Gr-1 1:50 in Blocking Solution;

Secondary antibodies: DakoCytomation EnVision+HRP Anti-Rabbit or Dako HRP rat/mouse (ENV)

Developing Reagent: AEC + High Sensitivity Substrate (Dako) ready to use reagent

Hematoxylin: 1:20 in ddH_2O

For straitening of the sections slides were pre-warmed to 55 °C for 5'

Deparaffinisation/Rehydration

- Incubate 2x in Xylene for 10'
- Incubate 2x in EtOH 100 % 5'

- Incubate 2x in EtOH 90 % 5‘
- Wash with ddH_2O (or tap water) 2x 5‘

Peroxidase was blocked by incubation for 10’ with 3 % H_2O_2 followed by washing twice for 5’ with tap water.

Antigen unmasking (from now on conducted in immunostaining chambers)
S. pyogenes: Incubation with ~100 µl Antigen Unmasking Solution at 37 °C for 10‘
Gr-1: Slides were boiled in Unmasking solution for 20´ – 30´ and cooled down for 30‘

After washing the slides 3x with wash buffer, sections were blocked for 30’ at RT with blocking solution. 150 µl primary antibody solution were added and slides were incubated 1 hr at RT or overnight at 4 °C. After 3x of washing 2-3 drops of secondary antibody were added. After 30’ of incubation at RT, slides were washed 3x and removed from immunostaining chambers. After encircling of the specimen with a fat pen, 2-3 drops of developing reagent were added. Slides were immersed in tap water as soon as the staining got visible (but after 20’ max). Specimen were counterstained with hematoxilin solution for 15-30’’ and washed afterwards for 10’ under running tap water.

Embedding
Slides were embedded with 1 drop/section Aquatex (MERCK), covered with microscope cover glass and dried over night at RT.

6.2.3 Microscopy and Grading of Histologic Specimen

Microscopic analysis was performed using an Axio/Stereomicroscope (Zeiss) and the according AxioVision software (Zeiss).

For the grading of infected tissue, the following criteria were taken into account: Vasodilation of blood vessels and thrombus formation, number of infiltrating cells (mainly neutrophils), depth of infection, swelling, acantosis and overall tissue destruction. Swiss rolls of colons from AOM-DSS treated mice were graded with respect to suggested criteria[181].

6.3 Cell Culture

Cells were grown in incubators providing: 37 °C, 5 % CO2 and 95 % humidity.

6.3.1 Taking Bone Marrow in Culture

Fresh: Bone marrow was flushed out of femur and tibia with 10 ml pre-warmed DMEM followed by centrifugation for 5' with 1100 rpm at RT to pellet the cells.

Frozen: 1 ml cell suspension was unfrozen quickly and transferred slowly into 10 ml pre-warmed (37 °C) DMEM. To get rid of toxic DMSO cells were pelleted by spinning the suspension for 5' with 1100 rpm at RT.

Pellet was resuspended either to differentiate bone marrow derived macrophages (BMDMs) or conventional dendritic cells (cDCs). Alternatively, pellet from freshly isolated bone marrow was resuspended in FCS + 10 % DMSO and frozen immediately (-80 °C).

6.3.2 Differentiation of Bone Marrow Derived Macrophages (BMDMs)

Cell pellet from fresh or thawed bone marrow was diluted with LC medium and split to five or four uncoated 10 cm square dishes with a total volume of 15 ml medium per dish. On day three of *in vitro* differentiation cells were fed with 5 ml of fresh LC medium. Cells were sometimes split depending on proliferation after day five, split and/or seeded for experiments on day seven or kept for experiments within the following two weeks. To split the cells, supernatant was aspirated and cells were scraped in about 2 ml remaining medium using a rubber wiper (sterilized with 70 % EtOH and flamed). Suspensions from one mouse were pooled, counted if necessary using Countess® Automated Cell Counter (invitrogen) and split onto the desired amount of fresh uncoated 10 cm square dishes, with a total volume of 15 ml LC medium per dish[182].

6.3.3 Differentiation of Conventional Dendritic Cells (cDCs)

For fresh bone marrow a red blood cell lysis was performed by resuspending the cell pellet in 1 ml red blood cell lysis buffer, followed by incubation for 1 to 2' in the incubator. Addition of 10 ml cDC medium stopped lysis. The suspension was centrifuged for 5' with 1200 rpm at RT. Supernatant was discarded, pellet was respuspended in cDC Medium + P/S and counted (1:10 dilution diluted 1:1 with Tryphanblue). $9x10^6$ to $13x10^6$ cells were seeded on 10 cm round, uncoated, bacterial petri dishes in 5 ml cDC medium.

Cells were fed 5 ml fresh cDC medium per dish on day three and were cultivated for seven days in total. This protocol is an adaptation of a published method[146]. For seeding for experiments non-adherent cells were pelleted (to avoid contamination by BMDMs), resuspended in cDC medium without P/S and counted.

6.3.4 *In Vitro* Infections of BMDMs and cDCs

Seeded $2x10^6$ BMDMs (the day before) or cDCs (approx. two hours before infection) on 6 cm tissue-culture dishes supplemented with 3 ml medium.

2 ml of streptococcal o/n culture were pelleted (6500 rpm, 6', RT) and resuspended in 2 ml sterile PBS. This suspension relates to $7x10^8$ cells/ml. BMDMs or cDCs were infected with MOI = 100 (equals ~ 290 µl cell-suspension for $2x10^6$ cells). After 30' medium of BMDMs was changed to LC medium containing 60 ng/ml Penicillin or 1000x Penicillin solution was added to cDCs.

Samples (supernatant, RNA or protein) were collected at indicated time points as described in the following:

BMDMs

- ELISA: Supernatant was taken, spun 1' at 4 °C with 13200 rpm and stored at -80 °C
- RNA: After washing the cells once with cold PBS using TRIzole method
- Protein: Cells were washed once with cold PBS and lysed with 80 µl lysis buffer. After scraping the lysate was transferred into a 1.5 ml Eppendorf tube and spun for 10' with 13200 rpm at 4 °C. Supernatant was mixed with 30 µl SDS Sample buffer, heated to 95 °C for 10' to denature proteins and stored at -20 °C.

cDCs

Cells were scraped within the medium and spun for 5' with 1200 rpm.

- ELISA: Supernatant was frozen at -80 °C.
- RNA: Pellet was resuspended in RA 1 buffer (of the NucleoSpin® RNA II kit from Macherey-Nagel). RNA was isolated following the protocol provided with the kit and stored at -80 °C.

- Protein: Pellet was resuspended in cell lysis buffer, spun for 10' at 4 °C with 13200 rpm. Supernatant was mixed with 30 µl SDS Sample buffer and boiled for 10' at 95 °C. Lysate was stored at -20 °C.

6.3.5 Colony Forming Unit Assay (CFU) of BMDMs

$2x10^5$ BMDMs per well were seeded the day before on a 24 well tissue-culture treated plate in 500 µl LC medium without P/S.

The next day, cells were infected with MOI = 100 and incubated for 45'. After washing once with sterile PBS, fresh LC medium supplemented with 60 ng/ml Penicillin was added and the cells were further incubated. At indicated time points post infection BMDMs were lysed by osmotic pressure using 500 µl autoclaved ddH_2O (5 to 10' at 37 °C). Lysate was pipetted up and down 5 times to lyse remaining BMDMs and to resuspend bacteria. 10-fold dilution series in PBS were plated on Trypticase Soy agar + 5 % sheep blood plates (Biomerieux) (5 drops of 10 µl per dilution, 4 dilutions per plate). After incubation over night, colonies were counted and CFU/ml were determined using **Equation 2**. To compare two different streptococcal strains (here: ISS3348 and EC700), inocula of both were determined and CFUs were expressed as percentage of total bacteria used for infection.

6.3.6 Phagocytosis Assay

This assay is an alternative to the *in vitro* CFU assay without bias of bacteria sticking at the membrane. BMDMs were differentiated and Stefanie Sigel (Knapp Group) performed the assay. In essence, bacteria were labeled using BacLight-green (molecular probes), washed 4 times and BMDMs were infected for 1 hour (additionally at 4 °C as negative control). After infection, cells were treated with Proteinase-K to digest bound but not phagocytozed bacteria. After washing, cells were analyzed by flowcytometry. Positive cells (FITC channel) were gated and phagocytosis index was calculated by mean fluorescence multiplied with total cell number within the gate. For comparing ISS3348 and EC700 phagocytosis indexes were normalized to inocula.

6.4 *In Vitro* Analysis

Following section describes the methods used to measure cytokine concentrations or kinase activation of samples obtained from above described experiments.

6.4.1 RNA Isolation with TRIzole Method

- Medium was removed and cells were washed 1x with ice cold PBS.
- 300 µl TRIzole (Sigma) were added and cells were scraped using a rubber wiper.
- Lysate was transferred to Safe Lock Tubes (Eppendorf) and was stored at -80 °C or further processed.
- Lysates were incubated 5’ on RT.
- 80 µl Chloroform were added, vortexed for 10’’ and left on RT for 10'
- After centrifugation (15’, 12000 rpm at 4 °C) upper aqueous phase was transferred to fresh tubes.
- 220 µl Isopropanol were added, tubes were inverted 5 times and incubated at RT for 10’.
- After centrifugation (10’, 12000 rpm at 4 °C) pellet was washed once with 500 µl 70 % EtOH.
- If Phenol-like smell was still present after centrifugation (5’, 12000 rpm, 4 °C), washing was repeated.
- Supernatant was taken off and pellets were air dried.
- RNA was resuspended with 25 (40) µl nuclease-free ddH_2O (on ice).
- RNA was stored at -80 °C.

6.4.2 Reverse Transcription of mRNA

- Mix: x µl RNA (0.5 to 1.0 µg of RNA were used)
  1 µl Oligo d(T) (100 pmol/µl) (Fermentas)
  ad 11 µl with nuclease-free ddH_2O
- Samples were incubated 5’ at 70 °C and subsequently transferred on ice.
- per sample: 4 µl 5x Reaction Buffer
  2 µl 10 mM dNTP (Fermentas)
  2 µl nuclease-free ddH_2O

- Incubation for 5’ at 37 °C and 1 µl of Mu-MLV Revert Aid Reverse Transcriptase (200 U/µl) (Fermentas) was added per sample.
- Samples were incubated for 60’ at 42 °C for reverse transcription, followed by inactivation of the enzyme (10’, 70 °C).
- reverse transcribed mRNA (=cDNA) was stored at -20 °C.

6.4.3 Quantitative RT-PCR (qRT-PCR)

- cDNA was diluted 1:10 with nuclease-free ddH_2O.
- Standards: 1:2 dilution series of sample where the highest signal was expected was prepared with nuclease-free ddH_2O (4 dilutions in total).
- qRT-PCR Mastermixes (without adding Ampli-Taq Polymerase) were prepared.
- 5 µl of cDNA solution per well were added in 96-well plates.
- Mastercycler was started to pre-heat.
- Ampli-Taq Polymerase was added to the qRT-PCR Mastermixes.
- 20 µl of Mastermixes were added to each well.
- Run was started as soon as possibl.

For analysis, C-values of gene-of-interest (*Tnfa* or *Il6*) were normalized to housekeeping gene of the same cDNA sample (*Hprt*) to give arbitrary units.

Used Primers:

murine *Hprt* fwd 5´-GGATTTGAATCACGTTTGTGTCAT -3´,

murine *Hprt* rev 5´-ACACCTGCTAATTTTACTGGCAA -3´

murine *TNFa* fwd 5´-TTCTGTCTACTGAACTTCGGGGTGATCGGTCC -3´

murine *TNFa* rev 5´-GTATGAGATAGCAAATCGGCTGACGGTGTGGG -3´

murine *Il6* fwd 5´- ATG GAT GCT ACC AAA CTG GAT -3´

murine *Il6* rev 5´- TGA AGG ACT CTG GCT TTG TCT -3´

6.4.4 Western Blotting

SDS PAGE

Preparing 10% separation gel and 5% stacking gel

10% separation gel			**5% stacking gel**		
	0.75 mm spacer	1.5 mm spacer		0.75 mm spacer	1.5 mm spacer
50% AA for TTP	0.8 ml 1.3 ml	1.6 ml 2.6	30% AA	0.25 ml	0.5 ml
4x 1.5 M Tris HCl (pH 8.8)	1 ml	2 ml	4x 0.5 M Tris HCl (pH 6.8)	0.5 ml	1 ml
ddH_2O for TTP	2.2 ml 1.7 ml	4.4 ml 3.4 ml	ddH_2O	1.25 ml	2.5 ml
10% SDS	40 µl	80 µl	10% SDS	20 µl	40 µl
mix well and add					
20% APS	12 µl	24 µl	20% APS	6 µl	12 µl
TEMED	8 µl	16 µl	TEMED	4 µl	8 µl

15 µl (50 µl for cDC samples) were loaded in each slot. 5 µl of prestained Protein Ladder (Fermentas) were used and gels were run with 200 V, 20 mA (15 mA in case of TTP)

SEMI-DRY BLOTTING

- 14 whatman filters and one nitrocellulose membrane (7x9 cm) were prepared
- papers were prewet in buffers and blot was assembled according to the scheme:

TOP (-)

6x filter papers in cathode buffer

Gel in ddH2O

Membrane in anode buffer II

3x filter paper in anode buffer II

5x filter paper in anode buffer I

BOTTOM (+)

Rolling on the top removed air bubbles, blot was run with 25 V, 60 mA (per gel) for 90'. After blotting membrane was cut to the size of the gel, washed once with ddH_2O and stained with Ponceau S (2-3 ml) to monitor successful blotting.

IMMUNODETECTION

- Ponceau S stain was washed off with 1x TBST and the membrane was blocked with milk in TBST (2.5 to 3g of low-fat milk powder) shaking for 1 hr at RT.
- After washing the membrane 3x with TBST (10-15' each wash) it was incubateed over night with first antibody diluted in TBST containing 1 % BSA and 0.05 % NaN_3 shaking at 4 °C.
- Next day antibody-solution was collected for re-use and stored at 4 °C.
- After washing again 3x with 1x TBST (10-15' each wash), membrane was incubated with secondary antibody-solution (1:20000 in 1x TBST containing 1 % BSA).
- Membrane was shaken protected from light for 30' at RT
- After washing again 3x with 1x TBST, membrane was scanned with ODYSSEY Imaging System (Li-Cor Biosciences)

Table 2: Used Antibodies for Immunodetection

	Antibody	Species	Dilution	Fluorophore
Primary AB	polyclonal anti TTP	rabbit	1:2500	-
	anti phospho-p38	rabbit	1:1000	-
	anti p38	rabbit	1:1000	-
Secondary AB (ODYSSEY AB)	anti rabbit green		1:20000	IRDye800
	anti rabbit red		1:20000	IRDye700

STRIPPING OF MEMBRANE

With this procedure bound antibodies and milk/BSA were removed from the nylon-membrane to be reprobed with another antibody, e.g. p38 as loading control.

- Membrane was washed 2 times shortly with ddH_2O.
- Stripped for 10' at RT (shaking) with stripping buffer.
- Washed 3x 10' with 1x TBST

6.4.5 Enzyme-linked Immunosorbent Assay (ELISA)

ELISA kits (R&D Systems) were used to detect TNF-α, IL-6, CXCL2, CXCL1, IL-10 in BMDM/cDC supernatants, protein-isolates from lesions, colons and blood sera.

Capture Antibody:

- stock: 144 µg/ml (if diluted in 1 ml PBS)
- working concentration: 0.8 µg/ml

Detection Antibody:

- stock: 27 µg/ml if diluted in 1 ml Reagent Diluent
- working concentration: 150 ng/ml

Standards:

	Working conc. [pg/ml]
TNF-α	2000
IL-10	2000
CXCL1	1000
IL-6	1000
CXCL2	1000

1:2 dilution-series for the standard curve were prepared as the following: Standard was diluted to working concentration in 300 µl Reagent diluent and further dilutions were made with 150 µl Reagent Diluent + 150 µl standard to reach 7 standard-dilutions

Day 1:

- Capture Antibody was diluted to 0.8 µg/ml in 1x PBS.
- wells of a 96-well microplate were coated overnight with 100 µl each at RT.

Day 2:

- After washing the wells with Wash Buffer, they were blocked for at least 1 hr at RT by adding 300 µl Reagent Diluent to each well, followed y 3x washing.
- Loading: 100 µl of samples and standards were loaded per well.
- After incubation for 2 hrs at RT followed by 3x washing, Detection Antibody was added to each well (100 µl) and plate was incubated for another 2 hrs at RT.
- 100 µl of Streptavidin-HRP (1:200 in Reagent Diluent) were added to each well after washing followed by incubation for 20’ at RT protected from light.
- After washing 3x, 100 µl Substrate Solution (1:1 mixture of Reagent A and Reagent B out of DuoSet® ELISA Development Reagents (R&D Systems)) were added to each well and plate was incubated for another 20’ protected from light at RT.

- Reaction was stopped by adding 50 µl Stop Solution to each well.
- Optical density was determined, using a microplate reader set to 450 nm.

6.4.6 Genotyping

ΔM mice were genotyped after experiments.

2-5 mm of tail tissue was taken and put in 200 µl Tail Lysis Buffer (peqlab) supplemented with 0.2 mg Proteinase K (Sigma-Aldrich®). Incubation o/n at 55 °C degraded tissue (=crude Proteinase K lysate) followed by inactivation of the enzyme by incubation for 30' on 85 °C the next day. Crude Proteinase K lysate was frozen or directly used for PCR and results were analyzed by gelelectrophoresis using 1 % Agarose in 1xTAE.

Cre		**$TTP^{fl/fl}$**	
Reagent	1x [µl]	Reagent	1x [µl]
IMR 3066	0.25	TTP KO Neo f2	0.1
IMR 3067	0.4	TTP KO Neo rv	0.1
IMR 3068	0.2	RedMix	10
RedMix (Ampliqon)	10	Nuclease-free ddH2O	6.8
Nuclease-free ddH2O	6.15		
add 3 µl of genomic DNA			
PCR program			
	95 °C 05:00		95 °C 05:00
35 cycles	95 °C 00:30	35 cycles	94 °C 00:30
	57 °C 00:30		60 °C 00:30
	72 °C 00:30		72 °C 01:10
	72 °C 05:00		72 °C 05:00
expected bands			
WT	~ 350 bp	$TTP^{fl/fl}$	1197 bp
Cre	~ 700 bp	$TTP^{\Delta M}$	~ 200 bp

IMR 3066 5- CCC AGA AAT GCC AGA TTA CG -3

IMR 3067 5- CTT GGG CTG CCA GAA TTT CTC -3

IMR 3068 5- TTA CAG TCG GCC AGG CTG AC -3

TTP KO Neo f2 5- ATC TAG CTG ATC CAT ACT GGG -3

TTP KO Neo rv 5- AGG TTC TCC CTG GAG TTT GTG TGA -3

6.5 Reagents

Ketamine/Xylazine Solution
1 ml Ketasol 0.5 ml Xylasol in 10 ml 0.9 % NaCl

Tris-Acetate-EDTA (TAE): 50x
242 g Tris (solubilize in ddH_2O)
57.1 ml Acetic Acid (CH_3COOH)
100 ml 0.5 M EDTA (pH = 8)
ad 1 l with ddH_2O

Rehydration Solution: 1 L
13.5 g glucose
2.9 g sodium citrate
2.6 g sodium chloride
1.5 potassium chloride
ad 1 liter with tap water

Phosphate Buffered Saline (PBS): 10x
1.4 M NaCl
25 mM KCl
81 mM $Na_2HPO_4x2H_2O$
15 mM KH_2PO_4
ad 1 liter with ddH_2O, adjust pH = 7.3 with HCl

Tris Buffered Saline Tween (TBST): 10x
100 mM Tris
1.5 M NaCl
0.5 % Tween20
ad 1 liter with ddH_2O, adjust pH = 8.0 with HCl

L-conditioned (LC) Medium: 500 ml

Dulbeccos modified Eagle's medium (DMEM)
10 % FCS (GIBCO)
10 – 20 % L929-cell derived CSF-1 (LC)
optional: 500 µl 1000x P/S

cDC medium: 500 ml

Dulbeccos modified Eagle's medium (DMEM)
10 % FCS (GIBCO)
10 % X6310 cell-derived GMCSF
optional: 500 µl 1000x P/S

Red blood cell lysis buffer: 1 L

37.2 mg EDTA
8.29 g NH_4Cl
1 g $KHCO_3$
filter sterilized (0.2 µm) or autoclave

Pen/Strep (P/S): 1000x

0.6 g Penicillin
1 g Streptomycin
ad 10 ml with ddH_2O
filter sterilized and stored aliquots at -20 °C

THY: 1x

15 g Bact. Todd Hewitt Broth
1 g Yeast Extract
ad 500 ml with dH_2O (!!)
autoclave immediately

Lysis Buffer

1 ml Frackelton Buffer
10 µl 10 mM Na3VO4 (Vanadate)
1 µl 1M DTT
50 µl 20x Protease-Inhibitor (Roche)

Frackelton Buffer

10 mM Tris
30 mM Na4P2O7
50 mM NaCl
50 mM NaF
1 % Triton X-100
adjust pH to 7.1 and store at 4 °C

SDS Sample Buffer: 20 ml

5 ml 0.5 M Tris-HCl PH 6.8
2.5 ml Glycerol
4 ml 10 % SDS
2 ml β-mercaptoethanol
0.2 ml 0.05 % bromphenol blue
9.5 ml ddH_2O
stored at -20 °C

qRT-PCR Mastermix: 20 µl (1 reaction)

1.5 mM $MgCl_2$ (2.5 µl of 25 mM stock)
1x AmpliTaq Buffer II (2.5 µl of 10x stock)
200 µM dNTPs (0.5 µl of stock with 10 mM of each)
300 nM primer-for (0.075 µl of 100 pmol/ µl stock)
300 nM primer-rev (0.075 µl of 100 pmol/ µl stock)
SYBR Green (1 µl of 1:1000 stock)
1 U AmpliTaq (0.2 µl of 5 U/µl)
Pipet the AmpliTaq Polymerase just before using the Mastermix

Ponceau S

0.1% Ponceau
3% Trichloracetic acid (TCA)
0.01 % SDS
solubilize in ddH_2O

Anode Buffer I

0.3 M Tris 20 % Methanol in ddH_2O; adjust pH to 10.4

Anode Buffer II

2.5 mM Tris 20 % Methanol in ddH2O; adjust pH to 10.4

Cathode Buffer

0.04 M 6-Aminocaproic Acid 20 % Methanol 0.01 % SDS solubilize in ddH2O

Stripping Buffer (pH 2.2)

200 mM Glycine 150 mM NaCl 0.01 % Tween20 Solubilize in ddH_2O and autoclave

Wash Buffer (for ELISA)

0,25 ml Tween20 in 500 ml filter-sterilized 1xPBS

Reagent Diluent (for ELISA)

1 % (v/w) BSA in PBS and filter sterilize

Stop Solution (for ELISA)

2 N H_2SO_4 1:10 in ddH_2O

7 REFERENCES

1. Mellor, J. It Takes a PHD to Read the Histone Code. *Cell* **126**, 22-24 (2006).

2. Derynck, R. & Zhang, Y.E. Smad-dependent and Smad-independent pathways in TGF-[beta] family signalling. *Nature* **425**, 577-584 (2003).

3. Sadzak, I. et al. Recruitment of Stat1 to chromatin is required for interferon-induced serine phosphorylation of Stat1 transactivation domain. *PNAS* **105**, 8944-9 (2008).

4. Nilsen, T.W. & Graveley, B.R. Expansion of the eukaryotic proteome by alternative splicing. *Nature* **463**, 457-463 (2010).

5. Hudson, N.J. et al. Eukaryotic Evolutionary Transitions Are Associated with Extreme Codon Bias in Functionally-Related Proteins. *PLoS ONE* **6**, e25457 (2011).

6. Hess, D.T., Matsumoto, A., Kim, S.-O., Marshall, H.E. & Stamler, J.S. Protein S-nitrosylation: purview and parameters. *Nature Rev. Mol. Cell Biol.* **6**, 150-66 (2005).

7. Greganova, E., Altmann, M. & Bütikofer, P. Unique modifications of translation elongation factors. *FEBS Journal* **278**, 2613-2624 (2011).

8. Huntzinger, E. & Izaurralde, E. Gene silencing by microRNAs: contributions of translational repression and mRNA decay. *Nature Rev Genetics* **12**, 99-110 (2011).

9. Parker, R. & Song, H. The enzymes and control of eukaryotic mRNA turnover. *Nat Structural & Molecular Biology* **11**, 121-7 (2004).

10. Siomi, H. & Siomi, M.C. On the road to reading the RNA-interference code. *Nature* **457**, 396-404 (2009).

11. Gardner, L.B. Nonsense-mMediated RNA Decay Regulation by Cellular Stress: Implications for Tumorigenesis. *Mol Cancer Res* **8**, 295-308 (2010).

12. Okada-Katsuhata, Y. et al. N- and C-terminal Upf1 phosphorylations create binding platforms for SMG-6 and SMG-5:SMG-7 during NMD. *Nucleic Acids Res.* 1-16 (2011).doi:10.1093/nar/gkr791

13. Nicholson, P. et al. Nonsense-mediated mRNA decay in human cells: mechanistic insights, functions beyond quality control and the double-life of NMD factors. *Cell. Mol. Life Sci.* **67**, 677-700 (2010).

14. Kim, Y.K., Furic, L., Desgroseillers, L. & Maquat, L.E. Mammalian Staufen1 recruits Upf1 to specific mRNA 3'UTRs so as to elicit mRNA decay. *Cell* **120**, 195-208 (2005).

15. Kim, Y.K. et al. Staufen1 regulates diverse classes of mammalian transcripts. *The EMBO Journal* **26**, 2670-81 (2007).

16. Gong, C., Kim, Y.K., Woeller, C.F., Tang, Y. & Maquat, L.E. SMD and NMD are competitive pathways that contribute to myogenesis : effects on PAX3 and myogenin mRNAs. *Genes & Development* 54-66 (2009).doi:10.1101/gad.1717309.translation

17. Häsler, J. & Strub, K. Alu elements as regulators of gene expression. *Nucleic Acids Res.* **34**, 5491-7 (2006).

18. Vergara, S.V., Puig, S. & Thiele, D.J. Early recruitment of AU-rich element-containing mRNAs determines their cytosolic fate during iron deficiency. *Molecular and Cellular Biology* **31**, 417-29 (2011).

19. Cairrao, F., Halees, A.S., Khabar, K.S. a, Morello, D. & Vanzo, N. AU-rich elements regulate Drosophila gene expression. *Mol Cell Biol* **29**, 2636-43 (2009).

20. Aoki, K., Matsumoto, K. & Tsujimoto, M. Xenopus cold-inducible RNA-binding protein 2 interacts with ElrA, the Xenopus homolog of HuR, and inhibits deadenylation of specific mRNAs. *JBC* **278**, 48491-7 (2003).

21. Hodson, D.J. et al. Deletion of the RNA-binding proteins ZFP36L1 and ZFP36L2 leads to perturbed thymic development and T lymphoblastic leukemia. *Nat Immunol* **11**, 717-724 (2010).

22. Shaw, G. & Kamen, R. A conserved AU sequence from the 3' untranslated region of GM-CSF mRNA mediates selective mRNA degradation. *Cell* **46**, 659-667 (1986).

23. Brewer, G. & Ross, J. Regulation of c-myc mRNA stability in vitro by a labile destabilizer with an essential nucleic acid component. *Molecular and Cellular Biology* **9**, 1996-2006 (1989).

24. Zhang, W. et al. Purification, characterization, and cDNA cloning of an AU-rich element RNA-binding protein, AUF1. *Molecular and Cellular Biology* **13**, 7652-65 (1993).

25. Barreau, C., Paillard, L. & Osborne, H.B. AU-rich elements and associated factors: are there unifying principles? *Nucleic Acids Res.* **33**, 7138-50 (2005).

26. Lagnado, C.A., Brown, C.Y. & Goodall, G.J. AUUUA Is Not Sufficient To Promote Poly (A) Shortening and Degradation of an mRNA : the Functional Sequence within AU-Rich Elements May Be UUAUUUA (U / A)(U / A). *Mol Cell Biol* **14**, 7984-7995 (1994).

27. Chen, C.-ying A. & Shyu, A.-gin AU-rich elements: characterization and importance in mRNA degradation. *Trends Biochem. Sci.* **20**, 465-470 (1995).

28. von Roretz, C. & Gallouzi, I.-E. Decoding ARE-mediated decay: is microRNA part of the equation? *JCB* **181**, 189-94 (2008).

29. Lai, W.S., Stumpos, J. & Blacksheart, P.J. Rapid Insulin-stimulated Protein * Accumulation of an mRNA Encoding a. *JBC* **265**, 16556-16563 (1990).

30. Blackshear, P.J. et al. Zfp36l3, a rodent X chromosome gene encoding a placenta-specific member of the Tristetraprolin family of CCCH tandem zinc finger proteins. *Biology of Reproduction* **73**, 297-307 (2005).

31. Hudson, B.P., Martinez-Yamout, M. a, Dyson, H.J. & Wright, P.E. Recognition of the mRNA AU-rich element by the zinc finger domain of TIS11d. *Nature Structural and Molecular Biology* **11**, 257-64 (2004).

32. Lykke-Andersen, J. & Wagner, E. Recruitment and activation of mRNA decay enzymes by two ARE-mediated decay activation domains in the proteins TTP and BRF-1. *Genes & Development* **19**, 351-61 (2005).

33. Yamashita, A. et al. Concerted action of poly(A) nucleases and decapping enzyme in mammalian mRNA turnover. *Nat Structural & Molecular Biology* **12**, 1054-63 (2005).

34. Sandler, H., Kreth, J., Timmers, H.T.M. & Stoecklin, G. Not1 mediates recruitment of the deadenylase Caf1 to mRNAs targeted for degradation by tristetraprolin. *Nucleic Acids Res.* **39**, 4373-86 (2011).

35. Jing, Q. et al. Involvement of microRNA in AU-rich element-mediated mRNA instability. *Cell* **120**, 623-34 (2005).

36. Baou, M., Jewell, A. & Murphy, J.J. TIS11 family proteins and their roles in posttranscriptional gene regulation. *J. Biomed. Biotech.* **2009**, (2009).

37. Hasan Zaki, Peter Vogel, Mathilde Body-Malapel, Mohamed Lamkanfi, T.-D.K. IL-18 production downstream of the Nlrp3 inflammasome confers protection against colorectal tumor formation. *J Immunol* **185**, 4912-4920 (2010).

38. Cao, H., Urban, J.F. & Anderson, R. a Cinnamon polyphenol extract affects immune responses by regulating anti- and proinflammatory and glucose transporter gene expression in mouse macrophages. *The Journal of Nutrition* **138**, 833-40 (2008).

39. Cao, H. et al. Green tea increases anti-inflammatory tristetraprolin and decreases pro-inflammatory tumor necrosis factor mRNA levels in rats. *Journal of Inflammation* **4**, (2007).

40. Huang, G., Shi, L.Z. & Chi, H. Regulation of JNK and p38 MAPK in the immune system: Signal integration, propagation and termination. *Cytokine* **48**, 161-169 (2009).

41. Ananieva, O. et al. The kinases MSK1 and MSK2 act as negative regulators of Toll-like receptor signaling. *Nat Immunol* **9**, 1028-36 (2008).

42. Anderson, P. & Kedersha, N. Stressful initiations. *J. Cell Science* **115**, 3227-34 (2002).

43. Kedersha, N. & Anderson, P. Stress granules : sites of mRNA triage that regulate mRNA stability Stress granules (SGs): a historical perspective. *Biochemical Society* **30**, 963-969 (2002).

44. Kedersha, N. et al. Stress granules and processing bodies are dynamically linked sites of mRNP remodeling. *The Journal of Cell Biology* **169**, 871-84 (2005).

45. Franks, T.M. & Lykke-Andersen, J. TTP and BRF proteins nucleate processing body formation to silence mRNAs with AU-rich elements. *Genes & Development* **21**, 719-35 (2007).

46. Sandler, H. & Stoecklin, G. Control of mRNA decay by phosphorylation of tristetraprolin. *Biochemical Society Transactions* **36**, 491-6 (2008).

47. Schaljo, B. et al. Tristetraprolin is required for full anti-inflammatory response of murine macrophages to IL-10. *J Immunol* **183**, 1197-206 (2009).

48. Taylor, G. a et al. A pathogenetic role for TNF alpha in the syndrome of cachexia, arthritis, and autoimmunity resulting from tristetraprolin (TTP) deficiency. *Immunity* **4**, 445-54 (1996).

49. Brooks, S.A., Connolly, J.E. & Rigby, W.F.C. The Role of mRNA Turnover in the Regulation of Tristetraprolin Expression: Evidence for an Extracellular Signal-Regulated Kinase-Specific, AU-Rich Element-Dependent, Autoregulatory Pathway. *J Immunol* **172**, 7263-7271 (2004).

50. Stoecklin, G. et al. Genome-wide analysis identifies interleukin-10 mRNA as target of tristetraprolin. *JBC* **283**, 11689-99 (2008).

51. Varnum, B.C., Ma, Q.F., Chi, T.H., Fletcher, B. & Herschman, H.R. The TIS11 primary response gene is a member of a gene family that encodes proteins with a highly conserved sequence containing an unusual Cys-His repeat. *Mol. Cell. Biol.* **11**, 1754-8 (1991).

52. Lai, W.S., Carballo, E., Thorn, J.M., Kennington, E. a & Blackshear, P.J. Interactions of CCCH zinc finger proteins with mRNA. Binding of tristetraprolin-related zinc finger proteins to Au-rich elements and destabilization of mRNA. *JBC* **275**, 17827-37 (2000).

53. Thompson, M.J., Lai, W.S., Taylor, G.A. & Blackshear, P.J. Cloning and characterization of two yeast genes encoding members of the CCCH class of zinc finger proteins: zinc finger-mediated impairment of cell growth. *Gene* **174**, 225-233 (1996).

54. Ramos, S.B.V. et al. The CCCH tandem zinc-finger protein Zfp36l2 is crucial for female fertility and early embryonic development. *Development* **131**, 4883-93 (2004).

55. Stumpo, D.J. et al. Chorioallantoic Fusion Defects and Embryonic Lethality Resulting from Disruption of Zfp36L1 , a Gene Encoding a CCCH Tandem Zinc Finger Protein of the Tristetraprolin Family. *Mol. Cell. Biol.* **24**, 6445-6455 (2004).

56. Stumpo, D.J. et al. Targeted disruption of Zfp36l2, encoding a CCCH tandem zinc finger RNA-binding protein, results in defective hematopoiesis. *Blood* **114**, 2401-10 (2009).

57. Maitra, S. et al. The AU-rich element mRNA decay-promoting activity of BRF1 is regulated by mitogen-activated protein kinase-activated protein kinase 2. *RNA* **14**, 950-9 (2008).

58. Good, P.J., Chen, Q., Warner, S.J. & Herring, D.C. A family of human RNA-binding proteins related to the Drosophila Bruno translational regulator. *JBC* **275**, 28583-92 (2000).

59. López de Silanes, I., Zhan, M., Lal, A., Yang, X. & Gorospe, M. Identification of a target RNA motif for RNA-binding protein HuR. *PNAS* **101**, 2987-92 (2004).

60. Uren, P.J. et al. Genomic analyses of the RNA binding protein Hu Antigen R (HuR) identify a complex network of target genes and novel characteristics of its binding sites. *JBC* **286**, 37063-37066 (2011).

61. Kim, H.S. et al. Different modes of interaction by TIAR and HuR with target RNA and DNA. *Nucleic Acids Res.* **39**, 1117-30 (2011).

62. Raineri, I., Wegmueller, D., Gross, B., Certa, U. & Moroni, C. Roles of AUF1 isoforms, HuR and BRF1 in ARE-dependent mRNA turnover studied by RNA interference. *Nucleic Acids Res.* **32**, 1279-88 (2004).

63. Young, L.E. et al. The mRNA Binding Proteins HuR and Tristetraprolin Regulate Cyclooxygenase 2 Expression During Colon Carcinogenesis. *Gastroenterology* **136**, 1669-1679 (2009).

64. Bhattacharyya, S.N., Habermacher, R., Martine, U., Closs, E.I. & Filipowicz, W. Relief of microRNA-mediated translational repression in human cells subjected to stress. *Cell* **125**, 1111-24 (2006).

65. David Gerecht, P.S., Taylor, M. a & Port, J.D. Intracellular localization and interaction of mRNA binding proteins as detected by FRET. *BMC Cell Biology* **11**, 69 (2010).

66. Bhattacharya, S., Giordano, T., Brewer, G. & Malter, J.S. Identification of AUF-1 ligands reveals vast diversity of early response gene mRNAs. *Nucleic Acids Res.* **27**, 1464-72 (1999).

67. Laroia, G. Control of mRNA Decay by Heat Shock-Ubiquitin-Proteasome Pathway. *Science* **284**, 499-502 (1999).

68. Knapinska, A.M. et al. Chaperone Hsp27 modulates AUF1 proteolysis and AU-rich element-mediated mRNA degradation. *Molecular and Cellular Biology* **31**, 1419-31 (2011).

69. Lu, J.-Y., Sadri, N. & Schneider, R.J. Endotoxic shock in AUF1 knockout mice mediated by failure to degrade proinflammatory cytokine mRNAs. *Genes & Development* **20**, 3174-84 (2006).

70. Phillips, K., Kedersha, N., Shen, L., Blackshear, P.J. & Anderson, P. Arthritis suppressor genes TIA-1 and TTP dampen the expression of tumor necrosis factor alpha, cyclooxygenase 2, and inflammatory arthritis. *PNAS* **101**, 2011-6 (2004).

71. Piecyk, M. et al. TIA-1 is a translational silencer that selectively regulates the expression of TNF-alpha. *The EMBO Journal* **19**, 4154-63 (2000).

72. Kedersha, N. et al. Dynamic shuttling of TIA-1 accompanies the recruitment of mRNA to mammalian stress granules. *The Journal of Cell Biology* **151**, 1257-68 (2000).

73. Murray, P.J. & Wynn, T. a Protective and pathogenic functions of macrophage subsets. *Nature Rev. Immunol.* doi:10.1038/nri3073

74. Gordon, S. & Taylor, P.R. Monocyte and macrophage heterogeneity. *Nature Rev. Immunol.* **5**, 953-64 (2005).

75. Hume, D. a Macrophages as APC and the Dendritic Cell Myth. *J Immunol* **181**, 5829-35 (2008).

76. Silva, M.T. When two is better than one: macrophages and neutrophils work in concert in innate immunity as complementary and cooperative partners of a myeloid phagocyte system. *Journal of Leukocyte Biology* **87**, 93-106 (2010).

77. McGaha, T.L., Chen, Y., Ravishankar, B., van Rooijen, N. & Karlsson, M.C.I. Marginal zone macrophages suppress innate and adaptive immunity to apoptotic cells in the spleen. *Blood* **117**, 5403-12 (2011).

78. Smith, P.D., Ochsenbauer-Jambor, C. & Smythies, L.E. Intestinal macrophages: unique effector cells of the innate immune system. *Immunological Reviews* **206**, 149-59 (2005).

79. Soehnlein, O. & Lindbom, L. Phagocyte partnership during the onset and resolution of inflammation. *Nature Rev. Immunol.* **10**, 427-39 (2010).

80. Medzhitov, R. Recognition of microorganisms and activation of the immune response. *Nature* **449**, 819-26 (2007).

81. Flannagan, R.S., Jaumouillé, V. & Grinstein, S. The Cell Biology of Phagocytosis. *Annu. Rev. Pathol. Mech. Dis.* **7**, 49-86 (2012).

82. Scheller, J., Chalaris, A., Schmidt-Arras, D. & Rose-John, S. The pro- and anti-inflammatory properties of the cytokine interleukin-6. *Biochim. Biophys. Acta* (2011).doi:10.1016/j.bbamcr.2011.01.034

83. Tester, A.M. et al. LPS Responsiveness and Neutrophil Chemotaxis In Vivo Require PMN MMP-8 Activity. *PLoS ONE* **2**, (2007).

84. Eash, K.J., Greenbaum, A.M., Gopalan, P.K. & Link, D.C. CXCR2 and CXCR4 antagonistically regulate neutrophil trafficking from murine bone marrow. *J. Clin. Invest.* **120**, 2423-31 (2010).

85. Williams, M.R., Azcutia, V., Newton, G., Alcaide, P. & Luscinskas, F.W. Emerging mechanisms of neutrophil recruitment across endothelium. *Trends in Immunology* **32**, 461-469 (2011).

86. Faurschou, M. & Borregaard, N. Neutrophil granules and secretory vesicles in inflammation. *Microbes and Infection* **5**, 1317-1327 (2003).

87. Papayannopoulos, V. & Zychlinsky, A. NETs: a new strategy for using old weapons. *Trends in Immunology* **30**, 513-21 (2009).

88. Buchanan, J.T. et al. DNase expression allows the pathogen group A Streptococcus to escape killing in neutrophil extracellular traps. *Current Biology* **16**, 396-400 (2006).

89. Nathan, C. Neutrophils and immunity: challenges and opportunities. *Nature Rev. Immunol.* **6**, 173-82 (2006).

90. Weiss, S.J., Young, J., LoBuglio, a F., Slivka, A. & Nimeh, N.F. Role of Hydrogen Peroxide in Neutrophil-mediated Destruction of Cultured Endothelial Cells. *J. Clin. Invest.* **68**, 714-21 (1981).

91. Massberg, S. et al. Reciprocal coupling of coagulation and innate immunity via neutrophil serine proteases. *Nature Medicine* **16**, 887-96 (2010).

92. Loof, T.G. et al. Coagulation, an ancestral serine protease cascade, exerts a novel function in early immune defense. *Blood* 2589-2598 (2011).doi:10.1182/blood-2011-02-337568

93. De Yang et al. LL-37, the Neutrophil Granule- and Epithelial cell-derived Cathelicidin, Utilizes Formyl Peptide Receptor-like 1 (FPRL1) as a Receptor to Chemoattract Human Peripheral Blood Neutrophils, Monocytes, and T cells. *J. Exp. Med.* **192**, 1069-74 (2000).

94. Serbina, N.V. & Pamer, E.G. Monocyte emigration from bone marrow during bacterial infection requires signals mediated by chemokine receptor CCR2. *Nat Immunol* **7**, 311-7 (2006).

95. Hurst, S.M. et al. Il-6 and Its Soluble Receptor Orchestrate a Temporal Switch in the Pattern of Leukocyte Recruitment Senn during Acute Inflammation. *Immunity* **14**, 705-14 (2001).

96. Ingersoll, M. a, Platt, A.M., Potteaux, S. & Randolph, G.J. Monocyte trafficking in acute and chronic inflammation. *Trends in Immunology* **32**, 470-477 (2011).

97. Serbina, N.V., Salazar-mather, T.P., Biron, C.A., Kuziel, W.A. & Pamer, E.G. TNF / iNOS-Producing Dendritic Cells Mediate Innate Immune Defense against Bacterial Infection. *Immunity* **19**, 59-70 (2003).

98. Schwab, J.M. & Serhan, C.N. Lipoxins and new lipid mediators in the resolution of inflammation. *Current Opinion in Pharmacology* **6**, 414-420 (2006).

99. Maddox, J.F. et al. Lipoxin A4 stable analogs are potent mimetics that stimulate human monocytes and THP-1 cells via a G-protein-linked lipoxin A4 receptor. *J. Biol. Chem.* **272**, 6972-8 (1997).

100. Scannell, M. et al. Annexin-1 and Peptide Derivatives Are Released by Apoptotic Cells and Stimulate Phagocytosis of Apoptotic Neutrophils by Macrophages. *J Immunol* **178**, 4595-605 (2007).

101. Perretti, M. & D'Acquisto, F. Annexin A1 and glucocorticoids as effectors of the resolution of inflammation. *Nature Rev. Immunol.* **9**, 62-70 (2009).

102. Voll, R.E., Herrmann, M., Roth, E.A., Stach, C. & Kalden, J.R. Immunosuppressive effects of apoptotic cells. *Nature* **390**, 350-1 (1997).

103. Fadok, V. a et al. Macrophages That Have Ingested Apoptotic Cells In Vitro Inhibit Proinflammatory Cytokine Production Through Autocrine/Paracrine Mechanims Involving TGF-b, PGE2, and PAF. *J. Clin. Invest.* **101**, 890-8 (1998).

104. Johansson, L., Thulin, P., Low, D.E. & Norrby-Teglund, A. Getting under the skin: the immunopathogenesis of Streptococcus pyogenes deep tissue infections. *Clinical Infectious Diseases* **51**, 58-65 (2010).

105. Cunningham, M.W. Pathogenesis of group A streptococcal infections and their sequelae. *Clin Microbiol Reviews* **13**, 470-511 (2000).

106. Aziz, R.K. Rise and Persistence of Global M1T1 Clone of Streptococcus pyogenes. *Emerging Infectious Diseases* **14**, 1511-1517 (2008).

107. Frick, I.-M., Schmidtchen, A. & Sjöbring, U. Interactions between M proteins of Streptococcus pyogenes and glycosaminoglycans promote bacterial adhesion to host cells. *Eur. J. Biochem.* **270**, 2303-2311 (2003).

108. Areschoug, T., Waldemarsson, J. & Gordon, S. Evasion of macrophage scavenger receptor A-mediated recognition by pathogenic streptococci. *Eur. J. Immunol.* **38**, 3068-79 (2008).

109. Macheboeuf, P. et al. Streptococcal M1 protein constructs a pathological host fibrinogen network. *Nature* **472**, 64-8 (2011).

110. McNamara, C. et al. Coiled-coil irregularities and instabilities in group A Streptococcus M1 are required for virulence. *Science* **319**, 1405-8 (2008).

111. Cole, J.N., Barnett, T.C., Nizet, V. & Walker, M.J. Molecular insight into invasive group A streptococcal disease. *Nature Rev Microbiology* **9**, 724-736 (2011).

112. Kotb, M. et al. An immunogenetic and molecular basis for differences in outcomes of invasive group A streptococcal infections. *Nature Medicine* **8**, 1398-404 (2002).

113. Cole, J.N. et al. Streptococcus M Protein and Hyaluronic Acid Capsule Are Essential for In Vivo Selection of covRS Mutations Characteristic of Invasive Serotype M1T1 Group A Streptococcus. *mBio* **1**, (2010).

114. Platt, A.M. & Mowat, A.M. Mucosal macrophages and the regulation of immune responses in the intestine. *Immunology Letters* **119**, 22-31 (2008).

115. Jarchum, I. & Pamer, E.G. Regulation of innate and adaptive immunity by the commensal microbiota. *Current Opinion in Immunology* **23**, 353-360 (2011).

116. Johansson, M.E.V., Larsson, J.M.H. & Hansson, G.C. The two mucus layers of colon are organized by the MUC2 mucin, whereas the outer layer is a legislator of host-microbial interactions. *PNAS* **108**, 4659-65 (2011).

117. Takahashi, K. et al. Epigenetic Control of the Host Gene by Commensal Bacteria in Large Intestinal Epithelial Cells. *JBC* **286**, 35755-35762 (2011).

118. Roda, G. Intestinal epithelial cells in inflammatory bowel diseases. *World J Gastroenterol* **16**, 4264-71 (2010).

119. Hu, B. et al. Inflammation-induced tumorigenesis in the colon is regulated by caspase-1 and NLRC4. *PNAS* **107**, 21635-40 (2010).

120. Elinav, E. et al. NLRP6 inflammasome regulates colonic microbial ecology and risk for colitis. *Cell* **145**, 745-57 (2011).

121. Zaki, M.H. et al. The NLRP3 inflammasome protects against loss of epithelial integrity and mortality during experimental colitis. *Immunity* **32**, 379-91 (2010).

122. Fritz, J.H., Le Bourhis, L., Magalhaes, J.G. & Philpott, D.J. Innate immune recognition at the epithelial barrier drives adaptive immunity: APCs take the back seat. *Trends in Immunology* **29**, 41-9 (2008).

123. Garrett, W.S., Gordon, J.I. & Glimcher, L.H. Homeostasis and inflammation in the intestine. *Cell* **140**, 859-70 (2010).

124. Mowat, A.M. Anatomical basis of tolerance and immunity to intestinal antigens. *Nature Rev. Immunol.* **3**, 331-41 (2003).

125. Qin, J. et al. A human gut microbial gene catalogue established by metagenomic sequencing. *Nature* **464**, 59-65 (2010).

126. Pédron, T. & Sansonetti, P. Commensals, bacterial pathogens and intestinal inflammation: an intriguing ménage à trois. *Cell Host & Microbe* **3**, 344-7 (2008).

127. Cerf-Bensussan, N. & Gaboriau-Routhiau, V. The immune system and the gut microbiota: friends or foes? *Nature Rev. Immunol.* **10**, 735-44 (2010).

128. Lathrop, S.K. et al. Peripheral education of the immune system by colonic commensal microbiota. *Nature* **478**, 250-254 (2011).

129. Takahashi, K. et al. Epigenetic control of host gene by commensal bacteria in large intestinal epithelial cells. *JBC* doi:10.1074/jbc.M111.271007

130. Saleh, M. & Trinchieri, G. Innate immune mechanisms of colitis and colitis-associated colorectal cancer. *Nature Rev. Immunol.* **11**, 9-20 (2011).

131. Shen, R. et al. Stromal down-regulation of macrophage CD4/CCR5 expression and NF-κB activation mediates HIV-1 non-permissiveness in intestinal macrophages. *PLoS Pathogens* **7**, e1002060 (2011).

132. Manicassamy, S. et al. Activation of beta-catenin in dendritic cells regulates immunity versus tolerance in the intestine. *Science* **329**, 849-53 (2010).

133. Worthington, J.J., Czajkowska, B.I., Melton, A.C. & Travis, M.A. Intestinal Dendritic Cells Specialize to Activate Transforming Growth Factor-β and Induce Foxp3+ Regulatory T Cells via Integrin αvβ8. *Gastroenterology* **141**, 1802-1812 (2011).

134. Saleh, M. & Elson, C.O. Experimental inflammatory bowel disease: insights into the host-microbiota dialog. *Immunity* **34**, 293-302 (2011).

135. Rossin, E.J. et al. Proteins encoded in genomic regions associated with immune-mediated disease physically interact and suggest underlying biology. *PLoS Genetics* **7**, e1001273 (2011).

136. Travis, M. a et al. Loss of integrin alpha(v)beta8 on dendritic cells causes autoimmunity and colitis in mice. *Nature* **449**, 361-5 (2007).

137. Dupaul-Chicoine, J. et al. Control of intestinal homeostasis, colitis, and colitis-associated colorectal cancer by the inflammatory caspases. *Immunity* **32**, 367-78 (2010).

138. Asquith, M. & Powrie, F. An innately dangerous balancing act: intestinal homeostasis, inflammation, and colitis-associated cancer. *J. Exp. Med.* **207**, 1573-7 (2010).

139. Hanahan, D. & Weinberg, R. a Hallmarks of Cancer: The Next Generation. *Cell* **144**, 646-74 (2011).

140. Jablonska, J., Leschner, S., Westphal, K., Lienenklaus, S. & Weiss, S. Neutrophils responsive to endogenous IFN-β regulate tumor angiogenesis and growth in a mouse tumor model. *J Clin. Invest.* **120**, 1151-1164 (2010).

141. Eaden, J. a, Abrams, K.R. & Mayberry, J.F. The risk of colorectal cancer in ulcerative colitis: a meta-analysis. *Gut* **48**, 526-35 (2001).

142. Salcedo, R. et al. MyD88-mediated signaling prevents development of adenocarcinomas of the colon: role of interleukin 18. *J. Exp. Med.* **207**, 1625-36 (2010).

143. Massi, E. et al. The AOM/DSS murine model for the study of colon carcinogenesis: From pathways to diagnosis and therapy studies. *Journal of Carcinogenesis* **10**, 9 (2011).

144. Clausen, B.E., Burkhardt, C., Reith, W., Renkawitz, R. & Förster, I. Conditional gene targeting in macrophages and granulocytes using LysMcre mice. *Transgenic Research* **8**, 265-77 (1999).

145. Van Tubergen, E. et al. Tristetraprolin regulates interleukin-6, which is correlated with tumor progression in patients with head and neck squamous cell carcinoma. *Cancer* **117**, 2677-89 (2011).

146. Lutz, M.B. et al. An advanced culture method for generating large quantities of highly pure dendritic cells from mouse bone marrow. *J. Immunol. Meth.* **223**, 77-92 (1999).

147. Loof, T.G., Goldmann, O. & Medina, E. Immune recognition of Streptococcus pyogenes by dendritic cells. *Infection and Immunity* **76**, 2785-92 (2008).

148. Tamayo, E., Montes, M., García-Medina, G., García-Arenzana, J.M. & Pérez-Trallero, E. Spread of a highly mucoid Streptococcus pyogenes emm3/ST15 clone. *BMC Infectious Diseases* **10**, (2010).

149. Zingaretti, C. et al. Streptococcus pyogenes SpyCEP: a chemokine-inactivating protease with unique structural and biochemical features. *The FASEB Journal* **24**, 2839-48 (2010).

150. Goldmann, O., Sastalla, I., Wos-Oxley, M., Rohde, M. & Medina, E. Streptococcus pyogenes induces oncosis in macrophages through the activation of an inflammatory programmed cell death pathway. *Cellular Microbiology* **11**, 138-55 (2009).

151. Park, D. et al. Continued clearance of apoptotic cells critically depends on the phagocyte Ucp2 protein. *Nature* **477**, 220-224 (2011).

152. Gratz, N. et al. Type I interferon production induced by Streptococcus pyogenes-derived nucleic acids is required for host protection. *PLoS Pathogens* **7**, e1001345 (2011).

153. Sauer, I. et al. Interferons limit inflammatory responses by induction of tristetraprolin. *Blood* **107**, 4790-7 (2006).

154. Carballo, E. Feedback Inhibition of Macrophage Tumor Necrosis Factor- Production by Tristetraprolin. *Science* **281**, 1001-1005 (1998).

155. Olsnes, C., Stavang, H., Brokstad, K., Olofsson, J. & Aarstad, H.J. Chemokines are secreted by monocytes following OK-432 (lyophilized Streptococcus pyogenes) stimulation. *BMC Immunology* **10**, (2009).

156. Loof, T.G., Rohde, M., Chhatwal, G.S., Jung, S. & Medina, E. The contribution of dendritic cells to host defenses against Streptococcus pyogenes. *The Journal of Infectious Diseases* **196**, 1794-803 (2007).

157. Daley, J.M., Thomay, A. a, Connolly, M.D., Reichner, J.S. & Albina, J.E. Use of Ly6G-specific monoclonal antibody to deplete neutrophils in mice. *Journal of Leukocyte Biology* **83**, 64-70 (2008).

158. Terao, Y. et al. Group A streptococcal cysteine protease degrades C3 (C3b) and contributes to evasion of innate immunity. *JBC* **283**, 6253-60 (2008).

159. Chou, R.C. et al. Lipid-cytokine-chemokine cascade drives neutrophil recruitment in a murine model of inflammatory arthritis. *Immunity* **33**, 266-78 (2010).

160. Semerad, C.L., Liu, F., Gregory, A.D., Stumpf, K. & Link, D.C. G-CSF Is an Essential Regulator of Neutrophil Trafficking from the Bone Marrow to the Blood. *Immunity* **17**, 413-23 (2002).

161. Sadik, C.D., Kim, N.D. & Luster, A.D. Neutrophils cascading their way to inflammation. *Trends in Immunology* **32**, 452-60 (2011).

162. Cox, D., Kerrigan, S.W. & Watson, S.P. Platelets and the innate immune system: mechanisms of bacterial-induced platelet activation. *JTH* (2011).doi:10.1111/j.1538-7836.2011.04264.x

163. Bogdan, C. Nitric oxide and the immune response. *Nat Immunol* **2**, 907-16 (2001).

164. Rakoff-Nahoum, S., Paglino, J., Eslami-Varzaneh, F., Edberg, S. & Medzhitov, R. Recognition of commensal microflora by toll-like receptors is required for intestinal homeostasis. *Cell* **118**, 229-41 (2004).

165. Kontoyiannis, D., Pasparakis, M., Pizarro, T.T., Cominelli, F. & Kollias, G. Impaired on/off regulation of TNF biosynthesis in mice lacking TNF AU-rich elements: implications for joint and gut-associated immunopathologies. *Immunity* **10**, 387-98 (1999).

166. Ogawa, K., Chen, F., Kim, Y.-J. & Chen, Y. Transcriptional regulation of tristetraprolin by transforming growth factor-beta in human T cells. *JBC* **278**, 30373-81 (2003).

167. Ogilvie, R.L. et al. Tristetraprolin down-regulates IL-2 gene expression through AU-rich element-mediated mRNA decay. *J Immunol* **174**, 953-61 (2005).

168. Clevers, H. At the Crossroads of Inflammation and Cancer. *Cell* **118**, 671-4 (2004).

169. Lee, H.H. et al. Tristetraprolin regulates expression of VEGF and tumorigenesis in human colon cancer. *International Journal of Cancer* **126**, 1817-27 (2010).

170. Zamarron, B.F. & Chen, W. Dual Roles of Immune Cells and Their Factors in Cancer Development and Progression. *Int. J. Biol. Sci.* **7**, 651-8 (2011).

171. Becker, C. et al. In vivo imaging of colitis and colon cancer development in mice using high resolution chromoendoscopy. *Gut* **54**, 950-4 (2005).

172. Musteanu, M. et al. Stat3 Is a Negative Regulator of Intestinal Tumor Progression in ApcMin Mice. *Gastroenterology* **138**, 1003-1011 (2010).

173. Yurchenko, E., Levings, M.K. & Piccirillo, C. a CD4(+) Foxp3(+) regulatory T cells suppress γ δ T-cell effector functions in a model of T cell-induced mucosal inflammation. *European Journal of Immunology* **1934**, 1-33 (2011).

174. Makita, S. et al. Intestinal lamina propria retaining CD4+CD25+ regulatory T cells is a suppressive site of intestinal inflammation. *J Immunol* **178**, 4937-46 (2007).

175. Varol, C., Zigmond, E. & Jung, S. Securing the immune tightrope: mononuclear phagocytes in the intestinal lamina propria. *Nature Rev. Immunol.* **10**, 415-26 (2010).

176. He, Z. et al. Interleukin-18. *Methods* **19**, 121-132 (1999).

177. Bartsch, I., Zschaler, I., Haseloff, M. & Steinberg, P. Establishment of a long-term culture system for rat colon epithelial cells. *IN Vitro Cell. Dev. Biol.* **40**, 278-84 (2004).

178. Konkel, J.E. & Chen, W. Balancing acts: the role of TGF-β in the mucosal immune system. *Trends in Molecular Medicine* 1-9 (2011).doi:10.1016/j.molmed.2011.07.002

179. Hennet, T., Hagen, F.K., Tabak, L. a & Marth, J.D. T-cell-specific deletion of a polypeptide N-acetylgalactosaminyl-transferase gene by site-directed recombination. *PNAS* **92**, 12070-4 (1995).

180. Becker, C., Fantini, M.C. & Neurath, M.F. High resolution colonoscopy in live mice. *Nature Protocols* **1**, 2900-4 (2006).

181. Boivin, G.P. et al. Pathology of mouse models of intestinal cancer: consensus report and recommendations. *Gastroenterology* **124**, 762-77 (2003).

182. Gratz, N. et al. Group A streptococcus activates type I interferon production and MyD88-dependent signaling without involvement of TLR2, TLR4, and TLR9. *JBC* **283**, 19879-87 (2008).

Ich habe mich bemüht, sämtliche Inhaber der Bildrechte ausfindig zu machen und ihre Zustimmung zur Verwendung der Bilder in dieser Arbeit eingeholt. Sollte dennoch eine Urheberrechtsverletzung bekannt werden, ersuche ich um Meldung bei mir.

I endeavored to descry all copyright holders of figures and gained the acceptance to use the figures for this thesis. If there is any copyright infringement, I ask to contact me.

8 CURRICULUM VITAE

Private Facts

Address	Linzerstrasse 160/7/1, 1140 Wien
Phone Number	0650 47 00 302
E-Mail	florian.ebner@univie.ac.at
Date of Birth	20.12.1985
Place of Birth	Villach
Family Status	unmarried
Citizenship	Austria

Education

Since October 2006	University of Vienna / Molecular Biology
2000-2005	Höhere Technische Bunds- Lehr- und Versuchsanstalt Villach Branch: Electronic Data Processing and Organisation Acquisition: Diplom- und Reifeprüfung
1996-2000	Hauptschule Gegendtal (secondary school)

Job-related Activities

Since Nov 2010	Diploma thesis in immunology at the Max F. Perutz Laboratories
17/05 – 23/07/10	Università degli Studi di Milano-Bicocca: Silvia Nicolis Lab *SMART Summer School* Roles of the Sox2 transcription factor in neural stem cells
Nov/Dec 2009	Max F. Perutz Laboratories: Andreas Hartig Lab *Internship (2 month)/Wahlbeispiel* Analysis of peroxisomal proteins in yeast
Summer 2009	Max F. Perutz Laboratories: Kristina Djinovic Carugo Lab *Internship (2 month)/Wahlbeispiel* Purification, crystallization and structural analysis of proteins

Conferences & Teaching

5th – 9th Juli 2011	15th International Conference of Mucosal Immunology (Paris)
21st – 23rd June 2011	P3AGI Summer School: Animal Models in Allergic Disease (Vienna)
May/June 2011	Tutoring twice "Uebung IIIA: EDV in der Molekularbiologie"
March 2011	Workshop on Intestinal Mucosal Homeostasis and Disease (Hannover)
February 2011	Introductory Course into Laboratory Animal Science (FELASA B)

Particular Skills

Languages	German – mother tongue English – fluent in written and spoken Italian – basics
IT-Knowledge	MS Office, GraphPad, various programming languages (Java, HTML, C++, C#, Visual Basic .Net, SQL, COBOL, etc.), databases (Access, Oracle), UML, Visual Studio (6.0 & .Net), etc. Basics: Linux, VMD, Ghemical, SAP, LabView, LotusNotes, CCP4, Wincoot, BallView, to mention but a few.

Interests

Foreign cultures and countries, cooking, science and technology, astronomy, new media, parlor games, etc.